

DEVELOPMENT AND APPLICATION OF DENDRITIC SYSTEMS FOR  
TARGETED INTRACELLULAR DELIVERY

By

Artez Laurant Sims

Dissertation

Submitted to the Faculty of the  
Graduate School of Vanderbilt University  
in partial fulfillment of the requirements

for the degree of

DOCTOR OF PHILOSOPHY

in

Chemistry

August, 2013

Nashville, TN

Approved:

Professor Eva M. Harth

Professor Timothy Hanusa

Professor David Wright

Professor James E. Crowe

## ACKNOWLEDGEMENTS

This work would not have been possible without the financial support of the VINSE Fellowship Award, the D. Stanley and Ann T. Tarbell Endowment fund. I thank my lab members that include Ghazal Hariri, Dain Beazer, Kelly Gilmore, Guangzho Li, Benjamin Spears, and David Stevens. I am grateful to my collaborators that I have had the pleasure to work with. Each of the members of my Dissertation Committee has provided invaluable insight and guidance for my scientific research. I would especially like to thank Dr. Eva M. Harth, the chairman of my committee. As my advisor, she has both inspired and aided me throughout the progression of the program.

Nobody has provided more support to me than my close friends and members of my family. I would like to thank my parents, whose love has been unmistakably present at all times. I would also like to thank individuals within Alpha Phi Alpha Fraternity Incorporated that I have met and have become life-long friends with. Most importantly, I wish to thank my cherished loved one Valitria Williams, who has given me undaunted courage to endure hardships faced.

## TABLE OF CONTENTS

	Page
ACKNOWLEDGEMENTS.....	ii
LIST OF TABLES.....	v
LIST OF FIGURES.....	vi
LIST OF SCHEMES.....	viii
LIST OF ABBREVIATIONS.....	ix
Chapter	
I. INTRODUCTION.....	1
Inorganic Approaches.....	3
Polymeric Approaches.....	5
Polymeric Nanoparticles.....	5
Liposomes.....	6
Micelles.....	8
Linear Polymers.....	8
Hydrogels.....	10
Dendrimers.....	12
Conclusion.....	15
References.....	16
II. INTRACELLULAR NEUTRALIZATION OF ROTAVIRUS USING MOLECULAR DENDRITIC TRANSPORTER ANTIBODY CONJUGATE .....	25
Introduction.....	25
Discussion.....	28
Initial Studies: Conjugation of RV6-26 Fab to MT.....	28
Conjugation Optimization: MT to RV6-26 scFv.....	33
Conclusion.....	40
Experimental.....	40
References.....	48
III. DEVELOPMENT OF THIRD GENERATION NEWKOME TYPE DENDRIMERS .....	50
Introduction.....	50

Discussion.....	55
Conclusion.....	61
Experimental.....	62
References.....	68
IV. DEVELOPMENT OF A MOLECULAR TRANSPORTER FOR MITOCHONDRIA DELIVERY .....	74
Introduction.....	74
Discussion.....	78
Colocalization Studies.....	83
Conclusion.....	87
Experimental.....	88
References.....	96
V. CONCLUSIONS AND FUTURE OUTLOOK.....	99

## LIST OF TABLES

### Table

2.1.	Various conditions to optimize MT-RV6-26 conjugation.....	11
4.1.	Ratios of cyclohexyl group G3LLMT synthesized.....	80

## LIST OF FIGURES

### Figure

1.1.	Intracellular barriers.....	1
1.2.	Liposome.....	6
1.3.	Polyethylene glycol.....	9
1.4.	Linear polymer systems .....	10
1.5.	Stimuli response hydrogels polymers. ....	11
1.6.	G3 Dendrimer.....	12
2.1.	Rotavirus particle.....	27
2.2.	SPDP linker was attachment to RV6-26 Fab.....	31
2.3.	MT is reduction via dithiothreitol (DTT). ....	32
2.4.	MT-RV6-26 Fab conjugation.....	33
2.5.	An alternative antibody comparison.....	33
2.6.	Reduction of RV6-26 scFv via Tris carboxy ethyly phosphine (TCEP).....	34
2.7.	MT-RV6-26 scFv conjugation. ....	35
2.8.	Gel Electrophoresis: MT-RV6-26 scFv conjugation improvement.....	37
2.9.	Quantification of MT-RV6-26 scFv internalization. ....	38
2.10.	ELISA assay and titer neutralization assay. ....	38
2.11.	Confocal imaging of MT-RV6-26 scFv cell internalization. ....	39
3.1.	Divergent and convergent dendrimer building approach.....	50
3.2.	Loading of dendrimers at the core, cavity spacing, or peripheral head group.....	52
3.3.	Proposed scheme for dendrimer solvation and back-folding .....	54

3.4.	Second generation dendrimer targets the cytosol.....	55
3.5.	<sup>1</sup> H NMR spectrum of dendrimer following guanidine addition.....	61
4.1.	The mitochondria.....	74
4.2.	Termini amines reaction with 2-cyclohexyl acetaldehyde .....	81
4.3.	<sup>1</sup> H NMR Characterization of G3LL(NH <sub>2</sub> ) <sub>14</sub> -Cyclohexyl <sub>13</sub> .....	82
4.4.	Termini amines reaction with guanidine groups. ....	82
4.5.	Confocal microscopy images of NIH-3T3 fibroblast cells. ....	83
4.6.	The Pearson Correlation Coefficient (PCC) Expression.....	85
4.7.	Confocal Image of G3 Transporter and Pearson's correlation value. ....	85

## LIST OF SCHEMES

Scheme	
2.1.	Synthesis of molecular transporter (MT).....30
3.1.	2 <sup>nd</sup> generation dendron formation.....56
3.2.	3 <sup>rd</sup> generation dendron formation.....58
3.3.	The alkyl spacers were attachment to 3 <sup>rd</sup> generation dendron.....59
3.4.	Guanidine addition to form the dendrimer periphery .....60
4.1.	Alternative synthetic pathway for third generation dendrimer.....79



## LIST OF ABBREVIATIONS

°C	degree Celsius
ATCC	American Type Culture Collection
DCM	dichloromethane
DSL	disulphide linker
DMEM	Dulbecco Modified Eagle Medium
DMF	dimethylformamide
EtOH	ethanol
g	gram
h	hour
M	molar
MeOH	methanol
mg	milligram
mL	milliliter
MT	molecular transporter
MWCO	molecular weight cut off
N	normal
nm	nanometer
NMR	nuclear magnetic resonance
PAMAM	Poly(amido amine)
ppm	parts per million
PSI	pounds per square inch

rt	room temperature
SL	short linker
TEA	triethylamine
TCEP	tris(2-carboxyethyl)phosphine hydrochloride
TFA	trifluoroacetic acid
THF	tetrahydrofuran
$\mu\text{L}$	microliter
$\mu\text{M}$	micromolar
$\mu\text{mol}$	micromole

## CHAPTER I

### Introduction

The pharmacological potential of many drugs, nanocarriers, and biologically relevant content could vastly be improved using targeted intracellular delivery.<sup>1</sup> As the cell is comprised of several targets including the cytoplasm, nucleus, and organelles, such as the mitochondria, endoplasmic reticulum, among others, there are numerous approaches for therapy. Due to the ever-growing potential in treating malignant, virus-related, or genetic dispositions, intracellular transport of biologically active compounds

#### Intracellular Barriers

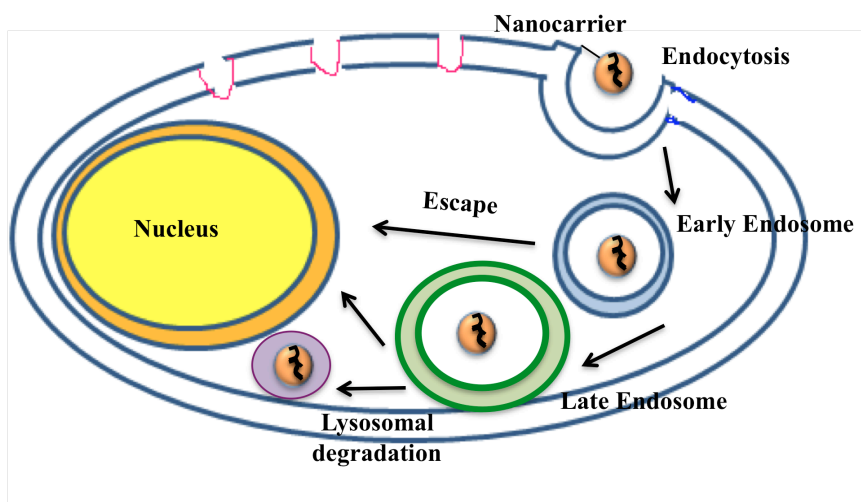


**Figure 1.1.** Following endocytosis nanocarriers must escape the endosome to prevent degradation.

remains at the forefront. Sadly there are many obstacles that prevent successful cellular uptake and drug delivery. The nature of compounds like antibodies, DNA, and many others suffer from inadequate cellular uptake, rendering therapeutic application less than favorable.<sup>2</sup>

Complications arise because even under circumstances where compounds show receptor-mediated absorption, endocytosis can lead to the formation of endosomes and eventually to lysosomes, where active degradation takes place (Figure 1.1).<sup>3</sup> To overcome such limitations, it is vital to develop systems that enable direct passage or provide a mediated route ensuring that biological integrity of the therapeutic is maintained and not degraded. An additional problem that raises concern is that once materials are able to enter cells and be delivered to the cytoplasm, the drug must also locate the specific subcellular target of interest.<sup>4</sup> The list of such targets includes the aforementioned organelles and others where treatment success is expected.<sup>5</sup>

Fortunately, advancements in nanotechnology have generated a number of delivery approaches<sup>6</sup> that have enabled successful cellular delivery and shown promise as targeted systems for therapeutic application.<sup>7</sup> This has fostered a greater understanding of diseases, disorders, and created treatment regimens that perform better. Over the last few decades, a greater emphasis has been placed on designing nanovehicle systems that utilize viral and non-viral strategies as approaches for drug delivery. Viral systems show promise as they demonstrate effective cellular penetration, but this has been marred by their capacity to mutate or illicit undesirable physiological responses.<sup>8</sup> Consequently, this has set the stage for non-viral systems, and while they exhibit a cumulative behavior of inefficient uptake,<sup>9</sup> there has been progress toward creating systems that address some of the challenges facing therapeutic delivery.

Non-viral nanocarriers have emerged as safer, tunable, alternative approaches to enhance uptake, and although these methods include inorganic and organic vectors alike, the use of polymer-based compounds suggests tremendous potential.<sup>4</sup> For *in vivo*

applications, they can be used to protect therapeutics creating tunable pharmacokinetics that allow for controlled absorption, delayed clearance, or reduced metabolism. They also have been shown to improve the solubility of water insoluble compounds.<sup>10, 11</sup>

To ensure success of developing polymer based systems, the carriers must ensure stable delivery of a therapeutic in an efficacious manner and also minimize unwanted biological side effects. In assessing the potential of these motifs for therapeutic delivery, there are immediate strengths, but also inherent drawbacks that have delayed clinical application. A major challenge, mentioned previously, alludes to difficulties with endosomal confinement,<sup>12</sup> and removal of materials.<sup>13, 14</sup> Therefore, it is vital that these limitations be overcome to create more sophisticated vehicles that provide intracellular delivery and sub-cellular targeting to specific organelles.

The list of polymers used to investigate intracellular delivery is extensive and describes approaches using linear systems, nanoparticles, micelles, liposomes, hydrogels, and dendrimer systems as they represent the most promising subclasses of this group of therapeutic transporters. To date, they make up a collection of compounds that have demonstrated the greatest potential to develop targeted delivery of therapeutics into cells and more specifically to cellular compartments. Further, the combinatory approaches using polymers and inorganic vectors has also been probed. Here the inorganic vectors and the potential as combined inorganic polymeric systems are discussed briefly. Polymeric-based delivery systems will also be discussed with a larger focus on the development and application of dendrimers for intracellular and targeted applications.

## **Inorganic Approaches**

The group of inorganic nanoparticles, which consists of gold, iron, silica, aluminum, cadmium and several other inorganic materials, has extensively been used for delivery applications. Their compositions are divided into degradable and non-degradable species with each category possessing characteristics that make them unique for delivery applications. For example, hydrotalcite-like particles are degradable particles and feature the ability to encapsulate drugs, specifically anionic compounds, using electrostatic interaction.<sup>15</sup>

The non-degradable approaches include gold nanoparticles, mesoporous silica particles, and quantum dots. Gold nanoparticles are inert, nontoxic structures that exhibit high stability<sup>16</sup> and undergo a facile preparation.<sup>17</sup> They have been applied to numerous investigations of cellular delivery ranging in size from 0.8 nm to 200 nm and can be modified with thiols.<sup>18-20</sup> Mesoporous silica nanoparticles (MSN) are silica based matrices and can range in functionalities. They are suitable as targeted nanocarriers due to their ability to encapsulate compounds efficiently, their excellent biocompatibility,<sup>21</sup> and ability to create tunable sizes. Quantum dots are cadmium based inorganic semiconductor nanocrystals and are highly fluorescent emitters. They contain a metalloid core and feature tunable physicochemical properties that vary based on metal selection. They are used mainly for imaging and due to their bright, fluorescent properties and resistance to photobleaching, they suggest vast potential for *in vivo* applications.<sup>22</sup>

The inorganic particles comprise a large group of delivery vectors with demonstrated potential for cellular delivery and subcellular targeting. However, these approaches have also been marked by challenges. As the general mode of uptake for

these structures follow endocytosis, this can lead to poor delivery efficiency due to endosomal entrapment. In addition, in some cases these particles raise concern due to water insolubility, toxicity, and aggregation which can severely limit delivery.<sup>23, 24</sup> Therefore there have been several polymeric approaches used to improve the performance of these compounds. As a result, there are many examples highlighting the advantages of inorganic nanoparticles surface functionalized with polymers, which have indicated enhanced biocompatibility and delivery.<sup>11, 25</sup> In discussing advantages that have been presented by polymeric entities it is also prudent to discuss their capacity for independent delivery as well.

### **Polymeric Approaches**

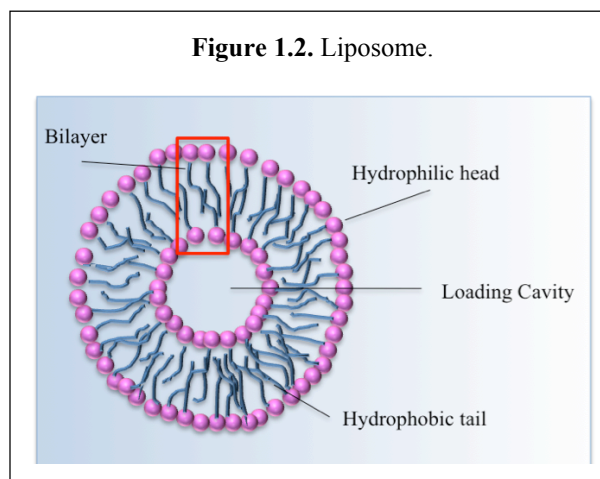
For years, polymers for pharmaceutical applications have used techniques such as adsorption, encapsulation, and compression. These strategies not only have provided cellular entry, but also feature a range of additional benefits that have been exploited to enhance drug dosing efficacy.<sup>26-28</sup> It is due to these macromolecular structures that include nanoparticles, liposomes, micelles, linear polymers, hydrogels, and dendrimers that the performance of drugs and also some inorganic delivery vectors have become more useful candidates for delivery.<sup>29</sup> Such improvements have been used to increase solubility, biocompatibility, “biological stealth,” or non-immunogenic potential, and provide targeted systems, setting the path for more intelligent forms of delivery treatment such as theranostic therapy.<sup>30, 31</sup>

## Polymer Nanoparticles

Nanoparticles are colloidal materials made of polymeric structures and can be divided into two main groups comprising of nanocapsules and nanospheres. Nanocapsules feature reservoirs used for drug encapsulation similar to liposomes while nanospheres conduct drug loading within a matrix. Over the years, they have been studied extensively for drug delivery systems, the majority of which has focused on developing biodegradable formulations. As their mode of delivery, loaded particles are internalized primarily through endocytosis where, depending on the properties and method of release from the particle, cargo is delivered. The surfaces of the particles can also be functionalized for targeting, or receptor mediated entry, the list of which is endless.<sup>32, 33</sup>

## Liposomes

Liposomes are synthetic and naturally occurring lipid-based bilayers that form vesicles. As they range in size dimensions between 50-1000 nm and can vary by the amount of layers, they are classified as multi-lamellar, large uni-lamellar, or small uni-lamellar structures.<sup>34</sup> With their initial inception being over half of a century



ago in the 1960's, they represent nanotechnology's first class of delivery vehicles and have been used to incorporate drugs, peptides, and even proteins.<sup>1, 34, 35</sup> To deliver compounds, a region of aqueous solution is surrounded by the hydrophobic bilayer



membrane, which is used for encapsulation of compounds. Once loaded within the layer, it can be used to protect the therapeutic of interest and mediate cell entry via endocytosis and released.

Liposomes have several features that make them nominal for systems of delivery. They are revered for being biologically inert, and generally biocompatible, exhibiting little to no toxic or antigenic response. However, despite these advantages, there are several limitations that arise using these formulations. During intracellular delivery, liposomes exhibit relatively low efficiency, and following endocytosis can remain confined to the endosomal compartment, thereby limiting uptake and subsequently inhibiting subcellular targeting.<sup>36</sup> In addition to the other limits, liposomes suffer from poor batch-to-batch reproducibility when synthesized, making their application daunting. Further, the required use of organic solvents can limit both application and loading of liposomes with drugs of interest, especially biological compounds such as proteins that function primarily in aqueous solution. Moreover, during *in vivo* application, most liposomes undergo rapid excretion from the body through the reticulo-endothelial system (RES).<sup>36, 37</sup>

Therefore, a proposed remedy to this dilemma has been to modify the carrier using conjugated materials to enhance uptake and overcome the lack of specificity with traditional liposome systems.<sup>38</sup> In order to mitigate these limitations, polymeric compounds have been attached and used to improve cellular uptake,<sup>39</sup> *in vivo* circulation<sup>40, 41</sup> and to reduce EPR effect.<sup>42</sup>

Further efforts to generate systems for intracellular targeting of compounds has prompted the development of a variety of modified systems such as liposomes,

possessing pH-sensitive responsiveness, or specialized ligands for enhanced uptake, selectivity, or immunogenicity. Liposome systems featuring pH response were initially developed to improve drug survival following the acidic degradation conditions during endosomal uptake.<sup>43</sup> As a mode of action, the modification of the liposome enables disruption of the endosome membrane and allows entry into the cellular cytoplasm. In other formulations used to promote delivery of charged compounds like DNA or RNA, cationic liposomes have been synthesized and the positive charge created is used to interact with the negatively charged material, causing an electrostatic interaction for delivery. In addition, the hydrophobic region holds DNA in place to ensure delivery.<sup>34, 44</sup> In another study using cationic liposomes, Boddapati and coworkers were able to create mitochondria-targeted liposomes by conjugating triphenylphosphonium (TPP), a well-known mitochondriotropic molecule, and use it to induce cellular apoptosis.<sup>5</sup> Unfortunately, although many of these strategies used to enhance liposomes have shown promise, limited clinical success<sup>45, 46</sup> indicates a need for more effective intracellular delivery systems.

## **Micelles**

Micelles are colloidal dispersions of aggregated surfactants, or polymers that form particles ranging in size from 5 to 50–100 nm. Unlike liposomes that contain a lipid bilayer and are mainly used to deliver water-soluble drugs, micelles comprise a lipid monolayer and are used mostly to deliver poorly soluble drugs. This property makes them ideal as carriers, as they form a barrier around compounds for delivery. However, current

problems of micelles include a limited capacity for loading of drug and poor stability, and must be overcome to create more effective delivery systems.<sup>47</sup>

### Linear Polymers

Traditional polymers are regarded as linear macromolecules containing covalently linked repeating monomer units and have been used for pharmacological enhancement. Their monomer building blocks can be blended using several approaches specific to application, and depending on the polymer selection, can be used to enhance therapeutic potential through covalent or noncovalent mediated delivery.<sup>33</sup>

Within the list of systems currently investigated that include polyglutamic acid, PEI, dextran, dextrans, chitosans, polylysine, and polyaspartamides, polyethylene glycol (PEG)<sup>48</sup> represents the most notable of this class of linear compounds, constituting the gold standard of polymers. This nonionic, hydrophilic material, containing glycol repeat units, is used widely to enhance water solubility, reduce toxicity, and

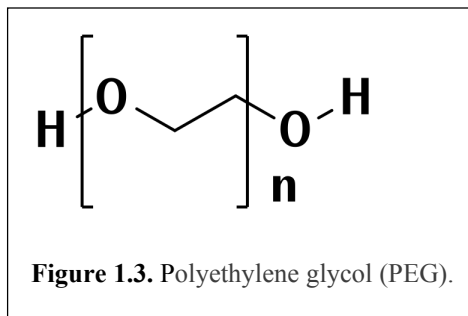
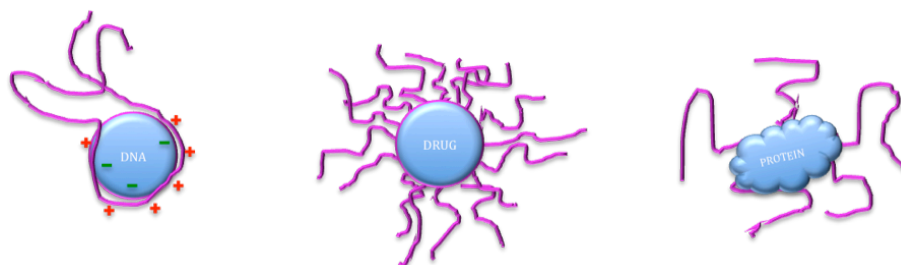


Figure 1.3. Polyethylene glycol (PEG).

provides increased biological circulation. It can be applied to compounds in a number of ways and also been shown in innumerable systems to reduce immunological response *in vivo* application. To date, PEG has been incorporated into numerous drugs for clinical evaluation. In fact, all polymer-based stealth drug-delivery systems have been developed featuring PEG<sup>49</sup> containing compounds and as it currently stands, there have been no other synthetic polymers that present comparable status.

## Linear Polymer Systems



**Figure 1.4.** Linear polymer systems can be used to mediate delivery of DNA, drugs and proteins.

Although PEG enhances the potential usefulness of drug formulations for application, much remains unknown about the intracellular fate of the polymer. Even further, despite reports that indicate PEG's ability to mask compounds, minimizing rapid renal clearance has been difficult to determine.<sup>29,50</sup>

In cases where PEG modification is used for therapeutic delivery, loss in binding affinity has been observed due to steric interference with drug or targeting moiety. Therefore, delivery systems must ensure that PEG does not compete with targeting.<sup>51</sup> PEG represents but one example of linear polymers, but other linear polymers demonstrate comparable limitations. Fortunately, many of these drawbacks can be mitigated by polymer addition or structural rearrangement to generate branched, crosslinked, or combined polymeric approaches.

## Hydrogels

Hydrogels represent an interesting group of polymers that have been applied to an array of biological applications. Their formation is described by a network of crosslinked hydrophilic natural and synthetic (co)polymers combinations and the selection of the crosslinking determines their behavior.<sup>27</sup> When covalently bound they are regarded as

permanent hydrogels and under ionic interactions or molecular entanglements they are regarded as physical gels.<sup>52, 53</sup>

Generally, they do not degrade and can be synthesized to feature responsiveness to different stimuli<sup>54, 55</sup> and undergo phase transitions. Stimuli range from fluctuations in pH, temperature, and solvent effects and can induce physiological change such as swelling. For drug loading, these features are maximized and used to load during formation or post-loaded for delivery applications.<sup>56</sup> When applied to cells nanogels, or

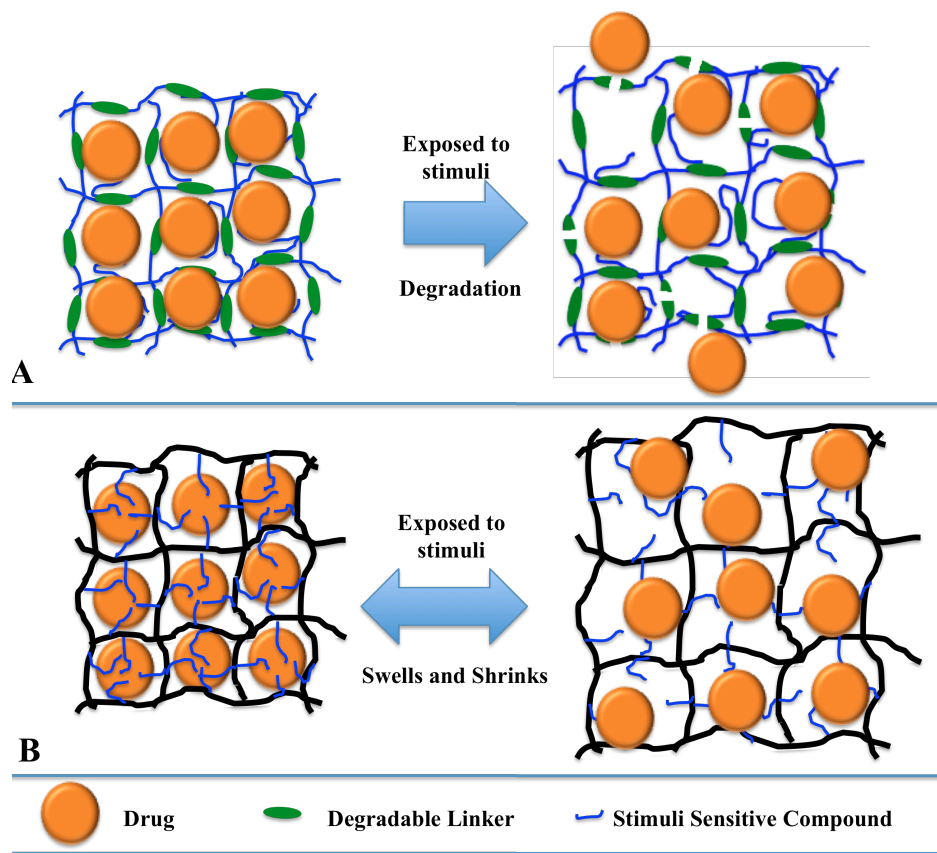


**Figure 1.5.** Hydrogels polymers feature stimuli responsive properties. Under various stimuli such as pH, temperature, in solvent they can degrade release drug or experience shrinking or swelling.

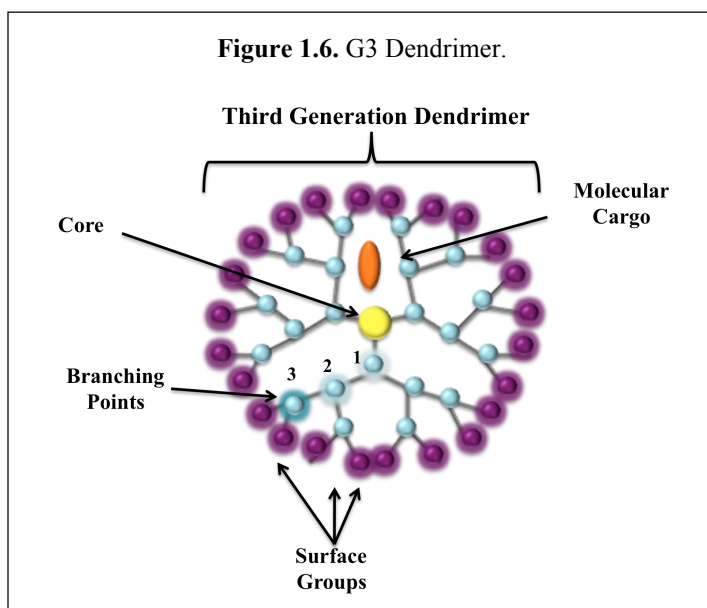
more accurately nano-sized hydrogels, are taken up primarily through endocytosis,<sup>57</sup> although more recent reports of Liu et al. suggest other methods of entry.<sup>58</sup>

To date, although the use of hydrogel systems for intracellular delivery has not been extensively studied,<sup>58-60</sup> hydrogels have shown marked progress in numerous applications of oral delivery systems,<sup>61</sup> optical devices,<sup>62</sup> and as biological implants.<sup>63</sup>

## Dendrimers

Dendrimers are unique highly organized group of polymers and demonstrate vast potential in therapeutic delivery. Unlike traditional polymer systems that feature mass ranges of 1000-800,000 kDa, they can be generated with low polydispersity.<sup>64-66</sup> Originating from the Greek word dendron, meaning tree, these branched macromolecules are comprised of an initiator core, branched repeating units, and a functional periphery.

From the core, denoted as generation zero, a series of iterative growth units form



dendritic generations and eventually terminal end groups. The selection of branched units varies drastically and combined with the terminal groups, contribute to the morphology and rheological properties.<sup>67, 68</sup>

For therapeutic loading,

larger generation structures can be used to encapsulate a compound of interest by

trapping it within cavity spacing<sup>69</sup> or attaching it covalently to the dendritic core<sup>70</sup> or periphery.<sup>28</sup> Encapsulated compounds within the void space offer an ideal advantage where compounds are retained better by steric forces, therefore reducing the chance of aggregation and toxicity. This has been observed especially for dendritic systems that employ metal components for catalysis that tend to aggregate independently.<sup>71, 72</sup> Archut et al. and coworkers explored this host-guest interaction by encapsulation using a photo-activated release system.<sup>73</sup> Similarly, Kojima and coworkers encapsulated poorly soluble drugs using a PEGylated dendrimer.<sup>74</sup>

The branched repeat units can also be tailored as macromolecular filters that selectively introduce compounds.<sup>75</sup> Furthermore, this enables systems that can be tuned with specific release or absorption through the manipulation of the branched repeat units and periphery. Finally, dendrimers can be tailored to transport insoluble cargo.<sup>76, 77</sup> As the solubility of dendrimers is heavily influenced by termini functionality, this can be exploited to form an internal region, more amendable to hydrophobic compounds, and also possess a region that enables transport under hydrophilic conditions.

When covalently linked to cargo, whether via the dendritic core or the terminal head groups, systems can reduce drug toxicity or also be used to create control-released systems. The number of readily available terminal groups is directed by the generation of the dendrimer and can be manipulated to feature uniform or multifunctional end groups. Previously, De Jesus and colleagues<sup>78</sup> were able to exploit this characteristic by attaching doxorubicin to the periphery. This attachment was mediated by a hydrazone linker and was able to minimize *in vitro* toxicity and circulate *in vivo* with minimal accumulation in vital organs when compared to free drug. The reports of Shabat *et al* demonstrate a

degradable dendrimer featuring an antibody core that was used to mediate uptake into cells and provide cellular delivery of the periphery-loaded anti-cancer agents, camptothecin and doxorubicin.<sup>79</sup>

In addition to drug loading, the periphery can also be functionalized to enhance dendritic performance.<sup>80, 81</sup> An example of this behavior is exhibited in the reports of dendrimers synthesized to model certain peptides.<sup>82</sup> Inspired by studies indicating the arginine residues to be significant in cell translocation by peptides (cell penetrating peptides),<sup>83-86</sup> many have sought to create architectures featuring arginine-like residues. This has been accomplished through the inclusion of peripheral guanidine groups.<sup>70, 82, 87</sup>

Exploitation of adjustment of the dendritic periphery has also been extended to organelle specific delivery. In the works of Biswas and coworkers, PAMAM dendrimers were modified with triphenylphosphonium to create mitochondria specific delivery.<sup>88</sup> In more recent efforts, Albertazzi et al. has reported dendrimer-based sensors that measure the pH of specific organelles.<sup>89</sup>

A promising feature of dendritic based delivery systems is evidenced with *in vivo* behavior and suggests potential for creating tunable pharmacokinetics. Depending on the branched system selected, they can be tuned for cellular delivery via an energy dependent<sup>81</sup> or independent manner.<sup>70</sup> For *in vivo* usage, distribution is contingent upon dendritic size. The reports of Kobayashi indicate that size can direct leakage from blood-circulation into other fluids in the body.<sup>90</sup>



## Conclusion

The body of delivery system continues to grow not only in vehicles for application, but also for the innovations to these systems. Such advancements are being developed to endow carriers with more sophisticated designs of cellular uptake and subcellular targeting. The potential in this approach lies not only in the creation of more efficient systems but also in the promise of developing novel therapies. It is because many of these therapies, which include drugs, antibodies, DNA and other compounds, are limited by ineffective penetration and intracellular selectivity, that there is a sincere need for more effective replacements. It stands to reason, that creating vehicles that encourage more efficient regimens of uptake will motivate further treatment strategies.

For applications of delivery, an ideal delivery vehicle would be based on a platform design that encourages intracellular selectivity through facile modification. This approach could then be used to create approaches to target delivery to the nucleus, mitochondria, or other specific intracellular compartments.

Obviously, strategies toward manifesting this approach have not yet been realized, yet efforts continue.<sup>91</sup> A common strategy adopted has been vested in the use of subcellular targeting ligands. In addition, understanding of compounds has also steadily been improving to determine how compounds selectively accumulate.<sup>92, 93</sup> Cooperatively, this may provide insight and lead to better methodologies to address dysfunctional conditions.

## References

1. Torchilin, V. P., Recent approaches to intracellular delivery of drugs and DNA and organelle targeting. *Annual Review of Biomedical Engineering* **2006**, *8*, 343-375.
2. Wolff, J. A.; Budker, V., The Mechanism of Naked DNA Uptake and Expression. *Non-Viral Vectors for Gene Therapy, Second Edition: Part 2* **2005**, *54*, 3-20.
3. Yoshimura, T.; Shono, M.; Imai, K.; Hong, K. L., Kinetic-Analysis of Endocytosis and Intracellular Fate of Liposomes in Single Macrophages. *Journal of Biochemistry* **1995**, *117* (1), 34-41.
4. Omid C. Farokhzad, R. L., Impact of Nanotechnology on Drug Delivery. *Acs Nano* **2009**, *3* (1), 16-20.
5. Boddapati, S. V.; D'Souza, G. G. M.; Erdogan, S.; Torchilin, V. P.; Weissig, V., Organelle-targeted nanocarriers: Specific delivery of liposomal ceramide to mitochondria enhances its cytotoxicity in vitro and in vivo. *Nano Letters* **2008**, *8* (8), 2559-2563.
6. Torchilin, V. P., Tat peptide-mediated intracellular delivery of pharmaceutical nanocarriers. *Advanced Drug Delivery Reviews* **2008**, *60* (4-5), 548-558.
7. Lim, C. S., Organelle-specific targeting in drug delivery and design - Preface. *Advanced Drug Delivery Reviews* **2007**, *59* (8), 697-697.
8. Xu, L.; Anchordoquy, T., Drug Delivery Trends in Clinical Trials and Translational Medicine: Challenges and Opportunities in the Delivery of Nucleic Acid-Based Therapeutics. *Journal of Pharmaceutical Sciences* **2011**, *100* (1), 38-52.
9. Khalil, I. A.; Kogure, K.; Akita, H.; Harashima, H., Uptake pathways and subsequent intracellular trafficking in nonviral gene delivery. *Pharmacological Reviews* **2006**, *58* (1), 32-45.
10. Gillies, E. R.; Frechet, J. M. J., Dendrimers and dendritic polymers in drug delivery. *Drug Discovery Today* **2005**, *10* (1), 35-43.
11. Joralemon, M. J.; Mcrae, S.; Emrick, T., PEGylated polymers for medicine: from conjugation to self-assembled systems. *Chemical Communications* **2010**, *46* (9), 1377-1393.
12. Conner, S. D.; Schmid, S. L., Regulated portals of entry into the cell. *Nature* **2003**, *422* (6927), 37-44.
13. Breunig, M.; Bauer, S.; Goefferich, A., Polymers and nanoparticles: Intelligent tools for intracellular targeting? *European Journal of Pharmaceutics and Biopharmaceutics* **2008**, *68* (1), 112-128.

14. Bulmus, V.; Woodward, M.; Lin, L.; Murthy, N.; Stayton, P.; Hoffman, A., A new pH-responsive and glutathione-reactive, endosomal membrane-disruptive polymeric carrier for intracellular delivery of biomolecular drugs. *Journal of Controlled Release* **2003**, *93* (2), 105-120.
15. Choi, S. J.; Oh, J. M.; Choy, J. H., Biocompatible ceramic nanocarrier for drug delivery with high efficiency. *Journal of the Ceramic Society of Japan* **2009**, *117* (1365), 543-549.
16. Connor, E. E.; Mwamuka, J.; Gole, A.; Murphy, C. J.; Wyatt, M. D., Gold nanoparticles are taken up by human cells but do not cause acute cytotoxicity. *Small* **2005**, *1* (3), 325-327.
17. Huang, T.; Meng, F.; Qi, L. M., Facile Synthesis and One-Dimensional Assembly of Cyclodextrin-Capped Gold Nanoparticles and Their Applications in Catalysis and Surface-Enhanced Raman Scattering. *Journal of Physical Chemistry C* **2009**, *113* (31), 13636-13642.
18. Mishra, B.; Patel, B. B.; Tiwari, S., Colloidal nanocarriers: a review on formulation technology, types and applications toward targeted drug delivery. *Nanomedicine-Nanotechnology Biology and Medicine* **2010**, *6* (1), 9-24.
19. Tkachenko, A. G.; Xie, H.; Liu, Y. L.; Coleman, D.; Ryan, J.; Glomm, W. R.; Shipton, M. K.; Franzen, S.; Feldheim, D. L., Cellular trajectories of peptide-modified gold particle complexes: Comparison of nuclear localization signals and peptide transduction domains. *Bioconjugate Chemistry* **2004**, *15* (3), 482-490.
20. Wuelfing, W. P.; Gross, S. M.; Miles, D. T.; Murray, R. W., Nanometer gold clusters protected by surface-bound monolayers of thiolated poly(ethylene glycol) polymer electrolyte. *Journal of the American Chemical Society* **1998**, *120* (48), 12696-12697.
21. Slowing, I. I.; Trewyn, B. G.; Lin, V. S. Y., Mesoporous silica nanoparticles for intracellular delivery of membrane-impermeable proteins. *Journal of the American Chemical Society* **2007**, *129* (28), 8845-8849.
22. Alivisatos, A. P.; Gu, W. W.; Larabell, C., Quantum dots as cellular probes. *Annual Review of Biomedical Engineering* **2005**, *7*, 55-76.
23. Salmaso, S.; Caliceti, P.; Amendola, V.; Meneghetti, M.; Magnusson, J. P.; Pasparakis, G.; Alexander, C., Cell up-take control of gold nanoparticles functionalized with a thermoresponsive polymer. *Journal of Materials Chemistry* **2009**, *19* (11), 1608-1615.

24. Hardman, R., A toxicologic review of quantum dots: Toxicity depends on physicochemical and environmental factors. *Environmental Health Perspectives* **2006**, *114* (2), 165-172.
25. Vivero-Escoto, J. L.; Slowing, I. I.; Trewyn, B. G.; Lin, V. S. Y., Mesoporous Silica Nanoparticles for Intracellular Controlled Drug Delivery. *Small* **2010**, *6* (18), 1952-1967.
26. Ihre, H. R.; De Jesus, O. L. P.; Szoka, F. C.; Frechet, J. M. J., Polyester dendritic systems for drug delivery applications: Design, synthesis, and characterization. *Bioconjugate Chemistry* **2002**, *13* (3), 443-452.
27. Peppas, N. A.; Bures, P.; Leobandung, W.; Ichikawa, H., Hydrogels in pharmaceutical formulations. *European Journal of Pharmaceutics and Biopharmaceutics* **2000**, *50* (1), 27-46.
28. Lee, C. C.; Gillies, E. R.; Fox, M. E.; Guillaudeu, S. J.; Frechet, J. M. J.; Dy, E. E.; Szoka, F. C., A single dose of doxorubicin-functionalized bow-tie dendrimer cures mice bearing C-26 colon carcinomas. *Proceedings of the National Academy of Sciences of the United States of America* **2006**, *103* (45), 16649-16654.
29. Veronese, F. M.; Pasut, G., PEGylation, successful approach to drug delivery. *Drug Discovery Today* **2005**, *10* (21), 1451-1458.
30. Mahe, B.; Vogt, A.; Liard, C.; Duffy, D.; Abadie, V.; Bonduelle, O.; Boissonnas, A.; Sterry, W.; Verrier, B.; Blume-Peytavi, U.; Combadiere, B., Nanoparticle-Based Targeting of Vaccine Compounds to Skin Antigen-Presenting Cells By Hair Follicles and their Transport in Mice. *Journal of Investigative Dermatology* **2009**, *129* (5), 1156-1164.
31. Andersson, L.; Davies, J.; Duncan, R.; Ferruti, P.; Ford, J.; Kneller, S.; Mendichi, R.; Pasut, G.; Schiavon, O.; Summerford, C.; Tirk, A.; Veronese, F. M.; Vincenzi, V.; Wu, G. F., Poly(ethylene glycol)-poly(ester-carbonate) block copolymers carrying PEG-peptidyl-doxorubicin pendant side chains: Synthesis and evaluation as anticancer conjugates. *Biomacromolecules* **2005**, *6* (2), 914-926.
32. Vauthier, C.; Bouchemal, K., Methods for the Preparation and Manufacture of Polymeric Nanoparticles. *Pharmaceutical Research* **2009**, *26* (5), 1025-1058.
33. Mora-Huertas, C. E.; Fessi, H.; Elaissari, A., Polymer-based nanocapsules for drug delivery. *International Journal of Pharmaceutics* **2010**, *385* (1-2), 113-142.
34. Immordino, M. L.; Dosio, F.; Cattel, L., Stealth liposomes: review of the basic science, rationale, and clinical applications, existing and potential. *International Journal of Nanomedicine* **2006**, *1* (3), 297-315.

35. Bangham, A. D.; Standish, M. M.; Watkins, J. C., Diffusion of Univalent Ions across Lamellae of Swollen Phospholipids. *Journal of Molecular Biology* **1965**, *13* (1), 238-&.
36. Straubinger, R. M.; Hong, K.; Friend, D. S.; Papahadjopoulos, D., Endocytosis of Liposomes and Intracellular Fate of Encapsulated Molecules - Encounter with a Low Ph Compartment after Internalization in Coated Vesicles. *Cell* **1983**, *32* (4), 1069-1079.
37. Torchilin, V. P., Recent advances with liposomes as pharmaceutical carriers. *Nature Reviews Drug Discovery* **2005**, *4* (2), 145-160.
38. Wadia, J. S.; Stan, R. V.; Dowdy, S. F., Transducible TAT-HA fusogenic peptide enhances escape of TAT-fusion proteins after lipid raft macropinocytosis. *Nature Medicine* **2004**, *10* (3), 310-315.
39. Muthu, M. S.; Kulkarni, S. A.; Xiong, J. Q.; Feng, S. S., Vitamin E TPGS coated liposomes enhanced cellular uptake and cytotoxicity of docetaxel in brain cancer cells. *International Journal of Pharmaceutics* **2011**, *421* (2), 332-340.
40. Woodle, M. C., Controlling liposome blood clearance by surface-grafted polymers. *Advanced Drug Delivery Reviews* **1998**, *32* (1-2), 139-152.
41. Torchilin, V. P.; Trubetskoy, V. S., Which Polymers Can Make Nanoparticulate Drug Carriers Long-Circulating. *Advanced Drug Delivery Reviews* **1995**, *16* (2-3), 141-155.
42. Maeda, H.; Sawa, T.; Konno, T., Mechanism of tumor-targeted delivery of macromolecular drugs, including the EPR effect in solid tumor and clinical overview of the prototype polymeric drug SMANCS. *Journal of Controlled Release* **2001**, *74* (1-3), 47-61.
43. Gardikis, K.; Hatziantoniou, S.; Bucos, M.; Fessas, D.; Signorelli, M.; Felekis, T.; Zervou, M.; Screttas, C. G.; Steele, B. R.; Ionov, M.; Micha-Screttas, M.; Klajnert, B.; Bryszewska, M.; Demetzos, C., New Drug Delivery Nanosystem Combining Liposomal and Dendrimeric Technology (Liposomal Locked-In Dendrimers) for Cancer Therapy. *Journal of Pharmaceutical Sciences* **2010**, *99* (8), 3561-3571.
44. Mahato, R. I., Water insoluble and soluble lipids for gene delivery. *Advanced Drug Delivery Reviews* **2005**, *57* (5), 699-712.
45. White, S. C.; Lorigan, P.; Margison, G. P.; Margison, J. M.; Martin, F.; Thatcher, N.; Anderson, H.; Ranson, M., Phase II study of SPI-77 (sterically stabilised liposomal cisplatin) in advanced non-small-cell lung cancer. *British Journal of Cancer* **2006**, *95* (7), 822-828.

46. Seetharamu, N.; Kim, E.; Hochster, H.; Martin, F.; Muggia, F., Phase II Study of Liposomal Cisplatin (SPI-77) in Platinum-sensitive Recurrences of Ovarian Cancer. *Anticancer Research* **2010**, *30* (2), 541-545.
47. Torchilin, V. P., Micellar nanocarriers: Pharmaceutical perspectives. *Pharmaceutical Research* **2007**, *24* (1), 1-16.
48. Pillai, O.; Panchagnula, R., Polymers in drug delivery. *Current Opinion in Chemical Biology* **2001**, *5* (4), 447-451.
49. Gregoriadis, G., Carrier Potential of Liposomes in Biology and Medicine .2. *New England Journal of Medicine* **1976**, *295* (14), 765-770.
50. Parr, M. J.; Masin, D.; Cullis, P. R.; Bally, M. B., Accumulation of liposomal lipid and encapsulated doxorubicin in murine Lewis lung carcinoma: The lack of beneficial effects by coating liposomes with poly(ethylene glycol). *Journal of Pharmacology and Experimental Therapeutics* **1997**, *280* (3), 1319-1327.
51. Fishburn, C. S., The pharmacology of PEGylation: Balancing PD with PK to generate novel therapeutics. *Journal of Pharmaceutical Sciences* **2008**, *97* (10), 4167-4183.
52. Hoffman, A. S., Hydrogels for biomedical applications. *Advanced Drug Delivery Reviews* **2002**, *54* (1), 3-12.
53. Lowman, A. M.; Peppas, N. A., Molecular analysis of interpolymer complexation in graft copolymer networks. *Polymer* **2000**, *41* (1), 73-80.
54. Qiu, Y.; Park, K., Environment-sensitive hydrogels for drug delivery. *Advanced Drug Delivery Reviews* **2001**, *53* (3), 321-339.
55. Qiu, Y.; Park, K., Environment-sensitive hydrogels for drug delivery. *Advanced Drug Delivery Reviews* **2012**, *64*, 49-60.
56. Lemieux, P.; Vinogradov, S. V.; Gebhart, C. L.; Guerin, N.; Paradis, G.; Nguyen, H. K.; Ochiatti, B.; Suzdaltseva, Y. G.; Bartakova, E. V.; Bronich, T. K.; St-Pierre, Y.; Alakhov, V. Y.; Kabanov, A. V., Block and graft copolymers and Nanogel (TM) copolymer networks for DNA delivery into cell. *Journal of Drug Targeting* **2000**, *8* (2), 91-105.
57. Hoffman, A. S., Hydrogels for biomedical applications. *Advanced Drug Delivery Reviews* **2012**, *64*, 18-23.
58. Liu, W. J.; Zhou, X. Y.; Mao, Z. W.; Yu, D. H.; Wang, B.; Gao, C. Y., Uptake of hydrogel particles with different stiffness and its influence on HepG2 cell functions. *Soft Matter* **2012**, *8* (35), 9235-9245.

59. Banquy, X.; Suarez, F.; Argaw, A.; Rabanel, J. M.; Grutter, P.; Bouchard, J. F.; Hildgen, P.; Giasson, S., Effect of mechanical properties of hydrogel nanoparticles on macrophage cell uptake. *Soft Matter* **2009**, *5* (20), 3984-3991.
60. Nie, S. F.; Hsiao, W. L. W.; Pan, W. S.; Yang, Z. J., Thermoreversible Pluronic (R) F127-based hydrogel containing liposomes for the controlled delivery of paclitaxel: in vitro drug release, cell cytotoxicity, and uptake studies. *International Journal of Nanomedicine* **2011**, *6*, 151-166.
61. Knuth, K.; Amiji, M.; Robinson, J. R., Hydrogel Delivery Systems for Vaginal and Oral Applications - Formulation and Biological Considerations. *Advanced Drug Delivery Reviews* **1993**, *11* (1-2), 137-167.
62. Chow, L. M.; Subbaraman, L. N.; Sheardown, H.; Jones, L., Kinetics of in Vitro Lactoferrin Deposition on Silicone Hydrogel and FDA Group II and Group IV Hydrogel Contact Lens Materials. *Journal of Biomaterials Science-Polymer Edition* **2009**, *20* (1), 71-82.
63. Sefc, L.; Pradny, M.; Vacik, J.; Michalek, J.; Povysil, C.; Vitkova, I.; Halaska, M.; Simon, V., Development of hydrogel implants for urinary incontinence treatment. *Biomaterials* **2002**, *23* (17), 3711-3715.
64. Quintana, A.; Raczka, E.; Piehler, L.; Lee, I.; Myc, A.; Majoros, I.; Patri, A. K.; Thomas, T.; Mule, J.; Baker, J. R., Design and function of a dendrimer-based therapeutic nanodevice targeted to tumor cells through the folate receptor. *Pharmaceutical Research* **2002**, *19* (9), 1310-1316.
65. Majoros, I. J.; Myc, A.; Thomas, T.; Mehta, C. B.; Baker, J. R., PAMAM dendrimer-based multifunctional conjugate for cancer therapy: Synthesis, characterization, and functionality. *Biomacromolecules* **2006**, *7* (2), 572-579.
66. Crespo, L.; Sanclimens, G.; Pons, M.; Giralt, E.; Royo, M.; Albericio, F., Peptide and amide bond-containing dendrimers. *Chemical Reviews* **2005**, *105* (5), 1663-1681.
67. Tande, B. M.; Wagner, N. J.; Kim, Y. H., Influence of end groups on dendrimer rheology and conformation. *Macromolecules* **2003**, *36* (12), 4619-4623.
68. Domanski, D. M.; Klajnert, B.; Bryszewska, M., Influence of PAMAM dendrimers on human red blood cells. *Bioelectrochemistry* **2004**, *63* (1-2), 189-191.
69. Jansen, J. F. G. A.; Debrabandervandenberg, E. M. M.; Meijer, E. W., Encapsulation of Guest Molecules into a Dendritic Box. *Science* **1994**, *266* (5188), 1226-1229.

70. Huang, K.; Voss, B.; Kumar, D.; Hamm, H. E.; Harth, E., Dendritic molecular transporters provide control of delivery to intracellular compartments. *Bioconjugate Chemistry* **2007**, *18* (2), 403-409.
71. Niu, Y. H.; Crooks, R. M., Preparation of dendrimer-encapsulated metal nanoparticles using organic solvents. *Chemistry of Materials* **2003**, *15* (18), 3463-3467.
72. Niu, Y. H.; Crooks, R. M., Dendrimer-encapsulated metal nanoparticles and their applications to catalysis. *Comptes Rendus Chimie* **2003**, *6* (8-10), 1049-1059.
73. Archut, A.; Azzellini, G. C.; Balzani, V.; De Cola, L.; Vogtle, F., Toward photoswitchable dendritic hosts. Interaction between azobenzene-functionalized dendrimers and eosin. *Journal of the American Chemical Society* **1998**, *120* (47), 12187-12191.
74. Kojima, C.; Turkbey, B.; Ogawa, M.; Bernardo, M.; Regino, C. A. S.; Bryant, L. H.; Choyke, P. L.; Kono, K.; Kobayashi, H., Dendrimer-based MRI contrast agents: the effects of PEGylation on relaxivity and pharmacokinetics. *Nanomedicine-Nanotechnology Biology and Medicine* **2011**, *7* (6), 1001-1008.
75. Crooks, R. M.; Zhao, M. Q.; Sun, L.; Chechik, V.; Yeung, L. K., Dendrimer-encapsulated metal nanoparticles: Synthesis, characterization, and applications to catalysis. *Accounts of Chemical Research* **2001**, *34* (3), 181-190.
76. SayedSweet, Y.; Hedstrand, D. M.; Spinder, R.; Tomalia, D. A., Hydrophobically modified poly(amidoamine) (PAMAM) dendrimers: Their properties at the air-water interface and use as nanoscopic container molecules. *Journal of Materials Chemistry* **1997**, *7* (7), 1199-1205.
77. Devarakonda, B.; Li, N.; de Villiers, M. M., Effect of polyamidoamine (PAMAM) dendrimers on the in vitro release of water-insoluble nifedipine from aqueous gels. *Aaps Pharmscitech* **2005**, *6* (3).
78. Jevprasesphant, R.; Penny, J.; Jalal, R.; Attwood, D.; McKeown, N. B.; D'Emanuele, A., The influence of surface modification on the cytotoxicity of PAMAM dendrimers. *International Journal of Pharmaceutics* **2003**, *252* (1-2), 263-266.
79. Shabat, D., Self-immolative dendrimers as novel drug delivery platforms. *Journal of Polymer Science Part a-Polymer Chemistry* **2006**, *44* (5), 1569-1578.
80. Devarakonda, B.; Hill, R. A.; de Villiers, M. M., The effect of PAMAM dendrimer generation size and surface functional group on the aqueous solubility of nifedipine. *International Journal of Pharmaceutics* **2004**, *284* (1-2), 133-140.



81. Albertazzi, L.; Serresi, M.; Albanese, A.; Beltram, F., Dendrimer Internalization and Intracellular Trafficking in Living Cells. *Molecular Pharmaceutics* **2010**, *7* (3), 680-688.
82. Chung, H. H.; Harms, G.; Seong, C. M.; Choi, B. H.; Min, C. H.; Taulane, J. P.; Goodman, M., Dendritic oligoguanidines as intracellular translocators. *Biopolymers* **2004**, *76* (1), 83-96.
83. Letoha, T.; Gaal, S.; Somlai, C.; Czajlik, A.; Perczel, A.; Penke, B., Membrane translocation of penetratin and its derivatives in different cell lines. *Journal of Molecular Recognition* **2003**, *16* (5), 272-279.
84. Hollins, A. J.; Benboubetra, M.; Omid, Y.; Zinselmeyer, B. H.; Schatzlein, A. G.; Uchegbu, I. F.; Akhtar, S., Evaluation of generation 2 and 3 poly(propyleneimine) dendrimers for the potential cellular delivery of antisense oligonucleotides targeting the epidermal growth factor receptor. *Pharmaceutical Research* **2004**, *21* (3), 458-466.
85. Fittipaldi, A.; Giacca, M., Transcellular protein transduction using the Tat protein of HIV-1. *Advanced Drug Delivery Reviews* **2005**, *57* (4), 597-608.
86. Esposito, C.; Tian, A. W.; Scrima, M.; Kieres, K.; Campiglia, P.; D'Ursi, A. M.; Baumgart, T., The role of Cell Penetrating Peptides (CPPs) in membrane lipid phase behavior: a novel aspect elucidating peptide-mediated delivery. *Peptides for Youth* **2009**, *611*, 605-606.
87. Amos, R. C.; Nazemi, A.; Bonduelle, C. V.; Gillies, E. R., Tuning polymersome surfaces: functionalization with dendritic groups. *Soft Matter* **2012**, *8* (21), 5947-5958.
88. Biswas, S.; Dodwadkar, N. S.; Piroyan, A.; Torchilin, V. P., Surface conjugation of triphenylphosphonium to target poly(amidoamine) dendrimers to mitochondria. *Biomaterials* **2012**, *33* (18), 4773-4782.
89. Albertazzi, L.; Storti, B.; Marchetti, L.; Beltram, F., Delivery and Subcellular Targeting of Dendrimer-Based Fluorescent pH Sensors in Living Cells. *Journal of the American Chemical Society* **2010**, *132* (51), 18158-18167.
90. Kobayashi, H.; Kawamoto, S.; Jo, S. K.; Bryant, H. L.; Brechbiel, M. W.; Star, R. A., Macromolecular MRI contrast agents with small dendrimers: Pharmacokinetic differences between sizes and cores. *Bioconjugate Chemistry* **2003**, *14* (2), 388-394.
91. D'Souza, G. G. M.; Weissig, V., Subcellular targeting: a new frontier for drug-loaded pharmaceutical nanocarriers and the concept of the magic bullet. *Expert Opinion on Drug Delivery* **2009**, *6* (11), 1135-1148.

92. Horobin, R. W.; Trapp, S.; Weissig, V., Mitochondriotropics: A review of their mode of action, and their applications for drug and DNA delivery to mammalian mitochondria. *Journal of Controlled Release* **2007**, *121* (3), 125-136.
93. Mailman, R. B.; Murthy, V., Ligand functional selectivity advances our understanding of drug mechanisms and drug discovery. *Neuropsychopharmacology* **2010**, *35* (1), 345-346.

## CHAPTER II

### INTRACELLULAR NEUTRALIZATION OF ROTAVIRUS USING MOLECULAR DENDRITIC TRANSPORTER ANTIBODY CONJUGATE

#### Introduction

The immune system produces antibodies to identify and neutralize objects that attack the body. This occurs either through natural infection or following vaccination, and once produced, antibodies can subsequently be used to protect against infection or even reinfection. They can also be harvested and used for therapeutic platforms displaying high specificity and affinity to targets of interest. When compared to other drug formats their success rate has been slightly more promising,<sup>1</sup> however, in some cases, therapeutic success has been variably tolerated from patient to patient. In addition, although antibodies can be introduced under scientific settings, they demonstrate inadequate cellular penetration and exhibit limited ability to combat intracellular targets. Therefore, antibodies are typically ineffective at clearing most established viral infections where the intracellular region serves as the site of viral replication.

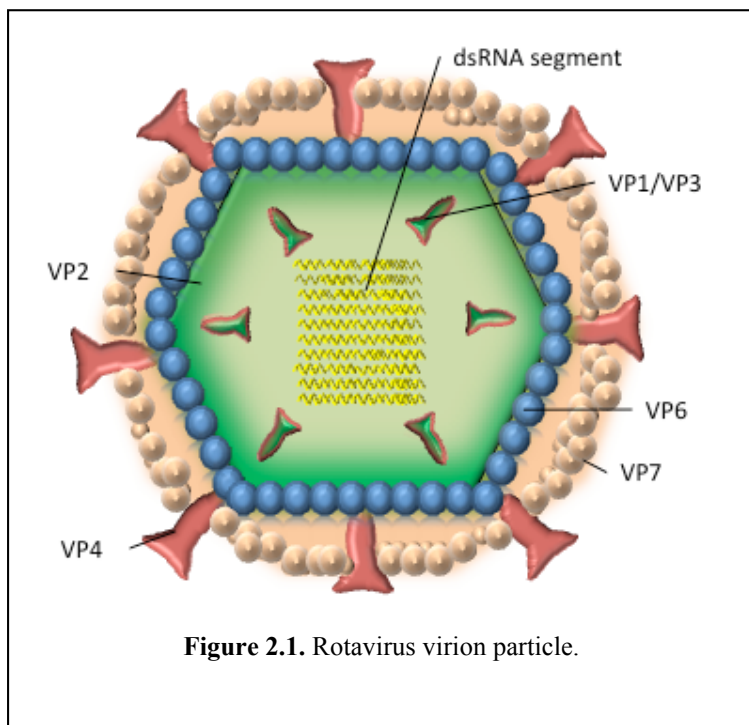
Under natural circumstances, cytolytic T cells are the principal immune effectors that eliminate virus-infected cells. T cell therapies are challenging, however, because a large numbers of cells are required. In addition, because recognition of infected cells is MHC-restricted, the virus first must be consumed by macrophages to produce the necessary peptides to mediate antibody production. Therefore, it would be desirable to develop a treatment capable of cellular penetration following viral onset. In generating

such a system, an ideal approach to treatment would be biocompatible, possess a mode of action that is not genetically restricted, and successfully inhibit viral replication. Recombinant antibodies satisfy several of these qualifications as they are nominal candidates for viral treatment and possess many advantages over conventional antibodies including enhanced efficacy, reduced immunogenicity,<sup>2</sup> and demonstrate an excellent record of safety in humans.<sup>3</sup> They can also be formulated without the need for animals, unlike traditionally harvested antibodies. Finally, the potential application of recombinant antibodies to the treatment of viral conditions could soon be realized for *in vitro* and *in vivo* use should effective strategies for intracellular delivery systems be realized.<sup>4</sup>

Rotavirus is one example marked by limitations to successful treatment that would benefit from treatment within the intracellular milieu. Rotavirus (RV) is a virus that infects infants and young children throughout the world and causes more than 600,000 deaths annually. During onset, the virus infects intestinal cells of the bowels causing severe diarrhea, dehydration, and even death in many Third World nations.<sup>5</sup> As rotavirus constitutes one of the most common etiological agents of diarrhea disorder, a condition ranking second in mortality for children under five, it becomes evident that treatment is vital. Currently, vaccination is available as a liquid or freeze-dried formulation, but cost of transport and storage has prevented availability to impoverished areas. To date, vaccination serves as the primary form of treatment to the virus, however, development of cost effective and safe approaches for Third World nations continues. In a collaborative effort between John Hopkins and Aridis Pharmaceuticals oral strips have been developed<sup>6,7</sup> and may show promise in minimizing the costs of delivery, although

such approaches constitute only a preemptive strategy. As it stands, formal approaches to treat rotaviral onset do not exist and, therefore, represent an unmet need.<sup>8</sup>

Rotavirus is comprised of three capsid layers surrounding a genome of 11



segments of double-stranded RNA (Figure 4.1). The outer layer proteins, viral protein 4 (VP-4) and viral protein 7 (VP7), facilitate viral attachment and entry within cells. Uptake of virus occurs via endocytosis, and during this process the external virion layer sheds exposing

the VP-6 coated double-layered particle for transcription and viral replication.<sup>9</sup> Previous findings indicate the primary antibody response to be directed to viral protein 6 (VP-6),<sup>10</sup> although intracellular treatment using antibodies remains in infancy.<sup>2</sup>

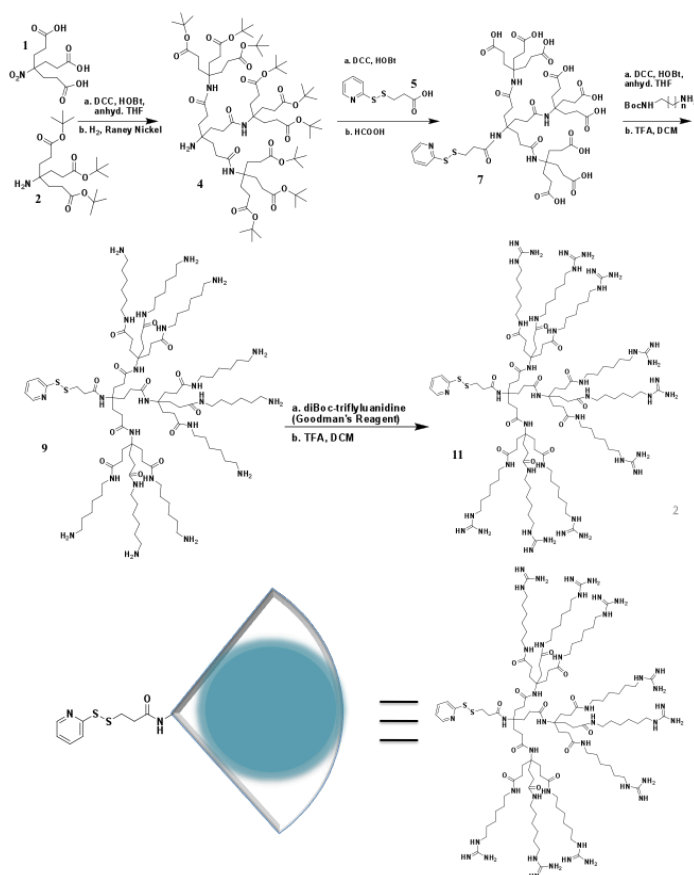
In a previous report, a recombinant antibody was shown to inhibit viral replication by rotavirus using artificial transfection.<sup>11</sup> Although promising as a method of treatment, a desire to create a more viable system of delivery for this antibody motivated a collaborative effort to design a bioconjugate for treatment. Therefore, we became interested in conjugating dendrimers to antibodies<sup>12</sup> for transport and treatment of infected cells.

We have previously demonstrated the dendritic molecular transporter (MT) to deliver siRNAs, peptides, and full monoclonal antibodies into cells.<sup>13-15</sup> Here, we sought to investigate using the transporter to provide delivery of novel recombinant antibodies and treat viral onset.

## DISCUSSION

### **Initial Studies: Conjugation of RV6-26 Fab to MT**

In previous reports, a human monoclonal antibody directed to rotavirus VP-6 protein was isolated and indicated to inhibit transcription. Corroborated by additional reports of the VP-6 role in transcription,<sup>10,16</sup> these findings further suggested a potential strategy for viral neutralization. Subsequent studies were conducted to evaluate the ability of a recombinant Fab antibody (RV6-26) to inhibit rotavirus *in vitro* transcription. During the investigation, successful inhibition of viral protein VP-6 was achieved using artificially transfected antibody suggesting its potential for a mechanism of rotavirus neutralization.<sup>12</sup> However, as previously mentioned, the inability of antibodies to independently inhibit VP-6 prompted effort to design a method for intracellular antibody transport.<sup>11, 12</sup> Therefore, to deliver RV6-26 effectively into cells, our molecular transporter was conjugated to the antibody to enhance cellular penetration. Prior to attachment, the molecular transporter was synthesized separately using a multi-step process. The design of the transporter is inspired by cell-penetrating peptide derivatives such as nona-arginine, and features guanidine head groups attached via a flexible alkyl spacer to a compact dendritic polyamide core.<sup>17</sup> Previously, we demonstrated uptake of the transporter into cells and reported a mechanism independent of active transport



**Scheme 2.1.** Synthesis of the hexyl-spaced dendritic molecular transporter (MT).

similar to previously reported Tat-peptides and other derivatives.<sup>18</sup> Additional findings indicated the effect of alkyl spacing on the performance of our transporter, where it was found that subcellular localization was directed by variations on length of the alkyl spacer between the guanidine head group and the dendritic core.<sup>19</sup> From our observations, the transporter uniquely can be tuned for preferential delivery within cells, and is achieved using an alkyl hexyl spacer for cytosol localization, and by use of an alkyl ethyl linker for localization within the nucleus. Previously described dendritic MTs do not distribute to specific subcellular localizations.<sup>17</sup>

In our approach, we selected the hexyl spaced MT for cytosolic delivery and attached an antibody to the transporter. We synthesized the transporter with slight modifications to the previous synthesis (Scheme 4.1).<sup>14</sup> Briefly, the amine triester (2)

was coupled with nitrotriacid (**1**) to form nitro dendron (**3**). The dendron was next hydrogenated and purified using amended work-up conditions to convert the nitro group at the focal point to yield amine dendron (**4**). The amine dendron (**4**) was reacted at the amine focal point with a pyridinyl dithio-protecting group (**5**) and the tert-butyl ester protecting groups were removed from the dendritic periphery using formic acid to yield (**7**). Next, the *N*-Boc-1,6-diaminohexane linker was added (**8**) and the Boc-protecting groups were removed using trifluoroacetic acid to provide free amines at the periphery (**9**). The end groups were treated with *N,N*-diboc-*N* triflylguanidine (**10**) and deprotected using trifluoroacetic acid to yield molecular transporter (**11**).

The transporter was given a pyridinyl dithio-protecting group to attach to the antibody. It features a disulfide bridge that can be exchanged with the free thiol group of



**Figure 2.2.** SPDP linker was attached to RV6-26 Fab to prepare for conjugation to MT.

another compound and, upon cellular entry, can undergo cleavage during exposure with glutathione or redox enzymes present at high concentrations in the cytoplasm of the cells. We previously used this cleavable pyridinyl disulfide group to conjugate transporter to siRNA and full monoclonal antibodies.<sup>13, 14</sup>



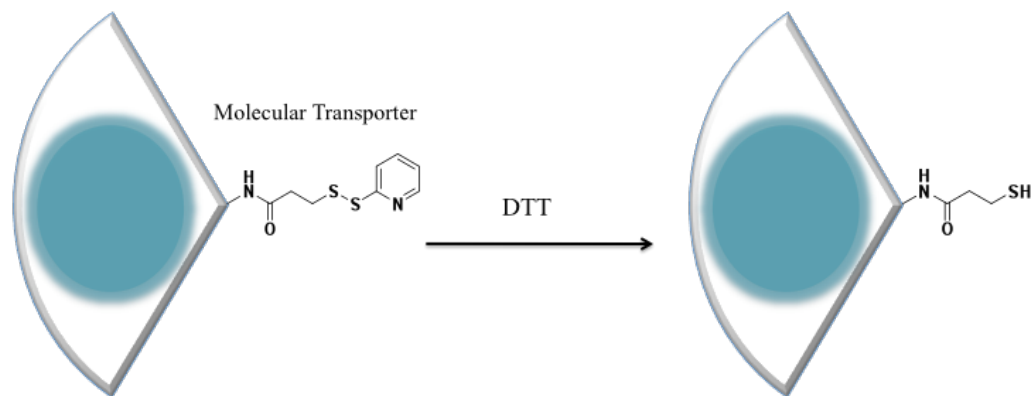


**Figure 2.3.** MT is reacted with dithiothreitol (DTT) to provide free thiol for antibody conjugation.

In preliminary investigations, recombinant Fab antibody could not be attached directly to the molecular transporter, and required prior modification to conjugate using thiol-disulfide exchange. Therefore, a molecular linker featuring a pyridinyl disulfide bridge was conjugated to the RV6-26 fragment antibody before conjugation (Figure 2.2.). Concurrently, the disulfide bridge of the molecular transporter was cleaved using dithiothreitol (DTT) to afford thiol functionality for thiol-disulfide exchange (Figure 2.3). Following modification to both compounds, the two were conjugated via thiol-disulfide exchange (Figure 2.4), purified, and applied to cells in a corresponding titer assay. For uptake experiments, the conjugate was labeled prior to application to cells, yet this approach demonstrated unconvincing results (data not shown). The findings from our investigation prompted further probing based on several concerns.

In our approach, concerns were raised regarding the effects of post modification to the structural integrity of fragment antibody following conjugation with the molecular linker and subsequent transporter addition. Moreover, the assessment of conjugation proved to be a daunting task and yielded ineffective characterization. Therefore, an alternative approach was sought out to overcome these limitations.

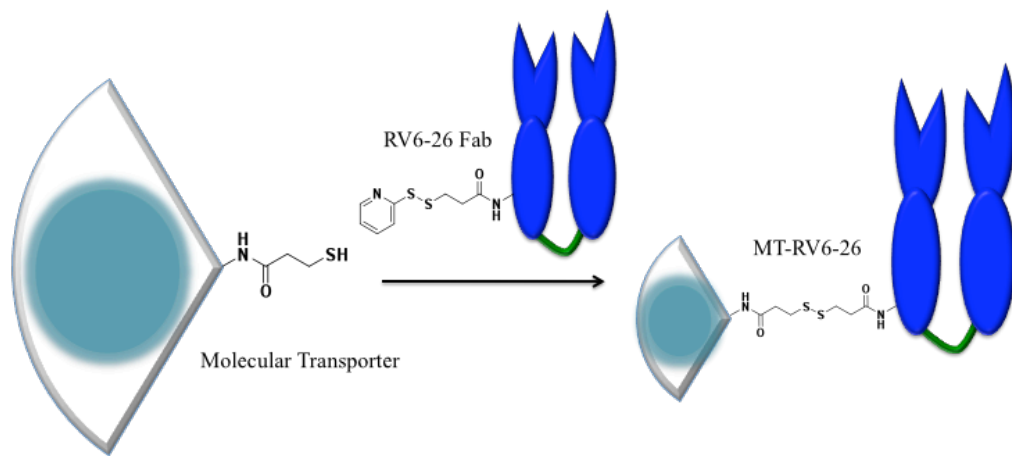


**Figure 2.4.** RV6-26 Fab antibody and MT undergo thiol-disulfide exchange to form MT-RV6-26 conjugate.

### Conjugation Optimization: MT to RV6-26 scFv

A smaller single-chained fragment variant (scFv) recombinant antibody was developed featuring a linked heavy and light chain, a His<sub>10</sub> tag for cellular detection, and an engineered cysteine group with a thiol that could be exchanged with the

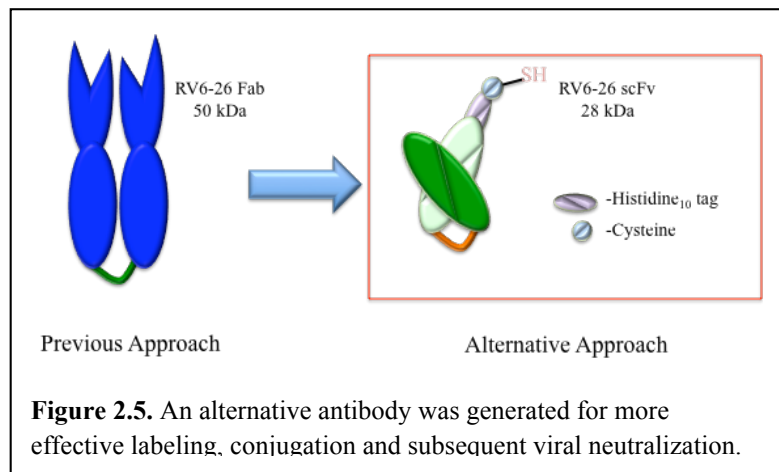


**Figure 2.5.** An alternative antibody was generated for more effective labeling, conjugation and subsequent viral neutralization.

transporter (Figure 2.5). It was also shown to inhibit transcription by the RV double layer particle similarly to the Fab fragment. Following optimization of the antibody, it became our goal to attach the transporter to the scFv antibody. Using this optimized approach, we could now achieve a facile, site-specific thiol-disulfide exchange between the transporter and antibody that could be characterized.

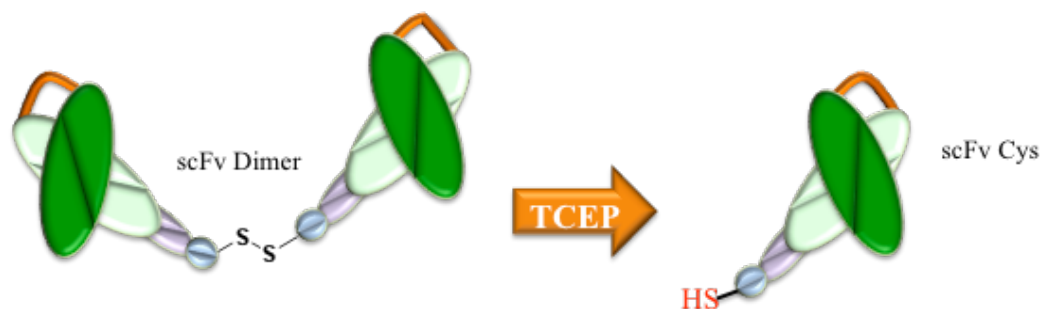


**Figure 2.6.** Dimeric form of the single chained fragment variable antibody was reduced using Tris carboxy ethyl phosphine (TCEP) to provide a free thiol on the cysteine.

Prior to attachment of the transporter, the RV6-26 scFv required reduction of its dimeric form to provide a free thiol for conjugation. A scFv for respiratory syncytial virus RSV (C781) was used as a control and required prior disulfide reduction as well. As an alternative to DTT, both dimers were reduced to the monomeric form using tris(2-carboxyethyl)phosphine (TCEP) to provide a more facile route that could be applied using lower concentrations of reductant. TCEP also ensured reduction of the recombinant antibody without compromised thiol production that occurs when using DTT. During conjugation, a disulfide linker between the scFv and the MT formed a bioconjugate that left the antigen-binding surface of the scFv unmodified, for optimal virus binding. The MT-scFv was prepared by adding the molecular transporter to the reduced single chain antibody (Figure 2.7.). After purification of the scFv and MT, the two were conjugated, purified by ultrafiltration (and labeled in some cases with a nickel–nitrilotriacetate fluorescent probe (Ni-NTA-Atto 647; Sigma, St. Louis, MO) for imaging purposes), and then stored at 4 °C until use.

Because the exchange between the transporter and recombinant scFv antibody required one-to-one exchange, it became vital to ensure that maximized conjugation was achieved. Therefore, preliminary reactive conditions were conducted with an excess of

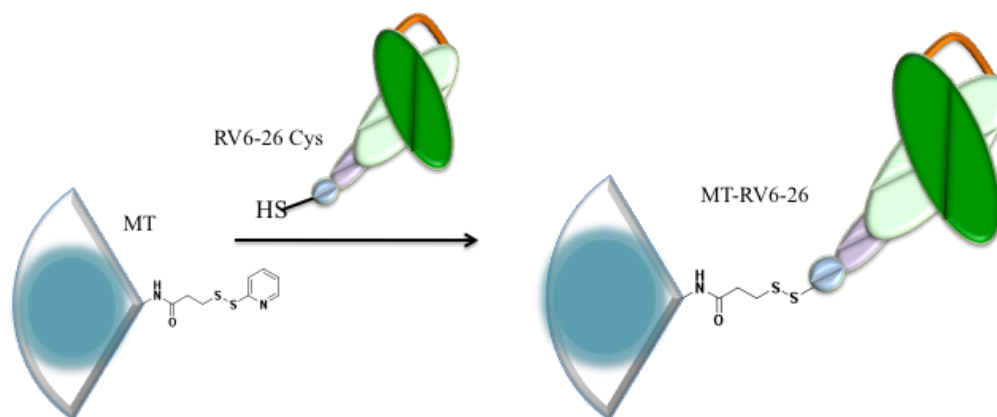


**Figure 2.7.** Attachment of MT to RV6-26 scFv Cys to form MT-RV6-26 conjugate.

the transporter. However, these conditions were found to produce less than favorable yields as substantial amounts of dimer was found with limited conjugation. These results suggested that either reduction conditions were ineffective at reduction of the antibody, or that prior to transporter attachment, the recombinant antibody began to form the dimer during TCEP removal. Consequently, an assay was conducted to determine if adequate concentrations of reductant were used for antibody reduction. In addition, several additional conjugations were performed to determine the most optimized concentration of transporter needed. To enhance attachment further and eliminate the chance of dimer formation following reduction, the molecular transporter was added before and after removal of reductant (Table 2.1). Successful conjugation was confirmed by shifting of the apparent molecular weight of the monomer on protein gels, as detected by electrophoresis under non-reducing conditions. Under reducing conditions, the RV6-26 scFv is 28 kDa and the dimeric form occurs at 52 kDa. Through modification, there was a significant reduction to the dimeric bond. Following attachment to the transporter, the bioconjugate forms a structure with an approximate molecular weight of ~31 kDa, as

indicated. As an additional improvement to the synthetic approach, the concentration of the desired concentration was also increased (Figure 2.8.).

**Table 2.1.** Various conditions were used to achieve optimized MT-RV6-26 conjugation.

<b>RV6-26 ScFv -Transporter Conjugation Conditions</b>				
	<b>Trial 1</b>	<b>Trial 2</b>	<b>Trial 3</b>	<b>Optimized Protocol</b>
<b>RV6-26 Starting concentration</b>	3.04 $\mu\text{M}$	4.87 $\mu\text{M}$	4.87 $\mu\text{M}$	<b>105.43 <math>\mu\text{M}</math></b>
<b>TCEP Equivalent to RV6-26</b>	2000 mol eq.	2 mole eq.	100 mole eq.	<b>10 mole eq.</b>
<b>Transporter Equivalent to RV6-26</b>	5,000 mole eq.	6 mole eq.	6 mole eq. before TCEP removal followed by 10 mol eq. after TCEP removal	<b>2 mole eq.; 10 mole eq</b>
<b>MT-RV6-26 Volume</b>	2.50 mL	2.5 mL	1.5 mL	<b>1.25 mL</b>
<b>RV6-26-MT Conjugate MT-RV6-26 Concentration</b>	3.71 $\mu\text{M}$	5.84 $\mu\text{M}$	2.26 $\mu\text{M}$	<b>101.34 <math>\mu\text{M}</math></b>

The MT-conjugated antibody was first tested for cellular internalization to determine if the conjugation improved uptake performance. Therefore, conjugated MT-RV6-26 and unconjugated RV6-26 were applied to MA104 kidney cell monolayers.

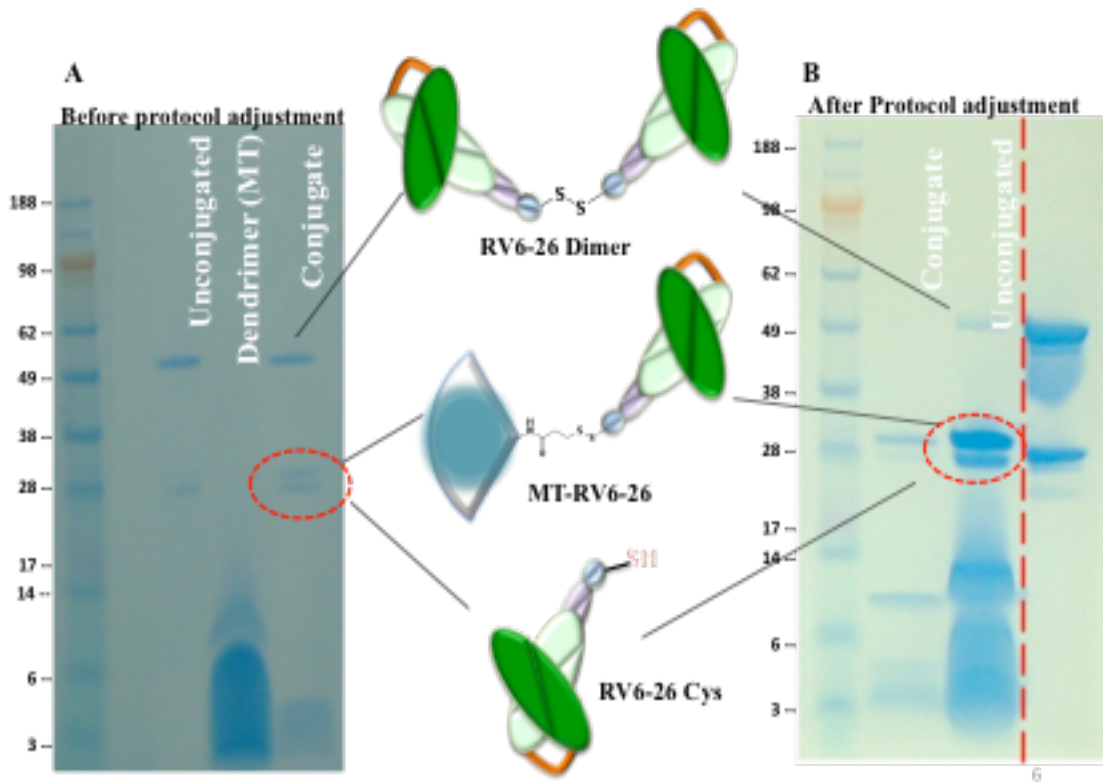


**Figure 2.8.** Gel Electrophoresis of MT-RV6-26 before and after protocol improvement. (performed by Gopal Sannarapu)

The His<sub>10</sub> tags of the RV6-26 were then stained, evaluated for fluorescence, and quantified. As indicated by figure 2.9, the addition of transporter to the antibody enabled more effective cellular penetration than the RV6-26 antibody alone (Figure 2.9). Following this, an ELISA assay was conducted to determine if conjugation to the molecular transporter inhibited the binding of RV6-26. This was evaluated using RV double-layered particles (DLPs) and it was shown that the MT-RV6-26 conjugate produced comparable binding, and confirmed that the binding capacity of scFv was not inhibited following modification with our transporter (Figure 2.10).

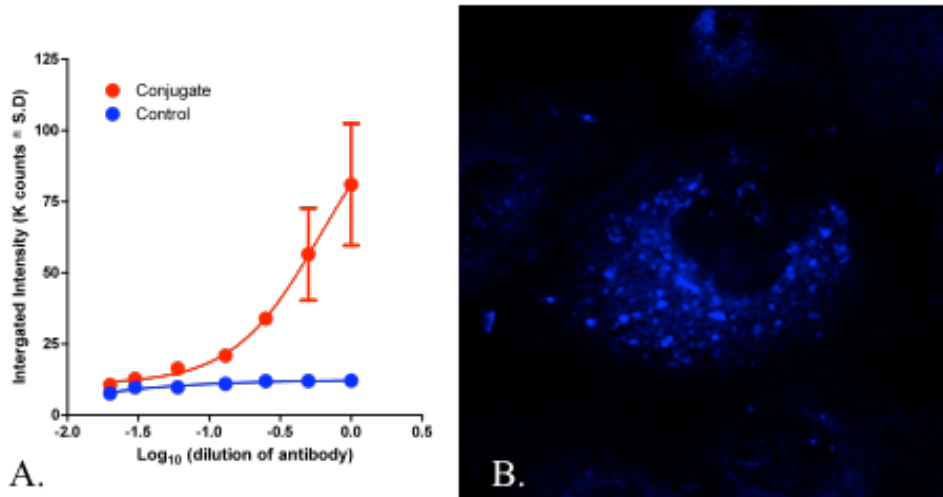


**Figure 2.9.** Internalization of MT-RV6-26 conjugate was evaluated against RV6-26 using MA104 kidney cells. Following application, the cells were stained with anti-histidine stain, imaged, and quantified. **A** depicts the quantified fluorescence **B** indicates MT-RV6-26 application. (performed by Gopal Sapparapu)

Following confirmation of the ability of the transporter to transfect cells and bind successfully to double layer particles, viral neutralization was tested to determine if use of the transporter enabled binding of the antibody to an intracellular virion following viral onset. MA104 cells were treated with RV6-26, MT-RV6-26 or control C781 or MT-

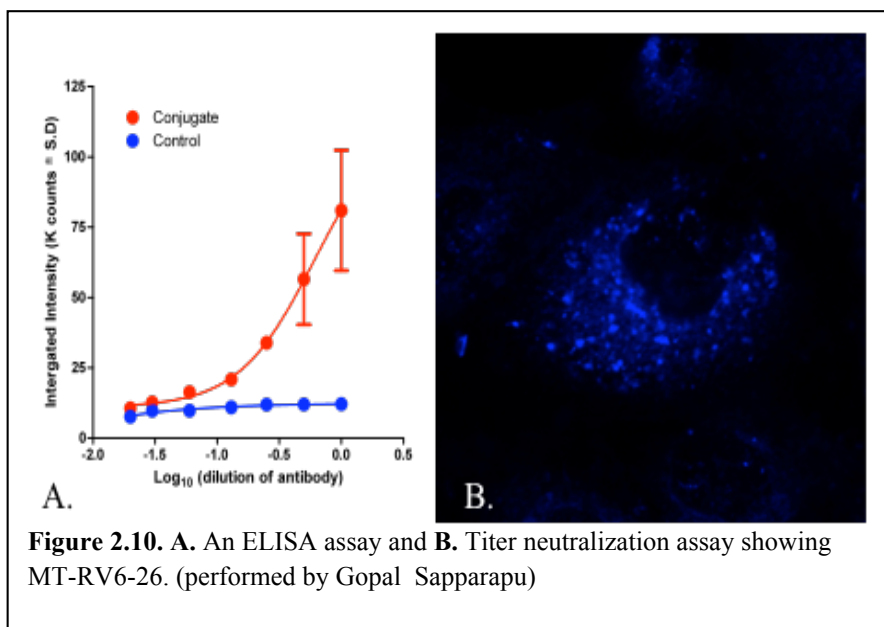


**Figure 2.10.** **A.** An ELISA assay and **B.** Titer neutralization assay showing MT-RV6-26. (performed by Gopal Sapparapu)

C781 antibodies, and subsequently cells were inoculated with the RRV strain. Viral replication was compared between treated and untreated cells

and it was found that MT-RV6-26 conjugate inhibited virus replication significantly, with more than 50% reduction following treatment. Additionally, treatment of viral cells with scFv C781 or MT-C781 was ineffective at inhibition to viral replication, suggesting that delivery of RV6-26 by transporter treated RV without any contributions of MT binding.

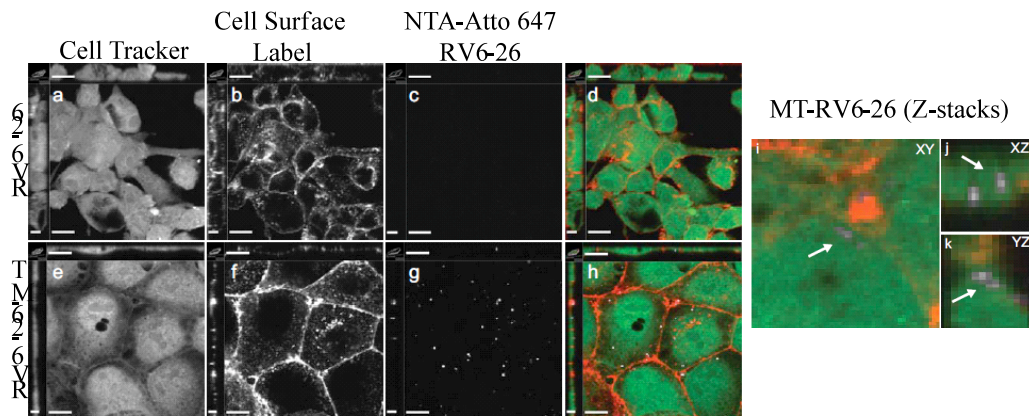


**Figure. 2.11.** Application of MT-RV6-26 to MA104 cells for internalization. (performed by Fyza Shaikh)

Imaging of cells was performed to confirm uptake of RV6-26 antibody by transporter into the cytoplasm (Figure 2.11). As previous reports indicate, the hexyl-spaced transporter promotes cellular penetration within the cytoplasm, and we were interested to see if this system of delivery enabled delivery of recombinant antibody into the cytoplasm as well. The location of the His<sub>10</sub> labeled scFv molecules was investigated using laser scanning confocal microscopy. The cytoplasm of cells was marked with a Cell Tracker dye, the plasma membranes were marked with a fluorescent wheat germ agglutinin (WGA), and scFv was detected using Ni-NTA-Atto 647. Confirmation of MT-RV6-26 scFv within cells was confirmed using reconstruction of XY, YZ, and XZ planes and determined to be found within cells. There was no indication of Ni-NTA-Atto 647 reagent or unmodified scFv detected, confirming that the transporter is required to



facilitate cell uptake. From our investigation, it can be concluded that successful neutralization of rotavirus-infected cells was achieved using MT-RV6-26.

### Conclusion

The application of recombinant antibody and dendritic transporter sheds light on the potential treatment of other conditions in a number of ways. First, it indicates the potential for treating other viral conditions via intracellular targeting. This is an important attribute, as many conditions possess preventive barriers that inhibit neutralization within the extracellular environment. Secondly, the use of recombinant antibody further illustrates the growing potential for the use of these compounds as an approach to viral treatment. Finally, it highlights the capacity of using a dendritic transporter for application of these novel therapies where independent cellular penetration is ineffective.

### EXPERIMENTAL

**Materials.** All reagents were purchased either from Alfa Aesar, Chem-Impex Int. (Wood Dale, IL), EMD Millipore, Fisher Scientific, Life Technologies (Eugene, OR), or Sigma-Aldrich (St. Louis, MO), and used without further purification unless noted. Analytical TLC was performed on commercial Merck plates coated with silica gel 60 F<sub>254</sub>. Amicon Ultra centrifugal filter devices (10 kDa MWCO) were obtained from Millipore Co. (Billerica, MA).

**Instrumentation.** Nuclear magnetic resonance (NMR) spectra were collected on a Bruker DPX-300 and a Bruker AV-400 Spectrometer. Chemical shifts were reported in parts per million and referenced to the corresponding residual nuclei in deuterated solvents. Hydrogenation was conducted using a Parr 3911 hydrogenation apparatus. Samples were centrifuged at 5,000 rpm on an Eppendorf centrifuge 5430. Column chromatography was conducted using Isolera biotage, and Confocal fluorescence microscopy experiments were performed using an LSM 510 laser scanning confocal microscope (Carl Zeiss, Thornwood, NY).

#### **Preparation of the Molecular Transporter.**

Molecular dendritic transporter was synthesized similarly to previously reported procedures<sup>14</sup> with amendments to reactive conditions and purifications steps.

**Synthesis of 4-(2-carboxyethyl)-4-nitroheptanedioic acid. 1.** To a round bottom flask, a solution of nitrotriester and formic acid (20 mL) was stirred overnight at room temperature. After the solvent was removed under reduced pressure, toluene was added and concentrated *in vacuo* to remove any residual formic acid to yield a white solid. <sup>1</sup>H NMR (400 MHz, MeOD):  $\delta$  = 2.29 (s, CH<sub>2</sub>, 12H). <sup>13</sup>C NMR (400 MHz CDCl<sub>3</sub>):  $\delta$  = 29.39, 31.40, 93.85, 175.65.

**Synthesis of di-tert-butyl 4-amino-4-(3-tert-butoxy-3-oxopropyl)heptanedioate, “Behera’s Amine<sup>20</sup>” 2.** A solution of nitrotriester (8.00 g, 17.9 mmol) in ethanol/

dichloromethane (13:1, 140 mL) in a Parr hydrogenation bottle with (4.00 g, 68.15 mmol) Raney-nickel was shaken at 60 psi for 48 h at room temperature. The suspension was gravity filtered, and solvent was removed, suspended in dichloromethane (100 mL). Materials were then washed with water (100 mL), dried over anhydrous MgSO<sub>4</sub>, and evaporated under reduced pressure to yield the white aminotriester. (7.27 g, 97%) <sup>1</sup>H NMR (400 MHz, CDCl<sub>3</sub>): δ = 1.17 (s, NH<sub>2</sub>, 2H), 1.44 (s, CH<sub>3</sub>, 27H), 1.95 (t, CH<sub>2</sub>, 6H), 2.43 (t, CH<sub>2</sub>, 6H). <sup>13</sup>C NMR (400 MHz CDCl<sub>3</sub>): δ = 27.98, 29.46, 31.47, 56.99, 80.96, 172.30.

**Synthesis of 9 Cascade: nitromethane [3]: (2-aza-3-oxopenylydyne): propionioate (Dendron G1). 3.** To a sealed three neck round bottom flask, a solution of nitrotriacid, **1**, (1.35 g, 4.87 mmol) in dried THF (50 mL), 1-hydrobenzotriazole (HOBt) (2.37 g, 17.49 mmol), and DCC (3.61 g, 17.49 mmol), were added sequentially and stirred under Argon. Following 2.5 h, Behera's amine (7.27 g, 17.49 mmol), **2**, was added to the solution and the reaction proceeded at room temperature for 40 h, after which it was filtered, and concentrated under reduced pressure. The crude product was purified using column chromatography, eluting with hexane/ethyl acetate (3:2) to afford the desired Dendron G1 (6.89 g, 96%). <sup>1</sup>H NMR (400 MHz, CDCl<sub>3</sub>): δ = 1.44 (m, CH<sub>3</sub>, 81H), 1.95 (m, CH<sub>2</sub>, 18H), 2.21 (m, CH<sub>2</sub>, 30H), 6.92 (s, NH, 3H). <sup>13</sup>C NMR (400 MHz, CDCl<sub>3</sub>): δ = 28.04, 29.74, 29.85, 31.28, 57.56, 80.69, 92.47, 170.46, 172.76.

**Amine G1 (Hydrogenation of Dendron G1).** 4. A solution of amine G1, **3**, (6.00 g, 4.08 mmol) in ethanol/ dichloromethane (13:1, 140 mL) in a Parr hydrogenation bottle with Raney-nickel (4.00 g, 68.15 mmol) was shaken at 70 psi for 4 days at room temperature. The suspension was gravity filtered, the solvent was removed, and the residue was suspended in dichloromethane (100 mL). The materials were then washed with water (100 mL), dried over anhydrous MgSO<sub>4</sub> and evaporated under reduced pressure to yield a white solid (5.65 g, 96%). <sup>1</sup>H NMR (400 MHz MeOD) δ = 1.45 (s, CH<sub>3</sub>, 81H), 1.61 (m, CH<sub>2</sub>, 6H), 1.94 (m, CH<sub>2</sub>, 18H), 2.19 (m, CH<sub>2</sub>, 24H), 6.92 (s, NH, 3H), 7.39 (s, NH<sub>2</sub>, 2H). <sup>13</sup>C NMR (400 MHz MeOD) δ = 28.5, 30.5, 30.7, 32.0, 36.0, 58.7, 81.7, 174.4, 175.7.

**Synthesis of 3-(pyridin-2-yl)disulfanylpropanoic acid (Disulfide Linker).** 5. To a round bottom flask, a stirred solution of aldrithiol (10.00g, 45.39 mmol) and 3-mercaptopropionic acid (2.6 mL, 24.4 mmol) in 50 mL of MeOH was allowed to stir overnight at room temperature. The solution was concentrated under reduced pressure and purified using column chromatography, eluting with hexane/ ethyl acetate (1:1) to afford the white solid (2.01 g, 31%). <sup>1</sup>H NMR (400 MHz, MeOD): δ = 2.71 (t, CH<sub>2</sub>, 2H), 3.03 (t, CH<sub>2</sub>, 2H), 7.22 (d, Ar-H, 1H), 7.81 (m, Ar-H, 2H), 8.39 (d, Ar-H, 1H). <sup>13</sup>C NMR (400 MHz, MeOD): δ = 32.9, 33.3, 119.7, 120.9, 137.7, 148.9, 159.8, 173.5.

**SSG1, (PDPOH attachment to amine G1).** 6. To a three neck round bottom flask, a solution of 3-(2-pyridinyldithio)propanoic acid (0.93 g, 4.31 mmol) in dried THF ( 50 mL), 1-hydrobenzotriazole (HOBt) (0.58 g, 4.31 mmol), and DCC (0.89 g, 4.31 mmol)

were added. After 2.5 h, amine G1 (5.65 g, 3.92 mmol) **4**, was added and the solution stirred at room temperature under argon for 40 h. Materials were filtered and concentrated under reduced pressure. The crude product was purified using column chromatography, eluting with 1% methanol in dichloromethane and gradually increasing to 10% in methanol to yield white SS-G1 (5.12 g, 80%).  $^1\text{H}$  NMR (400 MHz, MeOD)  $\delta$  = 1.44 (m,  $\text{CH}_3$ , 81H), 2.91-1.92 (m,  $\text{CH}_2$ , 48H), 2.64 (t, CH,  $J=6.9\text{Hz}$ , 2H), 3.08 (t,  $\text{CH}_2$ ,  $J=7.0\text{Hz}$ , 2H), 7.24 (ddd, ArH,  $J=1.5\text{Hz}$ ,  $J=4.9\text{Hz}$ ,  $J=6.7\text{Hz}$ , 1H), 7.33 (s, NH, 4H), 7.61 (s, ArH, 1H), 7.83 (td, ArH,  $J=4.9\text{Hz}$ ,  $J=8.2\text{Hz}$ , 1H), 8.42 (d, ArH, 1H).  $^{13}\text{C}$  NMR (400 MHz, MeOD)  $\delta$  = 28.5, 30.5, 30.7, 32.1, 32.3, 35.6, 36.8, 58.8, 59.2, 81.7, 121.3, 122.5, 139.2, 150.5, 161.2, 172.9, 174.4, 175.4.

**SSG1OH, (Deprotection of SSG1).** **7.** SSG1 (4.59 g, 2.81 mmol) was dissolved in formic acid (100 mL) and the reaction stirred at room temperature overnight. Upon completion, the formic acid was azeotropically distilled with toluene under reduced pressure to yield the product SSG1OH (3.83 g, 100%).  $^1\text{H}$  NMR (400 MHz MeOD)  $\delta$  = 1.89-2.32 (m,  $\text{CH}_2$ , 48H), 2.64 (t,  $J=7.0\text{Hz}$ ,  $\text{CH}_2$ , 2H), 3.08 (t,  $J=7.0\text{Hz}$ , 2H), 7.22 (m, ArH, 1H), 7.33 (m, NH, 4H), 7.53 (td,  $J=7.4\text{Hz}$ , ArH, 1H), 7.84 (m, ArH, 1H), 8.07 (s, COOH, 9H), 8.41 (d,  $J=4.4\text{Hz}$ , ArH, 1H).  $^{13}\text{C}$  NMR (400 MHz MeOD)  $\delta$  = 29.3, 30.5, 32.0, 35.6, 36.9, 58.7, 59.2, 121.5, 122.5, 139.4, 150.4, 164.5, 175.5, 175.6, 177.1.

**SSGGLL, (*N*-Boc-1,6-diaminohexane attachment to SSG1 and deprotection of peripheral Boc groups).** **8.** SSG1OH, (2.00 g, 1.77 mmol) in dry THF (150 mL) was

stirred under argon at 4 °C with HOBt (2.58 g, 19.1 mmol) and DCC (3.94 g, 19.1 mmol). Following 2.5 h, *N*-Boc-1,6-diaminohexane (4.13 g, 19.1 mmol) was dissolved in 10% methanol in dry dichloromethane and added to the solution and the reaction allowed to proceed for 72 h. Upon completion, materials were filtered, removing the DCC salt, and the filtrate was concentrated into silica to be purified via flash chromatography, eluting with 1% methanol in dichloromethane and gradually increasing to 10% methanol in dichloromethane to yield a brown solid. As an added purification step, the product was filtered through Siliaprep Carbonate filter cartridges. (1.40 g, 28%) <sup>1</sup>H NMR (400 MHz, MeOD) δ = 1.33 (s, CH<sub>2</sub>, 36H), 1.46 (m, CH<sub>2</sub>, CH<sub>3</sub>, 117H), 1.98-2.17 (m, CH<sub>2</sub>, 48H), 2.67 (s, CH<sub>2</sub>, 2H), 3.02 (t, J=6.9Hz, CH<sub>2</sub>, 18H), 3.08(s, CH<sub>2</sub>, 2H), 3.15 (t, J=6.6Hz, CH<sub>2</sub>, 18H), 6.55 (s, NH, 4H), 7.23 (dd, J=4.6Hz, J=8.0Hz, ArH, 1H), 7.52 (d, J=17.8Hz, ArH, 1H), 7.81 (m, NH, 18H), 7.98 (d, J=4.8Hz, ArH, 1H), 8.43 (m, ArH, 1H). <sup>13</sup>C NMR (400 MHz, MeOD): δ = 27.5, 27.7, 28.9, 30.3, 30.9, 31.3, 31.7, 31.8, 31.9, 35.6, 36.9, 40.4, 41.2, 59.0, 59.4, 79.6, 121.1, 122.4, 139.1, 150.5, 158.3, 161.0, 172.8, 174.8, 175.4. The resulting solid was dissolved in dichloromethane (5 mL), and a cooled solution of diluted (1:1) trifluoroacetic acid in dichloromethane was added to the reaction and allowed to stir for 24 h. Upon completion, solvent was removed under pressure, and the residue was washed with dichloromethane, dried and then suspended in methanol and filtered through Siliaprep Carbonate cartridges to yield a brown solid (1.12 g, 100%). <sup>1</sup>H (400 MHz, MeOD) δ = 1.42 (s, CH<sub>2</sub>, 36H), 1.60 (s, CH<sub>2</sub>, 36H), 2.05-2.41 (m, CH<sub>2</sub>, 48H), 2.83 (s, CH<sub>2</sub>, 2H), 2.96 (t, J=6.7Hz, CH<sub>2</sub>, 18H), 3.27 (s, CH<sub>2</sub>, 18H), 3.35 (d, J=1.8Hz, CH<sub>2</sub>, 2H), 7.92 (m, NH, ArH) 8.11 (s, NH<sub>2</sub>, 18H), 8.42 (d, J=5.9Hz, ArH, 1H), 8.58 (m, ArH, 1H), 8.89 (s, ArH, 1H), 9.15 (m, NH, 9H). <sup>13</sup>C NMR (400 MHz, MeOD) δ = 27.0, 27.3, 28.3,

29.6, 30.6, 31.8, 32.0, 40.7, 41.2, 59.3, 59.7, 125.5, 126.9, 144.2, 147.4, 157.7, 175.3, 176.1, 176.8.

**Attachment of Goodman's reagent to SSG1LL. 10.** To a cooled solution of SSG1LL (295.0 mg, 0.146 mmol) in methanol (12 mL) was added triethylamine (TEA) (0.315 mL, 2.28 mmol) followed by addition of *N,N'*-diboc-*N''*-trifylguanidine (793.0 mg, 1.98 mmol); the reaction stirred for 48 h at room temperature. Following removal of solvent under reduced pressure, the crude materials were purified via flash chromatography, eluting with 1% methanol in dichloromethane and gradually increasing to 10% methanol in dichloromethane to yield a brown solid (230.0 mg, 43%). <sup>1</sup>H NMR (400 MHz, MeOD)  $\delta$  = 1.38 (s, CH<sub>2</sub>, 54H), 1.50 (d, J=21.2Hz, CH<sub>3</sub>, 162H), 1.59 (t, J=10.9Hz, CH<sub>2</sub>, 18H), 1.98-2.17 (m, J=74.5Hz, CH<sub>2</sub>, 48H), 2.67 (d, J=5.5Hz, CH<sub>2</sub>, 2H), 3.08 (dd, J=9.1Hz, J=15.5, CH<sub>2</sub>, 2H), 3.16 (d, J=4.6Hz, CH<sub>2</sub>, 18H), 3.35 (t, J=7.0Hz, CH<sub>2</sub>, 18H), 7.23 (dd, J=4.8Hz, J=8.0Hz, ArH, 1H), 7.49 (d, J=14.9Hz, NH, ArH, 5H), 7.80 (d, J=13.0Hz, ArH, 1H), 7.97 (s, NH, 27H), 8.44 (m, ArH, 1H). <sup>13</sup>C NMR (400 MHz, MeOD)  $\delta$  = 27.7, 28.4, 28.4, 28.7, 30.1, 30.4, 31.4, 31.7, 31.9, 32.0, 40.5, 40.7, 41.8, 59.2, 80.3, 84.4, 121.2, 122.5, 139.2, 150.7, 154.2, 157.5, 161.1, 164.5, 172.9, 175.5, 175.6.

**MT, (Deprotection of Molecular Transporter). 11.** The guanidinylated dendrimer (230.0 mg, 54.61  $\mu$ mol) was dissolved in dichloromethane (1 mL) at 4 °C. A solution containing trifluoroacetic acid dissolved in dichloromethane (1:1) was next added and the reaction was allowed to stir for 24 h at room temperature. Materials were concentrated,

suspended in methanol and filtered using a Siliaprep Carbonate cartridge. (131.0 mg, 100%).  $^1\text{H}$  NMR (400 MHz, MeOD)  $\delta$  = 1.40 (s,  $\text{CH}_2$ , 36H), 1.58 (d,  $J=39.0\text{Hz}$ ,  $\text{CH}_2$ , 36H), 1.90-2.38 (m,  $\text{CH}_2$ , 48H), 2.6 (s,  $\text{CH}_2$ , 2H), 3.20 (d,  $J=5.9\text{Hz}$ ,  $\text{CH}_2$ , 36H), 3.28 (s,  $\text{CH}_2$ , 2H), 6.79 (br s, NH, 4H), 7.31 (br s, NH, 9H), 7.47 (br s, NH, 18H), 7.74 (t,  $J=6.8\text{Hz}$ , ArH, 1H), 8.08 (d,  $J=8.5\text{Hz}$ , ArH, 1H), 8.37 (q,  $J=8.5\text{Hz}$ , ArH, NH<sub>2</sub>, 19H), 8.65 (d,  $J=4.3\text{Hz}$ , ArH, 1H).  $^{13}\text{C}$  NMR (400 MHz, MeOD)  $\delta$  = 27.3, 29.8, 30.1, 31.3, 31.8, 32.1, 40.5, 42.4, 59.2, 59.6, 123.6, 123.8, 127.7, 127.8, 143.0, 146.1, 158.6, 159.2, 176.0.

### **General Procedure for RV6-26 Antibody Preparation.**

RV6-26 ScFv antibody (408.85  $\mu\text{g}$ , 14.60 nmole, 4.87  $\mu\text{M}$ ) was first diluted using PBS solution prior to addition to tris(2-carboxyethyl)phosphine (TCEP) (8.37  $\mu\text{g}$ , 29.20 nmole, 8.06  $\mu\text{M}$ ) in a total solution volume of 3.5 mL PBS and allowed to stir for 3h at room temperature to reduce the disulfide bond and provide free thiol to be exchanged with the disulfide of the molecular transporter.

### **General Procedure for RV6-26 ScFv-Molecular Transporter Purification**

Following the reduction with TCEP, the molecular transporter was added to the solution to stir for 10 minutes and then purified from excess TCEP via Millipore™ centrifugal filter units (MWCO: 3000). The concentrated solution was collected, and purified three additional times by adding PBS solution followed by centrifugation to remove residual TCEP. Additional molecular transporter (209.7  $\mu\text{g}$ , 87.61 nmole) was added and the reaction was allowed to stir for 1 h at room temperature and at 4°C for 12 h. The



conjugate was then filtered (MWCO 10 000) to concentrate the final conjugate in PBS solution to obtain the RV6-26-MT conjugate.

## References

1. Reichert, J. M., Monoclonal Antibodies as Innovative Therapeutics. *Current Pharmaceutical Biotechnology* **2008**, *9* (6), 423-430.
2. Carter, P. J., Introduction to current and future protein therapeutics: A protein engineering perspective. *Experimental Cell Research* **2011**, *317* (9), 1261-1269.
3. Naz, R. K.; Gupta, S. K.; Gupta, J. C.; Vyas, H. K.; Talwar, G. P., Recent advances in contraceptive vaccine development: a mini-review. *Human Reproduction* **2005**, *20* (12), 3271-3283.
4. Wu, A. M.; Senter, P. D., Arming antibodies: prospects and challenges for immunoconjugates. *Nature Biotechnology* **2005**, *23* (9), 1137-1146.
5. Parashar, U. D.; Hummelman, E. G.; Bresee, J. S.; Miller, M. A.; Glass, R. I., Global illness and deaths caused by rotavirus disease in children. *Emerging Infectious Diseases* **2003**, *9* (5), 565-572.
6. Roy, K.; Mao, H. Q.; Huang, S. K.; Leong, K. W., Oral gene delivery with chitosan-DNA nanoparticles generates immunologic protection in a murine model of peanut allergy. *Nature Medicine* **1999**, *5* (4), 387-391.
7. Hai-Quan Mao, C. Y., Rotavirus Vaccination Via Oral Thin Film Delivery. *News Release* **2006**.
8. Surendran, S., Rotavirus infection: Molecular changes and pathophysiology. *Excli Journal* **2008**, *7*, 154-162.
9. Ranheim, T.; Mathis, P. K.; Joelsson, D. B.; Smith, M. E.; Campbell, K. A.; Lucas, G.; Barmat, S.; Melissen, E.; Benz, R.; Lewis, J. A.; Chen, J.; Schofield, T.; Sitrin, R. D.; Hennessey, J. P., Development and application of a quantitative RT-PCR potency assay for a pentavalent rotavirus vaccine (RotaTeq (R)). *Journal of Virological Methods* **2006**, *131* (2), 193-201.
10. Ward, R. L.; McNeal, M. M., VP6: A Candidate Rotavirus Vaccine. *Journal of Infectious Diseases* **2010**, *202*, S101-S107.
11. Crowe, J. E.; Suara, R. O.; Brock, S.; Kallewaard, N.; House, F.; Weitkamp, J. H., Genetic and structural determinants of virus neutralizing antibodies. *Immunologic Research* **2001**, *23* (2-3), 135-145.
12. Kallewaard, N. L.; McKinney, B. A.; Gu, Y.; Chen, A.; Prasad, B. V. V.; Crowe, J. E., Functional maturation of the human antibody response to rotavirus. *Journal of Immunology* **2008**, *180* (6), 3980-3989.

13. Hamilton, S. K.; Sims, A. L.; Donovan, J.; Harth, E., Non-viral siRNA delivery vectors: dendritic molecular transporter and molecular transporter nanovectors for target gene silencing. *Polymer Chemistry* **2011**, *2* (2), 441-446.
14. Hamilton, S. K.; Ikizler, M. R.; Wallen, C.; Wright, P. F.; Harth, E., Effective delivery of IgG-antibodies into infected cells via dendritic molecular transporter conjugate IgGMT. *Molecular Biosystems* **2008**, *4* (12), 1209-1211.
15. Hamilton, S. K.; Harth, E., Molecular Dendritic Transporter Nanoparticle Vectors Provide Efficient Intracellular Delivery of Peptides. *ACS Nano* **2009**, *3* (2), 402-410.
16. Sandino, A.; Spencer, E., Role of the Inner Protein Capsid on In Vitro Human Rotavirus Transcription. *Archivos De Biología Y Medicina Experimentales* **1987**, *20* (2), R247-R247.
17. Goun, E. A.; Pillow, T. H.; Jones, L. R.; Rothbard, J. B.; Wender, P. A., Molecular transporters: Synthesis of oligoguanidinium transporters and their application to drug delivery and real-time imaging. *ChemBioChem* **2006**, *7* (10), 1497-1515.
18. Torchilin, V. P.; Lukyanov, A. N., Peptide and protein drug delivery to and into tumors: challenges and solutions. *Drug Discovery Today* **2003**, *8* (6), 259-266.
19. Huang, K.; Voss, B.; Kumar, D.; Hamm, H. E.; Harth, E., Dendritic molecular transporters provide control of delivery to intracellular compartments. *Bioconjugate Chemistry* **2007**, *18* (2), 403-409.
20. Newkome, G. R.; Moorefield, C. N.; Baker, G. R.; Johnson, A. L.; Behera, R. K., Chemistry of Micelles .11. Alkane Cascade Polymers Possessing Micellar Topology - Micellanoic Acid-Derivatives. *Angewandte Chemie-International Edition in English* **1991**, *30* (9), 1176-1178.

## CHAPTER III

### DEVELOPMENT OF THIRD GENERATION NEWKOME TYPE DENDRIMERS

#### Introduction

Dendrimers are a unique group of polymers that have been explored for many uses including drug delivery,<sup>1</sup> gene delivery,<sup>2</sup> targeting,<sup>3</sup> and diagnostic applications.<sup>4</sup> In comparison to traditional polymer systems, they offer numerous characteristic benefits. Originally developed by Tomalia, these synthetic polymers have been investigated heavily during the last two decades.<sup>5</sup> They are highly ordered, exhibit low polydispersity, and feature a tunable rate of growth. These nanosized polymers comprise a core, diverging branched units that repeat, and an end group, or periphery, each of which can be readily tuned at any part of synthetic development.

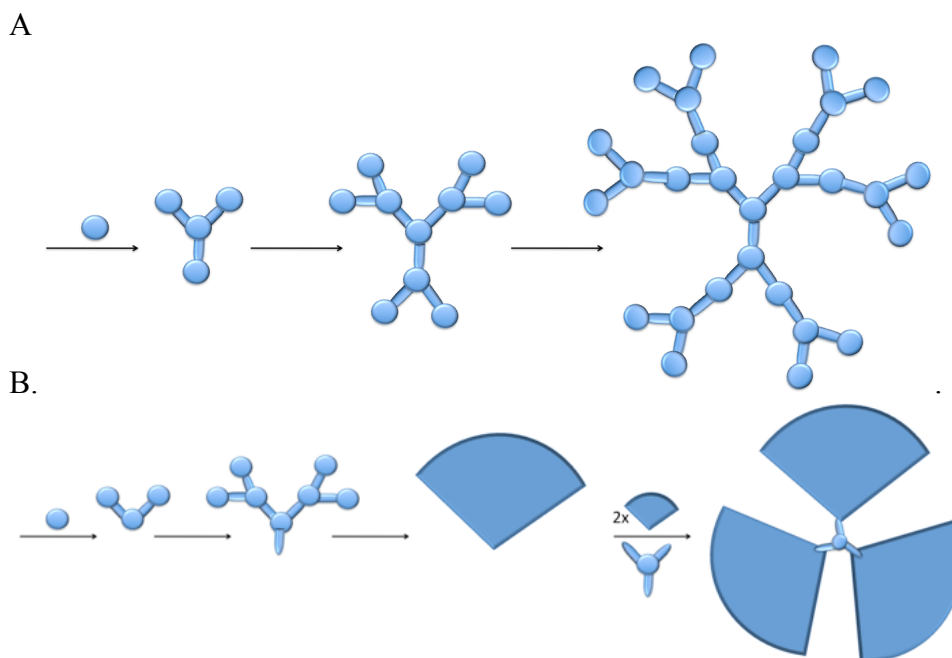


Figure 3.1. A. The divergent method; B. The convergent method.

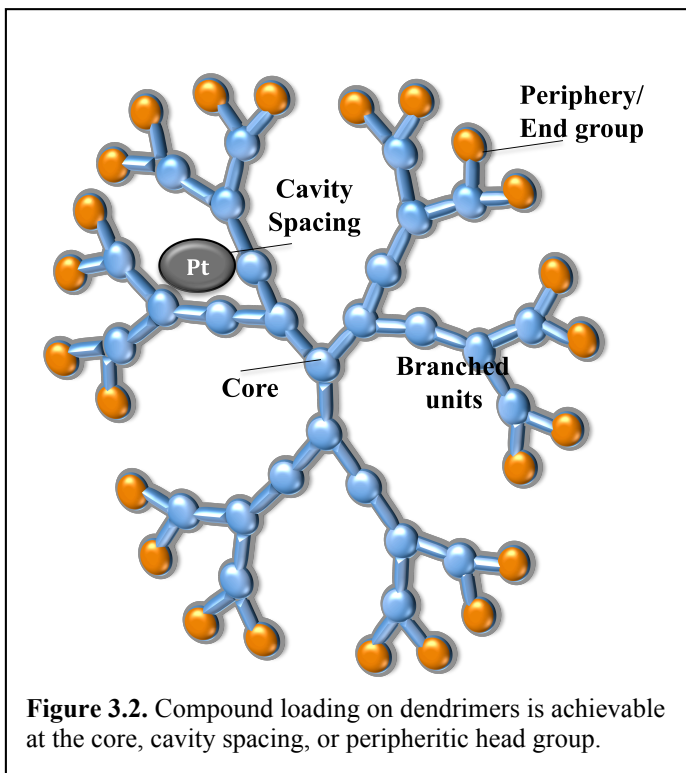
Synthesis is conducted through either of two routes which include divergent and convergent approaches.<sup>6</sup> The divergent approach begins with a core unit and is followed by the growth of repeating additional units, forming generations. Historically, this method represents the most used approach, however, because of the difficulties in functionalizing structures with larger generations, an alternative method was developed. As an alternative, a method utilizing a convergent approach was created.<sup>7</sup> In this approach, branched units, or dendritic wedges, were grown separately and combined simultaneously using a functional core. At present, both the divergent and convergent approaches have been used for several applications which include light-emitting diodes,<sup>8-</sup><sup>10</sup> chelating agents,<sup>11, 12</sup> diagnostics,<sup>4, 13</sup> catalyst,<sup>14</sup> and especially therapeutic applications.<sup>1-3</sup>

Recent years has brought with them a surge of advancements in the therapeutic use of dendrimers. These macromolecular compounds have generated vast interest in therapeutic application by virtue of their activity against prion diseases,<sup>15</sup> Alzheimer's disease,<sup>16</sup> inflammation,<sup>17</sup> HIV,<sup>18</sup> cancer,<sup>19, 20</sup> and tissue repair,<sup>21</sup> among others. In addition, one dendritic structure has even become commercially available as an active ingredient in Viva Gel™, where it inhibits viral infections, which include HIV, genital herpes virus, and the growth of bacteria.<sup>22, 23</sup>

The therapeutic strength of dendrimers is significantly affected by the structural size from lower ordered constructs to larger dendritic structures. Assessments of these effects have been evaluated extensively, and indicate clear distinctions regarding therapeutic behavior of structures containing different generation numbers.<sup>24, 25</sup>

Furthermore, in addition to the number of generations, the selection of compounds used for the core, repeat units, and periphery all contribute to the behavior as well.

The core of dendrimers can be functionalized or feature a specific compound for transport.<sup>26,27</sup> Following loading, increases within branched generations results in the compound of the structure becoming more shielded from surroundings and creates a microenvironment of protection. In structures featuring higher generations, this creates structures that provide a hydrophobic internal region and a



hydrophilic region externally or the chemistry can be manipulated to feature the inverse. Demonstration of this behavior was also seen in the findings of Tomalia and coworkers, who reported loading of water insoluble compounds into the apolar region of a dendrimer for delivery within the bloodstream.<sup>28</sup>

The periphery of the dendrimer can also be functionalized to feature groups for transport as well, and it has also been used to create structures modified with specific functionalities that enhance transport<sup>1, 27</sup> or enable drug loading.<sup>19</sup> By increasing generation numbers, this increases available head groups and also enables the formation of structures featuring different end groups.<sup>29-31</sup> An increase in generations also provides

a suitable cavity, or void space, where compounds can be encapsulated. Meijer demonstrated this process with the encapsulation of rose bengal into the cavities of a poly(propylene imine) dendrimer containing 64 branches.<sup>32</sup> These host-guest interactions are possible due to the peripheral groups that function as a shield, or as a filter against the external environment.<sup>33</sup>

Another interesting feature that is influenced by generation number is demonstrated in their rheological properties. Uniquely, dendritic polymers exhibit a lower viscosity than their linear counterparts.<sup>34, 35</sup> As the generation number increases so does viscosity, reaching a maximum followed by a decline.<sup>6, 36</sup> This is attributed to differences in behavior of branched morphology between structures as well as the influence of the peripheral functionality.

The differences in generations are also seen in the effects of solvation. Structurally, lower generation transporters feature flexible units while larger generation structures generally form rigid globular structures. This behavior also extends to the influence of solvent on size as well. While dendrimers of all generations experience back-folding due to solvent effects, this behavior is exhibited significantly more in lower generation dendrimers than higher ones.<sup>37-40</sup> For example, in the case of dendrimers featuring polar head groups, it has been proposed that dendritic structures demonstrate comparable behavior to proteins that fold to display more hydrophobic regions, or in this case back-folding, when exposed to aprotic solvents.<sup>41</sup> Conversely, when exposed to more protic solvents, the structures assume a more extended conformation (Figure 3.3.). In larger structures, the array of these peripheral functionalities form a more stable intramolecular network and reduces folding. Such effects also explain how generation

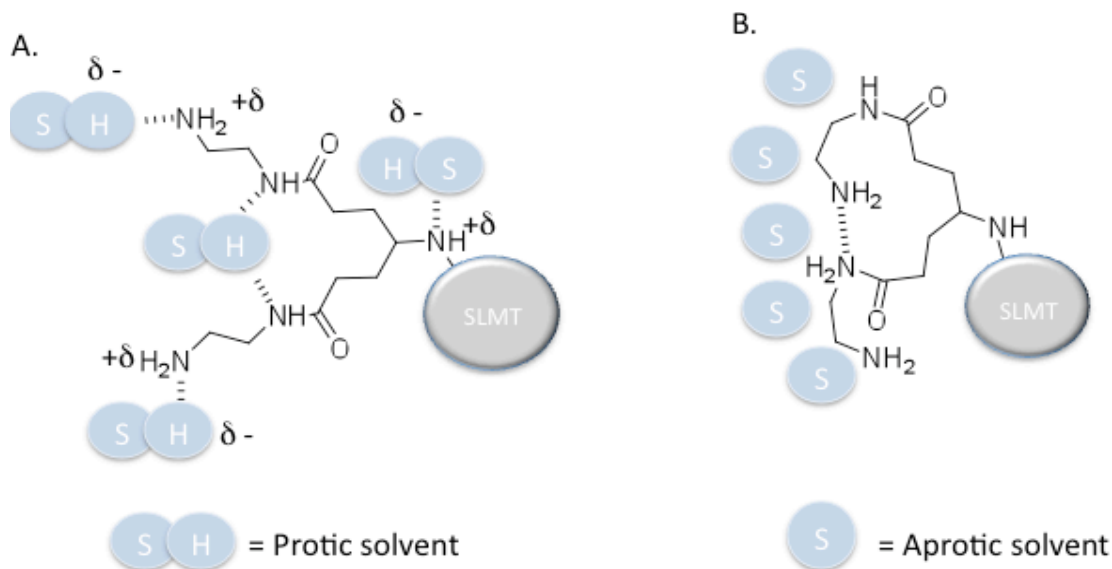


**Figure 3.3.** Proposed scheme for dendrimer solvation. **A:** Solvation of a polar dendrimer in a protic solvent leads to extended conformation. **B:** Polar dendrimer in an apolar aprotic solvent leads to back-folding.

number can affect solubility. An increase in generation number of dendrimers inherently results in greater amounts of peripheral functional groups. As a result, the selection of the functional head groups can be used to direct solubility. Consequently, lower generations with minimal solubility in polar or non-polar solvent will exhibit amplified solvent effects with higher generation structures.<sup>42</sup> The effects on solubility are also seen in the capacity to solubilize compounds as well. In an investigation using PAMAM dendrimer (generations 0-3), nifedipine water solubility was improved as the number of dendritic generations was increased.<sup>43, 44</sup>

The distribution of generation number also plays a role with *in vivo* application as well. In the reports of Kobayashi, PAMAM dendrimers ranging from second to fourth



generations were cleared rapidly when applied *in vivo*. Furthermore, in investigating structures from the fifth to the tenth generation, delayed renal secretion was exhibited due to a larger hydrodynamic volume. These results suggest potential for creating tunable dendritic systems for *in vivo* application.<sup>45</sup>

Because of the unique properties that dendrimers possess, the creation of novel structures would enhance their use in many areas of therapy. As a result, their potential is being realized in applications and continues to be ongoing. Although there are countless investigations with dendrimers, large majorities are either insoluble, known to induce cytotoxic affects, or are not effective at transport of biological compounds, limiting their potential for both *in vitro* and *in vivo* use.<sup>46, 47</sup> The exception to this of course represents a small class of dendrimers used for biomedical applications and include polyesters,<sup>48, 49</sup> polylysine,<sup>50</sup> polypropyleneimine (PPI),<sup>51, 52</sup> and the more popular PAMAM.<sup>53</sup> Obviously with such a small group and a plethora of literature supporting PAMAM dendrimers, there remains untapped potential in the development and application of other dendrimers.

## DISCUSSION

We have previously synthesized Newkome type-second generation dendrimers.<sup>27</sup>

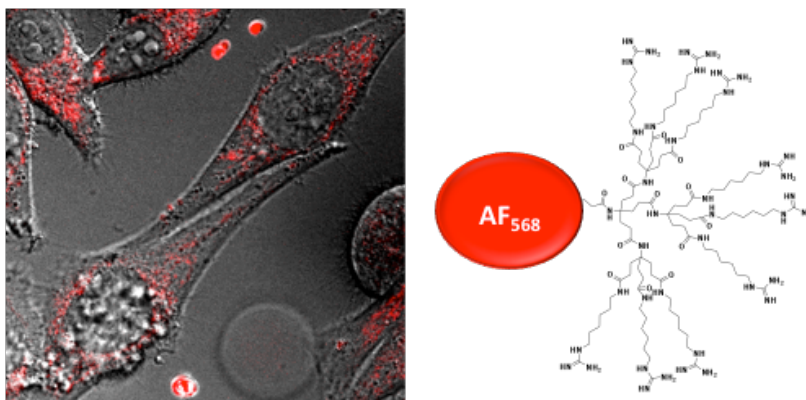
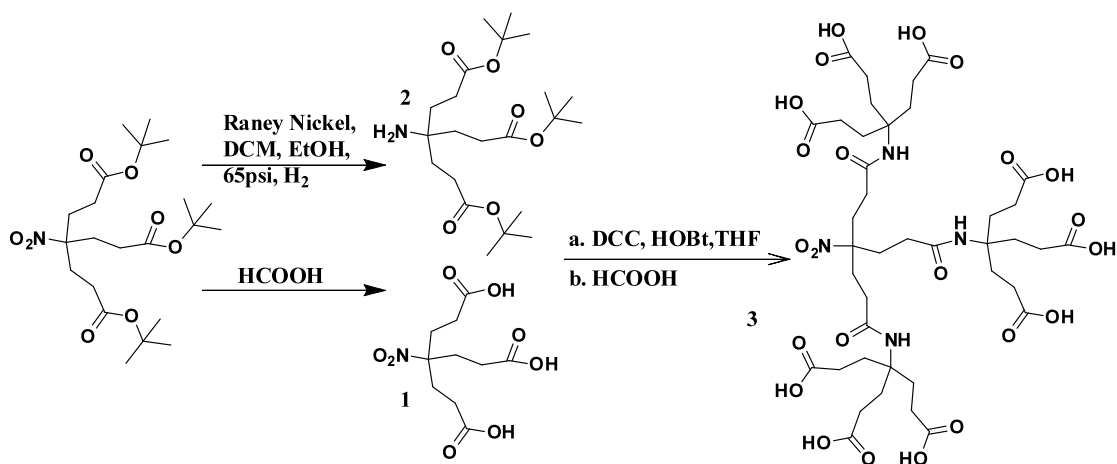


**Figure 3.4.** Second generation dendrimer targets the cytosol in cells.

Their architecture of the dendrimers is comprised of a polyamide backbone and feature guanidine peripheral head groups. Using ethyl and hexyl-spaced alkyl spacers we are able to direct the cellular localization to the nucleus and cytosol respectively. An example of the specificity is shown using the hexyl spaced second generation dendrimer in Figure 3.4. This dendrimer has also been demonstrated to transport biological cargo into cells as well.<sup>26,54,55</sup> However, until now an investigation to synthesize third generation structures has not yet been shown.

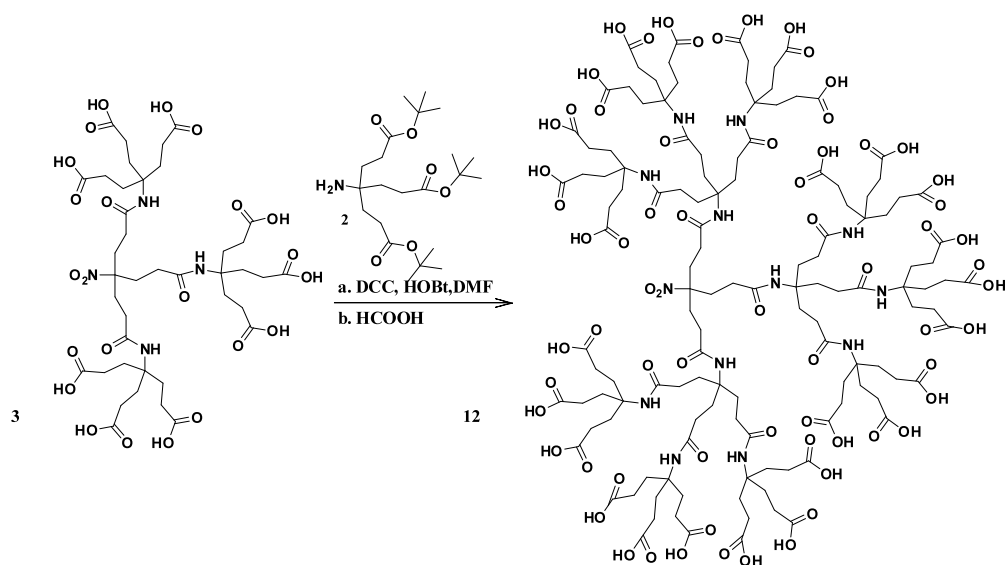
We wanted to construct additional dendritic transporters for several reasons. The primary interest was to develop systems featuring a tunable periphery. In previous attempts, modification to the dendritic periphery with multifunctional head groups proved to be challenging due to difficulties achieving effective conjugation of groups and subsequent purification. Therefore, we decided to create a third generation structure. Using this approach, a desire to modify the termini head groups with polyvalent



**Scheme 3.1.** 2<sup>nd</sup> generation was synthesized to provide nine available carboxylic acid groups.

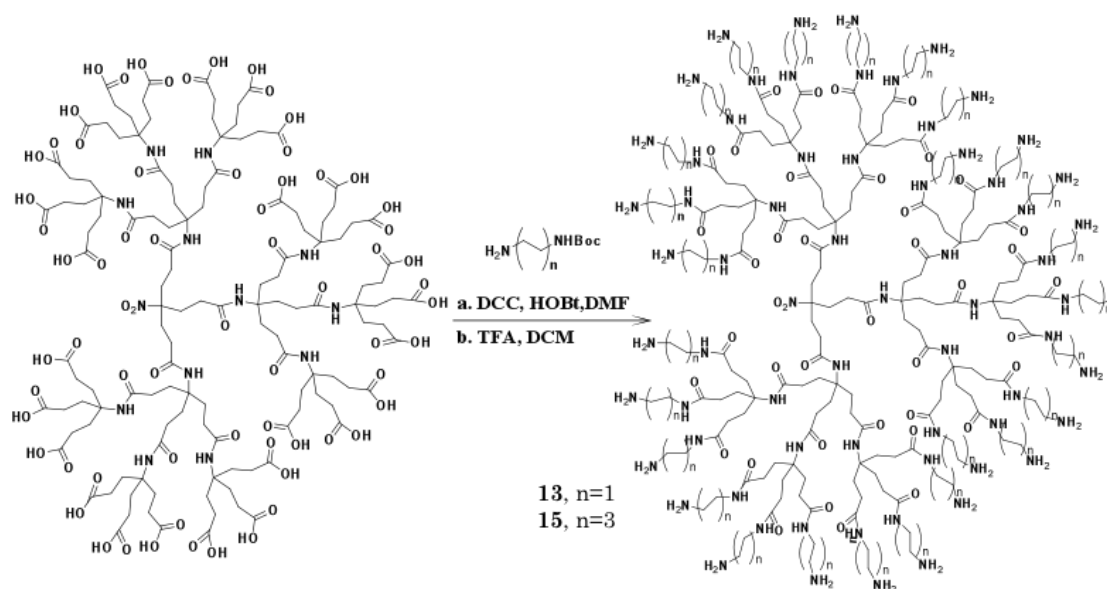
functionalities could be achieved and would also assure purification ease through the use of dialysis. In preliminary investigation, we sought first to synthesize two different third generation transporters. One transporter would feature an ethyl alkyl spacer emanating from the periphery and the other would feature a hexyl alkyl spacer.

To synthesize the macromolecules, the second generation dendron was first synthesized using the previously reported procedure<sup>55</sup> with modifications. Briefly, using a nitrotriester, the precursor monomer units were synthesized separately to form nitro triacid and “Behera’s amine.” The two were then reacted using amide coupling conditions to yield the second generation dendron. The tert. butyl ester protecting groups were next deprotected using formic acid, providing nine available carboxylic acid functional groups at the periphery (Scheme 3.1).



**Scheme 3.2.** 2<sup>nd</sup> generation dendron is coupled with amine monomer in the first step and in the next step deprotected to provide twenty-seven available groups.

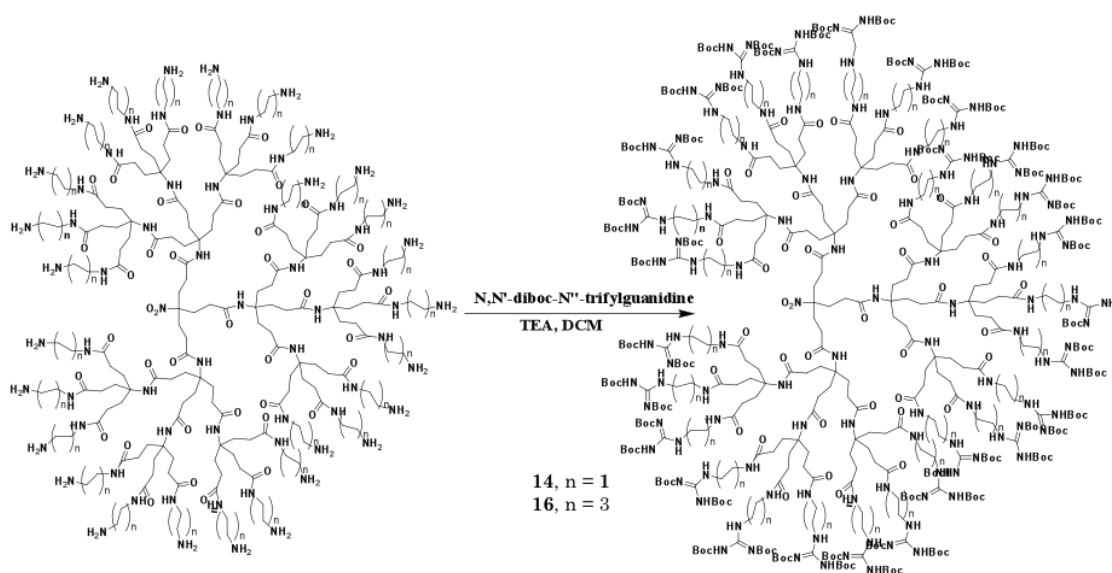
The available carboxylic acid groups of the second-generation dendron were then coupled with amine monomers using amide coupling. To purify, the third generation dendron was concentrated and dialyzed first against methanol and subsequently against dichloromethane to yield the product. The tert-butyl ester groups of the periphery were deprotected with formic acid to yield twenty-seven available carboxylic acid groups (Scheme 3.2).



**Scheme 3.3.** The alkyl spacers were attached and deprotected to form the amine terminated dendron.

The carboxylic acid groups of the periphery were then coupled to an N-Boc-ethylene diamine or N-Boc-1,6-diaminohexane and were purified using dialysis first in methanol and subsequently in dichloromethane to yield boc-protected ethyl and hexyl spaced dendrimer respectively. Deprotection of the boc protecting groups was conducted using trifluoroacetic acid and yielded structures with twenty-seven terminal amines (Scheme 3.3). These groups were coupled to triflyl guanidine and purified using dialysis once again (Scheme 3.4).

Successful synthesis of third generation dendrimers provided several insights. A significant benefit is the ease of purification. To provide a more facile alternative to previous methods of column separation, an alternative approach of dialysis was employed in several steps, leading to the formation of the third generation transporters. Using this method, materials could easily be obtained and characterized.



**Scheme 3.4** Guanine groups were added to form the dendrimer periphery.

It was also observed that solvent selection influenced purification success. As the works of Frechet and others suggests, the polar head groups of the dendritic periphery are heavily influenced by solvation and assume an extended confirmation in polar solvent while back-folding within aprotic non-polar solvents.<sup>38, 56</sup> Further elucidations of their findings suggests that with this behavior the extended confirmation enables removal of any impurities and the nature of back-folding behavior prevents interaction between solvent and dendrimer. Several inferences lead to this observation, as the selection of each solvent independently was ineffective at obtaining the desired product. Under polar conditions, impurities were removed more efficiently; however, *in vacuo* concentration of product yielded an oily residue unlike that of its natural solid composition. Conversely, the use of nonpolar solvent was ineffective at removal of undesired starting materials. Therefore, purification by a polar solvent removed unwanted impurities and subsequent purification in a non-polar solvent assisted with removal and provided solid product. While further characterization may be of interest regarding the behavior of the third generation transporter, it does suggest that our structure conforms to this behavior.

Characterization of the third generation dendrimer was conducted using  $^1\text{H}$  NMR and was used to determine attachment effectiveness. As indicated by Figure 3.5, the alkyl spacing (ethyl or hexyl) on the dendrimer can be identified by the region at 3.2 ppm (green color) and can easily be integrated to confirm attachment to the third generation

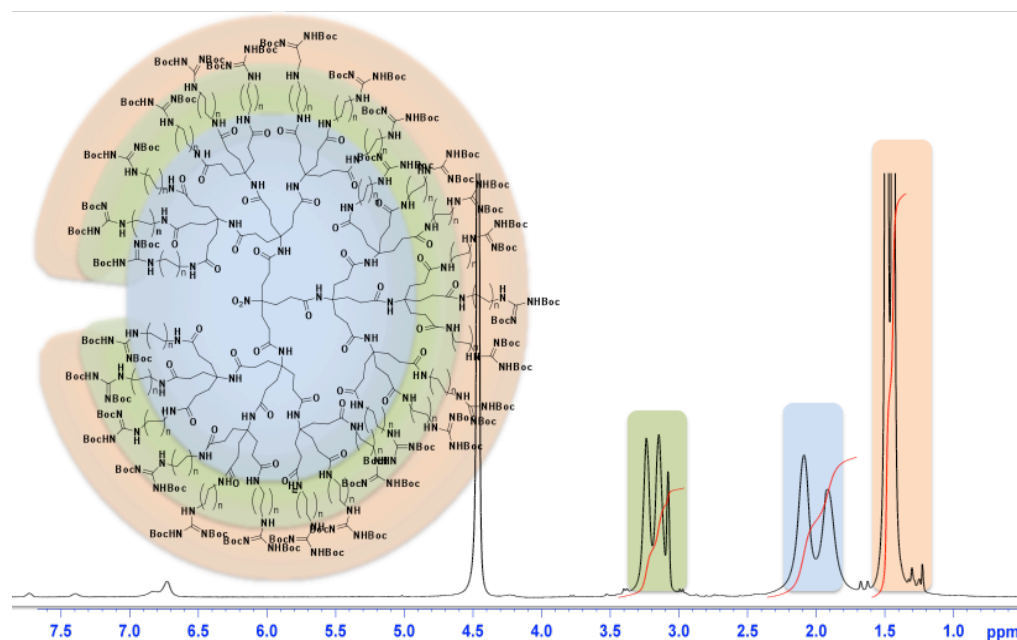


**Figure 3.5.**  $^1\text{H}$  NMR spectrum of Dendrimer following guanidine addition.

dendron (blue). Further, the integration at 1.44 ppm (orange) indicates guanidine attachment and was also used to confirm complete functionalization of the desired compound.

### Conclusion

In summation, third generation Newkome-type dendrimers were synthesized. One structure was synthesized using an ethyl spacer and another was synthesized using a hexyl spacer to create novel structures. In each case both constructs provided

monodispersed compounds that were characterized using  $^1\text{H}$  NMR. The purification used provides a facile alternative to previous methods. This approach circumvents the need for difficult column separation and will enable further development of third generation structures with polyvalent peripheral functionalities, a difficult task to achieve using second generation dendrimers.

## EXPERIMENTAL

**Materials.** All reagents were purchased either from Alfa Aesar, Chem-Impex Int. (Wood Dale, IL), EMD Millipore, Fisher Scientific, Life Technologies (Eugene, OR), or Sigma-Aldrich (St. Louis, MO), and used without further purification unless noted. Analytical TLC was performed on commercial Merck plates coated with silica gel 60 F<sub>254</sub>. Spectra/Por® Biotech Regenerated Cellulose Dialysis Membranes (1000 MWCO) were obtained from Spectrum Laboratories, Inc. (Rancho Dominguez, CA).

**Instrumentation:** Nuclear magnetic resonance was performed on a Bruker DPX-300 and a Bruker AV-400 Spectrometer. Chemical shifts were reported in parts per million and referenced to the corresponding residual nuclei in deuterated solvents. Hydrogenation was conducted using Parr 3911 hydrogenation apparatus. Column chromatography was conducted using an Isolera Biotage. Cell imaging was performed using Zeiss LSM 510 Confocal microscope.

**Synthesis of 4-(2-carboxyethyl)-4-nitroheptanedioic acid. 1.** To a round bottom flask, a solution of nitrotriester, **1**, (3.00 g, 6.73 mmol) and formic acid (20 mL) was stirred at room temperature for 12 h. After the solvent was removed under reduced pressure, toluene was added and removed via concentration *in vacuo* to remove residual formic



acid to yield a white solid (1.87 g, 100%).  $^1\text{H}$  NMR (400 MHz, MeOD):  $\delta = 2.29$  (s,  $\text{CH}_2$ , 12H).  $^{13}\text{C}$  NMR (400 MHz MeOD):  $\delta = 29.39, 31.40, 93.85, 175.65$ .

**Synthesis of di-tert-butyl 4-amino-4-(3-tert-butoxy-3-oxopropyl)heptanedioate, “Behera’s Amine”. 2.** A solution of nitrotriester (10.00 g, 22.4 mmol) in ethanol/dichloromethane (10:1, 150 mL) in a Parr hydrogenation bottle with (4.5 g, 76.67 mmol) Raney-nickel was shaken at 65 psi for 48 h at room temperature. The suspension was gravity filtered, and solvent was removed under reduced pressure to give the crude product. Materials were dissolved in chloroform (100 mL), washed with water (100 mL), and dried over anhydrous  $\text{MgSO}_4$ . Evaporation under reduced pressure yielded white aminotriester (9.05 g, 97%).  $^1\text{H}$  NMR (400 MHz, MeOD):  $\delta = 1.445$  (s,  $\text{CH}_3$ , 27H), 1.62 (t,  $\text{CH}_2$ , 6H), 2.26 (t,  $\text{CH}_2$ , 6H).  $^{13}\text{C}$  NMR (400 MHz MeOD):  $\delta = 26.68, 26.88, 29.39, 33.61, 51.97, 80.07, 173.37$ .

**Synthesis of 9 Cascade: nitromethane [3]: (2-aza-3-oxopenylydyne): propionioate (Dendron G2). 3.** To a sealed three neck round bottom flask, a solution of nitrotriacid (1.11 g, 4.01 mmol) in dried THF (50 mL), 1-hydroxybenzotriazole (HOBt) (1.95 g, 14.43 mmol), and DCC (2.97 g, 14.43 mmol), were added sequentially and stirred under argon. After 2.5 h, Behera’s amine (6.00 g, 14.43 mmol) was added to the solution and the reaction proceeded at room temperature for 40 h. The crude product was filtered, and concentrated under reduced pressure. Materials were purified using column chromatography, eluting with hexane/ethyl acetate (3:2) to afford the desired Dendron G1 (5.65 g, 96%).  $^1\text{H}$  NMR (400 MHz, MeOD):  $\delta = 1.44$  (m,  $\text{CH}_3$ , 81H), 1.95 (m,  $\text{CH}_2$ ,

18H), 2.21 (m, CH<sub>2</sub>, 30H), 6.92 (s, NH, 3H). <sup>13</sup>C NMR (400 MHz, MeOD): δ = 28.04, 29.74, 29.85, 31.28, 57.56, 80.69, 92.47, 170.46, 172.76. To a round bottom flask, a solution of dendron (G2) and formic acid (35 mL) was stirred at room temperature for 12 h. After removal of solvent under reduced pressure, toluene was added and concentrated *in vacuo* to remove residual formic acid to yield nona-acid, **5**, (5.58 g, 100%). <sup>1</sup>H NMR (400 MHz, MeOD): δ = 1.95 (m, CH<sub>2</sub>, 18H), 2.21 (m, CH<sub>2</sub>, 30H), 6.92 (s, NH, 3H). <sup>13</sup>C NMR (400 MHz, MeOD): δ = 29.74, 29.85, 31.28, 57.56, 92.47, 170.46, 172.76.

**Synthesis of (Dendron G3) 12.** To a sealed three neck round bottom flask, a solution of nona-acid, **5**, (1.93 g, 2.01 mmol) in dried DMF (50 mL), 1-hydroxybenzotriazole (HOBt) (2.92 g, 21.65 mmol), and DCC (4.47 g, 21.65 mmol), were added sequentially and stirred under argon at 4 °C. After 2.5 h, Behera's amine (9.00 g, 21.65 mmol) was added to the solution and the reaction proceeded at room temperature for 40 h. The crude product was filtered, dialyzed (MWCO: 1000) in methanol and dichloromethane. The dialyzed material was concentrated *in vacuo* to yield a white solid (6.21 g, 77%). <sup>1</sup>H NMR (300 MHz, MeOD): δ = 1.44 (s, CH<sub>3</sub>, 243H) 2.17 (t, CH<sub>2</sub>, 84H), 1.98 (t, CH<sub>2</sub>, 72H). <sup>13</sup>C NMR (400 MHz, MeOD): δ = 26.13, 26.99, 27.73, 28.29, 28.98, 29.20, 30.30, 30.95, 32.54, 32.70, 33.68, 33.87, 50.84, 50.92, 57.29, 67.78, 80.18, 92.59, 172.91, 177.26. To a round bottom flask, dendron G3 was dissolved in formic acid (40 mL) and stirred for 12 h at room temperature. The solvent was removed under reduced pressure, dialyzed in methanol (MWCO: 1000) and dichloromethane before being concentrated *in vacuo* to yield a white solid (3.52 g, 85%). <sup>1</sup>H NMR (300 MHz, MeOD): δ = 2.17 (t, CH<sub>2</sub>, 84H), 1.98 (t, CH<sub>2</sub>, 72H). <sup>13</sup>C NMR (400 MHz, MeOD): 26.13, 27.73, 28.29, 28.98, 29.20,

30.30, 30.95, 32.54, 32.70, 33.68, 33.87, 50.84, 50.92, 57.29, 67.78, 92.59, 172.91, 177.26.

### **Third Generation Short (ethyl) Linker Transporter**

#### **G3SLBoc, (N-Boc-1,6-diaminohexane attachment to G3 dendron acid G3OH). 13.**

G3OH (1.73 g, 0.57 mmol) in dry DMF (100 mL) was stirred under argon at 4 °C with HOBt (6.26 g, 46.3 mmol) and DCC (9.55 g, 46.3 mmol). After 2.5 h, N-Boc-ethylene diamine (7.42 g, 46.3 mmol) was dissolved in DMF and added to the solution and the reaction proceeded for 48 h. Upon completion, the materials were filtered, removing the DCC salt, and then dialyzed (MWCO: 1000) in methanol and dichloromethane before being concentrated *in vacuo* to yield a white solid (1.43 g, 36%). <sup>1</sup>H NMR (300 MHz, MeOD): δ =1.44-1.35 (s, CH<sub>3</sub>, 243H) 2.17 (t, CH<sub>2</sub>, 84H), 1.98 (t, CH<sub>2</sub>, 72H), 3.03 (t, CH<sub>2</sub>, 54H), 3.16 (t, CH<sub>2</sub>, 54H). <sup>13</sup>C NMR (400 MHz, MeOD): 29.88, 30.26, 30.58, 38.92, 39.19, 57.52, 112.41, 115.32, 118.24, 160.98, 161.32, 161.67, 174.05.

**G3SLBoc Deprotection.** G3SLBoc was dissolved in (50/50) dichloromethane/TFA (30 mL) solution and allowed to stir at room temperature for 12 h. The crude product was concentrated, dialyzed (MWCO: 1000) in methanol followed by dichloromethane, and concentrated *in vacuo* to yield a white solid (0.86 g, 100%). <sup>1</sup>H NMR (300 MHz, MeOD): δ =1.7-2.2 (t, CH<sub>2</sub>, 156H), 3.03 (t, CH<sub>2</sub>, 54H), 3.16 (t, CH<sub>2</sub>, 54H). <sup>13</sup>C NMR (400 MHz, MeOD): 29.88, 30.26, 30.58, 38.92, 39.19, 57.52, 112.41, 115.32, 118.24, 160.98, 161.32, 161.67, 174.05.

**Attachment of Goodman's reagent to G3SLNH<sub>2</sub> dendrimer. 15.** G3 dendrimer (0.86 g, 0.207 mmol) was dissolved in cooled dichloromethane (15 mL). Triethylamine (TEA) (1.35 mL) was added, followed by addition of *N,N'*-diboc-*N''*-triflylguanidine (3.267 g, 8.35 mmol), and the reaction stirred for 24 h at room temperature. The crude materials were dialyzed (MWCO: 1000) in methanol and dichloromethane before being concentrated to yield a white solid (0.82 g, 39%). <sup>1</sup>H NMR (400 MHz, MeOD): δ = 1.20-1.85 (s, CH<sub>3</sub>, 486H) 1.98 (broad s, CH<sub>2</sub>, 72H), 2.17 (broad s, CH<sub>2</sub>, 84H), 2.59 (broad s, CH<sub>2</sub>, 54H), 2.87 (broad s, CH<sub>2</sub>, 54). <sup>13</sup>C NMR (400 MHz, MeOD): δ = 25.68, 25.75, 25.84, 25.91, 25.99, 26.71, 26.80, 26.87, 27.22, 27.24, 29.70, 30.44, 32.39, 32.59, 32.64, 35.38, 50.86, 50.97, 80.66, 82.48, 82.57, 83.88, 115.01, 115.11, 121.45, 121.59, 124.57, 124.63, 124.78, 149.97, 151.72, 151.75, 153.00, 157.19, 173.91.

### **Third Generation Long (hexyl) Linker Transporter**

**G3LLBoc, (N-Boc-1,6-diaminohexane attachment to G3 dendron acid G3OH). 14.** G3OH (1.04 g, 0.34 mmol) in dry DMF (150 mL) was stirred under argon at 4 °C with HOBt (3.75 g, 27.78 mmol) and DCC (5.73 g, 27.78 mmol). After 2.5 h, N-Boc-1,6-diaminohexane (6.00 g, 27.78 mmol) was dissolved in DMF and added to the solution and the reaction proceeded for 48 h. Upon completion, the crude materials were filtered, removing DCC salt, and then concentrated and dialyzed (MWCO: 1000) in methanol to yield a brown solid (2.50 g, 87%). <sup>1</sup>H NMR (300 MHz, MeOD): δ = 1.44-1.35 (s, CH<sub>3</sub>, CH<sub>2</sub>, 459H) 2.17 (t, CH<sub>2</sub>, 84H), 1.98 (t, CH<sub>2</sub>, 72H), 3.03 (t, CH<sub>2</sub>, 54H), 3.16 (t, CH<sub>2</sub>, 54H). <sup>13</sup>C NMR (400 MHz, MeOD): 24.62, 25.66, 26.03, 27.02, 28.73, 29.88, 30.26,

30.58, 38.92, 39.19, 57.52, 78.33, 112.41, 115.32, 118.24, 160.98, 161.32, 161.67, 174.05.

**G3LLBoc Deprotection.** G3LLBoc was dissolved in (50/50) dichloromethane/TFA (30 mL) solution and allowed to stir at room temperature for 12 h. The crude product was concentrated, dialyzed (MWCO: 1000) in methanol, and concentrated *in vacuo* to yield a white solid (1.08 g, 64%). <sup>1</sup>H NMR (300 MHz, MeOD): δ =1.10-1.60 (s, CH<sub>3</sub>, CH<sub>2</sub>, 216H) 1.7-2.2 (t, CH<sub>2</sub>, 156H), 3.03 (t, CH<sub>2</sub>, 54H), 3.16 (t, CH<sub>2</sub>, 54H). <sup>13</sup>C NMR (400 MHz, MeOD): 25.66, 26.03, 27.02, 28.73, 29.88, 30.26, 30.58, 38.92, 39.19, 57.52, 112.41, 115.32, 118.24, 160.98, 161.32, 161.67, 174.05.

**Attachment of Goodman's reagent to G3LLNH<sub>2</sub> dendrimer. 16.** G3 dendrimer (490.6 mg, 92.6 μmol) was dissolved in cooled dichloromethane (12 mL). Triethylamine (TEA) (0.315 mL) was added, followed by addition of *N,N'*-diboc-*N''*-triflylguanidine (1.272 g, 3.25 mmol) and the reaction stirred for 48 h at room temperature. The crude materials were dialyzed (MWCO: 1000) in methanol and concentrated to yield a white solid (621.6 mg, 55%). <sup>1</sup>H NMR (400 MHz, MeOD): δ =1.20-1.85 (s, CH<sub>3</sub>, CH<sub>2</sub>, 702H) 1.98 (broad s, CH<sub>2</sub>, 72H), 2.17 (broad s, CH<sub>2</sub>, 84H), 2.59 (broad s, CHNHCH<sub>2</sub>, 54H), 3.16 (broad s, CONHCH<sub>2</sub>, 54). <sup>13</sup>C NMR (400 MHz), MeOD): δ = 25.68, 25.75, 25.84, 25.91, 25.99, 26.71, 26.80, 26.87, 27.22, 27.24, 29.70, 30.44, 32.39, 32.59, 32.64, 35.38, 50.86, 50.97, 80.66, 82.48, 82.57, 83.88, 115.01, 115.11, 115.21, 118.20, 118.28, 118.40, 121.39, 121.45, 121.59, 124.57, 124.63, 124.78, 149.97, 151.72, 151.75, 153.00, 157.19, 173.91, 174.01.

## References

1. Gillies, E. R.; Frechet, J. M. J., Dendrimers and dendritic polymers in drug delivery. *Drug Discovery Today* **2005**, *10* (1), 35-43.
2. Pack, D. W.; Hoffman, A. S.; Pun, S.; Stayton, P. S., Design and development of polymers for gene delivery. *Nature Reviews Drug Discovery* **2005**, *4* (7), 581-593.
3. Patri, A. K.; Kukowska-Latallo, J. F.; Baker, J. R., Targeted drug delivery with dendrimers: Comparison of the release kinetics of covalently conjugated drug and non-covalent drug inclusion complex. *Advanced Drug Delivery Reviews* **2005**, *57* (15), 2203-2214.
4. Tomalia, D. A.; Reyna, L. A.; Svenson, S., Dendrimers as multi-purpose nanodevices for oncology drug delivery and diagnostic imaging. *Biochemical Society Transactions* **2007**, *35*, 61-67.
5. Svenson, S.; Chauhan, A. S.; Reyna, L. A.; Tomalia, D. A., Coll 105-Starburst (R) and Priostar (Tm) Dendrimers for Enhanced Drug Solubilization. *Abstracts of Papers of the American Chemical Society* **2006**, 232.
6. Klajnert, B.; Bryszewska, M., Dendrimers: properties and applications. *Acta Biochimica Polonica* **2001**, *48* (1), 199-208.
7. Hawker, C. J.; Frechet, J. M. J., Preparation of Polymers with Controlled Molecular Architecture - a New Convergent Approach to Dendritic Macromolecules. *Journal of the American Chemical Society* **1990**, *112* (21), 7638-7647.
8. Li, J. Y.; Liu, D., Dendrimers for organic light-emitting diodes. *Journal of Materials Chemistry* **2009**, *19* (41), 7584-7591.
9. Kwon, T. W.; Alam, M. M.; Jenekhe, S. A., n-type conjugated dendrimers: Convergent synthesis, photophysics, electroluminescence, and use as electron-transport materials for light-emitting diodes. *Chemistry of Materials* **2004**, *16* (23), 4657-4666.
10. Burn, P. L.; Lo, S. C.; Samuel, I. D. W., The development of light-emitting dendrimers for displays. *Advanced Materials* **2007**, *19* (13), 1675-1688.
11. Dagani, R., Chemists explore potential of dendritic macromolecules as functional materials. *Chemical & Engineering News* **1996**, *74* (23), 30-38.
12. Berndt, U. E. C.; Zhou, T.; Hider, R. C.; Liu, Z. D.; Neubert, H., Structural characterization of chelator-terminated dendrimers and their synthetic intermediates by mass spectrometry. *Journal of Mass Spectrometry* **2005**, *40* (9), 1203-1214.

13. Kojima, C.; Turkbey, B.; Ogawa, M.; Bernardo, M.; Regino, C. A. S.; Bryant, L. H.; Choyke, P. L.; Kono, K.; Kobayashi, H., Dendrimer-based MRI contrast agents: the effects of PEGylation on relaxivity and pharmacokinetics. *Nanomedicine-Nanotechnology Biology and Medicine* **2011**, 7 (6), 1001-1008.
14. Piotti, M. E.; Rivera, F.; Bond, R.; Hawker, C. J.; Frechet, J. M. J., Synthesis and catalytic activity of unimolecular dendritic reverse micelles with "internal" functional groups. *Journal of the American Chemical Society* **1999**, 121 (40), 9471-9472.
15. Solassol, J.; Crozet, C.; Perrier, V.; Leclaire, J.; Beranger, F.; Caminade, A. M.; Meunier, B.; Dormont, D.; Majoral, J. P.; Lehmann, S., Cationic phosphorus-containing dendrimers reduce prion replication both in cell culture and in mice infected with scrapie. *Journal of General Virology* **2004**, 85, 1791-1799.
16. Wasiak, T.; Ionov, M.; Nieznanski, K.; Nieznanska, H.; Klementieva, O.; Granell, M.; Cladera, J.; Majoral, J. P.; Caminade, A. M.; Klajnert, B., Phosphorus Dendrimers Affect Alzheimer's (A beta(1-28)) Peptide and MAP-Tau Protein Aggregation. *Molecular Pharmaceutics* **2012**, 9 (3), 458-469.
17. Rele, S. M.; Cui, W. X.; Wang, L. C.; Hou, S. J.; Barr-Zarse, G.; Tatton, D.; Gnanou, Y.; Esko, J. D.; Chaikof, E. L., Dendrimer-like PEO glycopolymers exhibit anti-inflammatory properties. *Journal of the American Chemical Society* **2005**, 127 (29), 10132-10133.
18. McCarthy, T. D.; Karellas, P.; Henderson, S. A.; Giannis, M.; O'Keefe, D. F.; Heery, G.; Paull, J. R. A.; Matthews, B. R.; Holan, G., Dendrimers as drugs: Discovery and preclinical and clinical development of dendrimer-based microbicides for HIV and STI prevention. *Molecular Pharmaceutics* **2005**, 2 (4), 312-318.
19. Lee, C. C.; Gillies, E. R.; Fox, M. E.; Guillaudeu, S. J.; Frechet, J. M. J.; Dy, E. E.; Szoka, F. C., A single dose of doxorubicin-functionalized bow-tie dendrimer cures mice bearing C-26 colon carcinomas. *Proceedings of the National Academy of Sciences of the United States of America* **2006**, 103 (45), 16649-16654.
20. Wolinsky, J. B.; Grinstaff, M. W., Therapeutic and diagnostic applications of dendrimers for cancer treatment. *Advanced Drug Delivery Reviews* **2008**, 60 (9), 1037-1055.
21. Sontjens, S. H. M.; Nettles, D. L.; Carnahan, M. A.; Setton, L. A.; Grinstaff, M. W., Biodendrimer-based hydrogel scaffolds for cartilage tissue repair. *Biomacromolecules* **2006**, 7 (1), 310-316.
22. Jiang, Y. H.; Emau, P.; Cairns, J. S.; Flanary, L.; Morton, W. R.; McCarthy, T. D.; Tsai, C. C., SPL7013 gel as a topical microbicide for prevention of vaginal transmission of SHIV89.6P in macaques. *Aids Research and Human Retroviruses* **2005**, 21 (3), 207-213.

23. Rupp, R.; Rosenthal, S. L.; Stanberry, L. R., VivaGel (TM) (SPL7013 Gel): A candidate dendrimer microbicide for the prevention of HIV and HSV infection. *International Journal of Nanomedicine* **2007**, *2* (4), 561-566.
24. Zinselmeyer, B. H.; Mackay, S. P.; Schatzlein, A. G.; Uchegbu, I. F., The lower-generation polypropylenimine dendrimers are effective gene-transfer agents. *Pharmaceutical Research* **2002**, *19* (7), 960-967.
25. Karatasos, K.; Posocco, P.; Laurini, E.; Pricl, S., Poly(amidoamine)-based Dendrimer/siRNA Complexation Studied by Computer Simulations: Effects of pH and Generation on Dendrimer Structure and siRNA Binding. *Macromolecular Bioscience* **2012**, *12* (2), 225-240.
26. Hamilton, S. K.; Wallen, C.; Harth, E., BIOT 406-Multifunctional protein mimics for the delivery of peptides and oligonucleotides. *Abstracts of Papers of the American Chemical Society* **2008**, 236.
27. Huang, K.; Voss, B.; Kumar, D.; Hamm, H. E.; Harth, E., Dendritic molecular transporters provide control of delivery to intracellular compartments. *Bioconjugate Chemistry* **2007**, *18* (2), 403-409.
28. Tomalia, D. A.; Baker, H.; Dewald, J.; Hall, M.; Kallos, G.; Martin, S.; Roeck, J.; Ryder, J.; Smith, P., A New Class of Polymers - Starburst-Dendritic Macromolecules. *Polymer Journal* **1985**, *17* (1), 117-132.
29. Kurtoglu, Y. E.; Navath, R. S.; Wang, B.; Kannan, S.; Romero, R.; Kannan, R. M., Poly(amidoamine) dendrimer-drug conjugates with disulfide linkages for intracellular drug delivery. *Biomaterials* **2009**, *30* (11), 2112-2121.
30. Morgan, J. R.; Cloninger, M. J., Heterogeneously functionalized dendrimers. *Current Opinion in Drug Discovery & Development* **2002**, *5* (6), 966-973.
31. Vogtle, F.; Fakhrnabavi, H.; Lukin, O.; Muller, S.; Friedhofen, J.; Schalley, C. A., Towards a selective functionalization of amino-terminated dendrimers. *European Journal of Organic Chemistry* **2004**, (22), 4717-4722.
32. Jansen, J. F. G. A.; Debrabandervandenberg, E. M. M.; Meijer, E. W., Encapsulation of Guest Molecules into a Dendritic Box. *Science* **1994**, *266* (5188), 1226-1229.
33. Zhao, M. Q.; Crooks, R. M., Dendrimer-encapsulated Pt nanoparticles: Synthesis, characterization, and applications to catalysis. *Advanced Materials* **1999**, *11* (3), 217-+.



34. Farrington, P. J.; Hawker, C. J.; Frechet, J. M. J.; Mackay, M. E., The melt viscosity of dendritic poly(benzyl ether) macromolecules. *Macromolecules* **1998**, *31* (15), 5043-5050.
35. Hawker, C. J.; Farrington, P. J.; Mackay, M. E.; Wooley, K. L.; Frechet, J. M. J., Molecular Ball-Bearings - the Unusual Melt Viscosity Behavior of Dendritic Macromolecules. *Journal of the American Chemical Society* **1995**, *117* (15), 4409-4410.
36. Wooley, K. L.; Frechet, J. M. J.; Hawker, C. J., Influence of Shape on the Reactivity and Properties of Dendritic, Hyperbranched and Linear Aromatic Polyesters. *Polymer* **1994**, *35* (21), 4489-4495.
37. Chai, M. H.; Niu, Y. H.; Youngs, W. J.; Rinaldi, P. L., Structure and conformation of DAB dendrimers in solution via multidimensional NMR techniques. *Journal of the American Chemical Society* **2001**, *123* (20), 4670-4678.
38. Recker, J.; Tomcik, D. J.; Parquette, J. R., Folding dendrons: The development of solvent-, temperature-, and generation-dependent chiral conformational order in intramolecularly hydrogen-bonded dendrons. *Journal of the American Chemical Society* **2000**, *122* (42), 10298-10307.
39. De Backer, S.; Prinzie, Y.; Verheijen, W.; Smet, M.; Desmedt, K.; Dehaen, W.; De Schryver, F. C., Solvent dependence of the hydrodynamical volume of dendrimers with a rubicene core. *Journal of Physical Chemistry A* **1998**, *102* (28), 5451-5455.
40. Young, J. K.; Baker, G. R.; Newkome, G. R.; Morris, K. F.; Johnson, C. S., Smart Cascade Polymers - Modular Syntheses of 4-Directional Dendritic Macromolecules with Acidic, Neutral, or Basic Terminal Groups and the Effect of Ph Changes on Their Hydrodynamic Radii. *Macromolecules* **1994**, *27* (13), 3464-3471.
41. Maiti, P. K.; Cagin, T.; Lin, S. T.; Goddard, W. A., Effect of solvent and pH on the structure of PAMAM dendrimers. *Macromolecules* **2005**, *38* (3), 979-991.
42. Sakthivel, T.; Toth, I.; Florence, A. T., Synthesis and physicochemical properties of lipophilic polyamide dendrimers. *Pharmaceutical Research* **1998**, *15* (5), 776-782.
43. Devarakonda, B.; Hill, R. A.; de Villiers, M. M., The effect of PAMAM dendrimer generation size and surface functional group on the aqueous solubility of nifedipine. *International Journal of Pharmaceutics* **2004**, *284* (1-2), 133-140.
44. Devarakonda, B.; Li, N.; de Villiers, M. M., Effect of polyamidoamine (PAMAM) dendrimers on the in vitro release of water-insoluble nifedipine from aqueous gels. *Aaps Pharmscitech* **2005**, *6* (3).

45. Kobayashi, H.; Kawamoto, S.; Jo, S. K.; Bryant, H. L.; Brechbiel, M. W.; Star, R. A., Macromolecular MRI contrast agents with small dendrimers: Pharmacokinetic differences between sizes and cores. *Bioconjugate Chemistry* **2003**, *14* (2), 388-394.
46. Aillon, K. L.; Xie, Y. M.; El-Gendy, N.; Berkland, C. J.; Forrest, M. L., Effects of nanomaterial physicochemical properties on in vivo toxicity. *Advanced Drug Delivery Reviews* **2009**, *61* (6), 457-466.
47. Duncan, R.; Izzo, L., Dendrimer biocompatibility and toxicity. *Advanced Drug Delivery Reviews* **2005**, *57* (15), 2215-2237.
48. De Jesus, O. L. P.; Ihre, H. R.; Gagne, L.; Frechet, J. M. J.; Szoka, F. C., Polyester dendritic systems for drug delivery applications: In vitro and in vivo evaluation. *Bioconjugate Chemistry* **2002**, *13* (3), 453-461.
49. Morgan, M. T.; Carnahan, M. A.; Immoos, C. E.; Ribeiro, A. A.; Finkelstein, S.; Lee, S. J.; Grinstaff, M. W., Dendritic molecular capsules for hydrophobic compounds. *Journal of the American Chemical Society* **2003**, *125* (50), 15485-15489.
50. Bourne, N.; Stanberry, L. R.; Kern, E. R.; Holan, G.; Matthews, B.; Bernstein, D. I., Dendrimers, a new class of candidate topical microbicides with activity against herpes simplex virus infection. *Antimicrobial Agents and Chemotherapy* **2000**, *44* (9), 2471-2474.
51. Hollins, A. J.; Benboubetra, M.; Omid, Y.; Zinselmeyer, B. H.; Schatzlein, A. G.; Uchegbu, I. F.; Akhtar, S., Evaluation of generation 2 and 3 poly(propyleneimine) dendrimers for the potential cellular delivery of antisense oligonucleotides targeting the epidermal growth factor receptor. *Pharmaceutical Research* **2004**, *21* (3), 458-466.
52. Wang, S. J.; Brechbiel, M.; Wiener, E. C., Characteristics of a new MRI contrast agent prepared from polypropyleneimine dendrimers, generation 2. *Investigative Radiology* **2003**, *38* (10), 662-668.
53. Majoros, I. J.; Myc, A.; Thomas, T.; Mehta, C. B.; Baker, J. R., PAMAM dendrimer-based multifunctional conjugate for cancer therapy: Synthesis, characterization, and functionality. *Biomacromolecules* **2006**, *7* (2), 572-579.
54. Hamilton, S. K.; Ikizler, M. R.; Wallen, C.; Wright, P. F.; Harth, E., Effective delivery of IgG-antibodies into infected cells via dendritic molecular transporter conjugate IgGMT. *Molecular Biosystems* **2008**, *4* (12), 1209-1211.
55. Hamilton, S. K.; Sims, A. L.; Donavan, J.; Harth, E., Non-viral siRNA delivery vectors: dendritic molecular transporter and molecular transporter nanovectors for target gene silencing. *Polymer Chemistry* **2011**, *2* (2), 441-446.

56. Hawker, C. J.; Wooley, K. L.; Frechet, J. M. J., Solvatochromism as a Probe of the Microenvironment in Dendritic Polyethers - Transition from an Extended to a Globular Structure. *Journal of the American Chemical Society* **1993**, *115* (10), 4375-4376.

## CHAPTER IV

### DEVELOPMENT OF A MOLECULAR TRANSPORTER FOR MITOCHONDRIA DELIVERY

#### Introduction

The mitochondria function in cells to generate adenosine triphosphate (ATP) through oxidative phosphorylation and to provide cellular energy. They are elongated, thread-like organelles comprised of

an outer membrane, an inner membrane, and an inter membrane space separating the two regions. The outer membrane features a protein/phospholipid (1:1) region comprised similarly to the plasma membrane of cells and contains

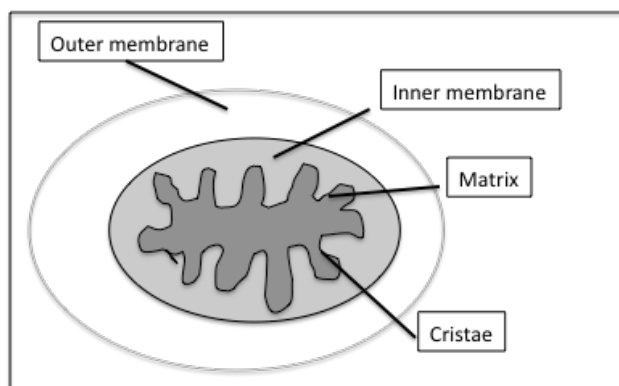


**Figure 4.1.** The mitochondria includes the outer, inter, and inner membrane region and cristae which contain the matrix.

channels, called porins, that allows diffusion of molecules under 6 kDa.<sup>1</sup> The inner membrane consists of a layer featuring a large ratio of tightly packed proteins and phospholipids (3:1). It contains enzymes used for oxidative phosphorylation, carrier proteins, and compartmentalized folds, called cristae, which contain the mitochondrial matrix. The intermembrane space contains specialized proteins that are used for oxidative phosphorylation as well.

However, the production of ATP represents only one facet of mitochondria function and they also play a role in several metabolic pathways, which include the citric acid cycle, oxidation of fatty acids, and the induction of cellular apoptosis, among others.<sup>2</sup> They add to this group of functions additional characteristics that make them a unique organelle. They feature genomic DNA specific to the organelle only. They also produce reactive oxygen species (ROS) for redox signaling. Under elevated stress, an imbalance in the amount of ROS occurs, resulting in overproduction. This can induce oxidative stress to the organelle and lead to mitochondria dysfunction, a condition linked to many mitochondrial related disorders.<sup>3</sup> Mitochondria dysfunction has been implicated in many debilitating conditions, including Alzheimer's, cancer, Parkinson's disease, diabetes, and aging and therefore represents an attractive target for therapeutic delivery.<sup>4</sup> Unfortunately, approaches toward creating targeted delivery systems are only at a very early stage of development. Therefore, it is important to probe further understanding of mitochondria disorders to develop applicable therapy.

Improved understanding begins with developing systems to treat failing mitochondria. However, designing a treatment system to treat or repair damaged mitochondria remains an unmet challenge. For successful treatment, the therapeutic must enter cells, target the mitochondria, and be delivered in relevant amounts. Much of the success of acquiring treatment by pharmacologically active components is highly dependent on the ability to be selectively targeted. Due to lack of specific targeting, creating treatment regimens for mitochondria disorder continues to be a daunting task. Currently, much effort has been focused on developing approaches for mitochondrial repair, and while targeted treatment would be a boon to developing effective therapies,

few reports have demonstrated effective mitochondria targeting.<sup>5, 6</sup> It is because the mitochondria play vital roles in numerous cellular functions that creating a targeted system of delivery would further understanding of the pathology of diseases and provide strategies for novel treatment.

During the production of ATP, the mitochondria in cells produce a transmembrane electrochemical gradient that includes contributions from the negative potential internally, and from the external pH difference. An approach that can be utilized for mitochondria targeting is to maximize this electrochemical potential. This potential falls between 180 and 200 mV *in vitro*,<sup>7</sup> and causes an attraction between mitochondria and positively charged molecules without penetration. In cancer cells this is especially significant where the mitochondrial membrane potential is higher.<sup>8</sup> A barrier to complete accumulation stems from tight packing of the phospholipids within the inner membrane. Previous reports suggest that amphiphilic compounds featuring delocalized cationic charge accumulate in mitochondria,<sup>9</sup> examples of which include Rhodamine 123, tetraphenylphosphonium chloride (TPP-Cl), and other cationic aryl phosphonium salts.<sup>10,11, 12</sup> The attachment of delocalized cationic compounds to current platforms of delivery such as polymers for targeting would be a rational design.<sup>13, 14</sup> Unfortunately, attachment of polar forms of cargo can heavily impact the performance of these compounds, and further investigation is needed. Additionally, the toxicity by these compounds disrupts mitochondrial function following overaccumulation. Therefore, the selection of vehicles for targeted delivery has been challenging. The scattered reports of targeted nanocarriers<sup>15, 16</sup> corroborated with the only two reports that use dendrimers for

mitochondria targeting<sup>17, 18</sup> demonstrate an immeasurable need for new mitochondrial targeted systems.

More recently, Kelley and coworkers indicated a promising approach for achieving specific targeting to mitochondria.<sup>5, 19, 20</sup> As they report, a cellular penetrating peptide can be modified to direct accumulation through use of the electrochemical gradient of mitochondria. These “mitochondria penetrating peptides” were synthesized using variations in the residues found on HIV tat-peptide. Previously, tat-peptide has been shown in several reports to provide cellular penetration and inspired findings of both additional peptide sequences and even dendritic structures for cellular delivery.<sup>5, 21, 22</sup> Adjustments to the tat-peptide sequence were made to create a library of targeted peptides and investigate their propensity for mitochondria accumulation. Motivated by these findings,<sup>20</sup> we became interested in developing a dendritic transporter for mitochondria targeting.

In recent years, dendrimers have increased as viable candidates for drug delivery. These macromolecules can be functionalized in numerous ways for improved biocompatibility and increased water solubility, characteristics ideal for therapeutic delivery.<sup>23</sup> These highly organized polymers feature a core with emanating branches that repeat. The branched architecture provides the ability to tune molecular weight, size, and surface head groups at the periphery for the specific application.<sup>24</sup> As a result, modifications to these groups have demonstrated improved bioavailability,<sup>25</sup> reduced toxicity,<sup>26</sup> and even applied to specific therapeutic targeting.<sup>27</sup>

We were interested in designing a macromolecular approach to develop targeting to mitochondria. To do so we created a dendritic structure to demonstrate cellular uptake

using confocal imaging and mitochondria targeting (i.e. colocalization) with fluorescently labeled mitochondria in live cells. To circumvent the ambiguity in fluorescent imaging that leads to the Potter's Stewart approach<sup>28</sup> of colocalization, in our investigation we further corroborated our images using an objective method for assessment.

Because it has become a recent interest to extract statistical representation of fluorescent overlap to effectively ascertain the spatial and co-occurrent nature of fluorescent images, recent investigations have adopted the use of Pearson's Correlation Coefficient (PCC) to extract better understanding of colocalization.<sup>29</sup> In this case, colocalization is not determined by looking at merged colors, but by analyzing the emitted spectra of the fluorescent dyes. This method measures each pixel of the image and provides a logarithmic expression of colocalization.<sup>30</sup> In our investigation, we evaluated the success of our nanovehicle using this method to provide objective information and further identify localization behavior. Our transporter presents one of few known approaches using dendrimers for mitochondria targeting,<sup>17, 18</sup> but it is the first, to employ statistically correlated colocalization by a dendritic transporter.

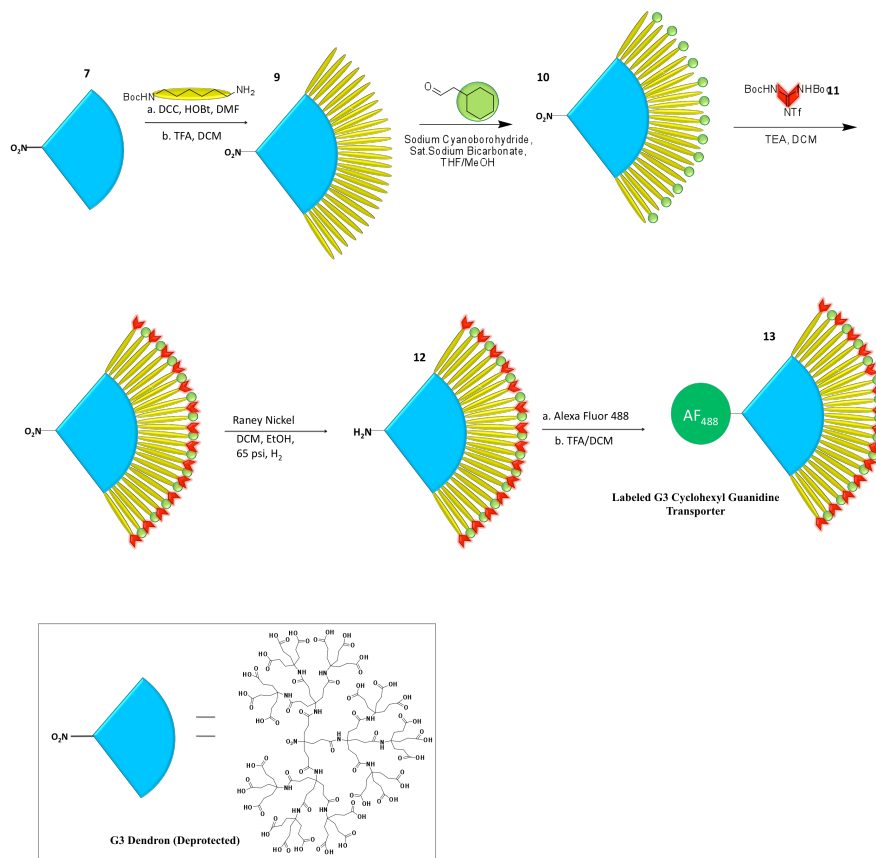
## DISCUSSION

In the interest of developing a targeted dendrimer, we began our efforts with the synthesis of second generation Newkome-type dendrimer that would be subsequently appropriately modified. We were motivated to create a transporter featuring a balanced ratio of lipophilic and cationic distribution for targeted delivery. In our previous reports, we show a Newkome dendrimer featuring nine arginines,<sup>22</sup> inspired by the cellular



penetration capabilities of nona-arginine peptide<sup>31</sup> and tat-peptide.<sup>32</sup> We selected this second generation transporter as our scaffold to achieve targeted delivery, and synthesized the dendrimer using previously described steps with the exception of the final step of guanidine addition. To synthesize a dendrimer with our desired functionalities, we sought to attach a cyclohexyl group and incorporate the guanidine group afterwards. To do so, attachment was conducted using a series of molar equivalents of cyclohexyl groups. The yields from these attachments produced unfavorable results and we observed very limited attachment success. Difficult purification steps further complicated the results.

**Approach Alternative: G3 Cyclohexyl-Guanidine Dendrimer**



**Scheme 4.1.** Alternative synthetic pathway for third generation cyclohexyl guanidine transporter.

Therefore, efforts were redirected to an alternative approach (Scheme 4.1). Current interest in third generation transporters prompted our efforts toward synthesizing a targeted system using a third generation dendron. Such transporters offer more facile synthesis and purification than earlier systems. This was described in the preceding chapter, but we note here that the approach presents a more effective strategy for achieving tunable ratios of peripheral functionality. Using the third generation dendron as a scaffold, we sought to synthesize dendrimers featuring various ratios of cyclohexyl groups.

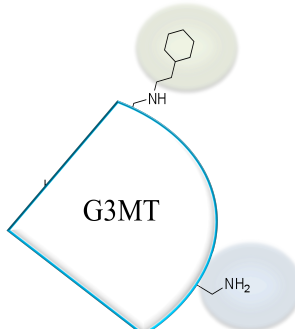
The first generation of the dendron was synthesized using a slight modification to the previously reported literature procedure<sup>33</sup> to increase yield. Formation of “Behera’s amine” was achieved using modified work-up procedures. This monomer was subsequently used with nitrotriacid to synthesize the second generation dendron. The nine tert-butyl ester protecting groups on the dendrimer were deprotected to provide nine

available carboxylic acid groups that were coupled with Behera’s amine to form the third generation dendron featuring twenty-seven peripheral arms. These groups

were removed similarly to the previous deprotection and the end groups were coupled with *N*-boc-1,6-diaminohexane. The boc groups were deprotected yielding terminal amine groups for subsequent reaction. Next, we conducted several reactions in series using various molar equivalents

**Table 4.1.** Indicates various ratios of cyclohexyl groups synthesized.

Third Generation Reductive Aminations		
	Cyclohexyl Attached	Remaining Amines
Trial 1	3	24
Trial 2	4	23
Trial 3	8	19
Trial 4	14	13
Trial 5	20	7



The diagram shows a large blue circular structure labeled 'G3MT'. Two smaller circular structures are attached to its perimeter: one is a light green circle containing a cyclohexane ring with an -NH- group, and the other is a light blue circle containing an -NH<sub>2</sub> group.

of cyclohexyl groups to acquire a library of third generation transporters. This provided us with transporters featuring different ratios of cyclohexyl functional groups (Table 4.1).

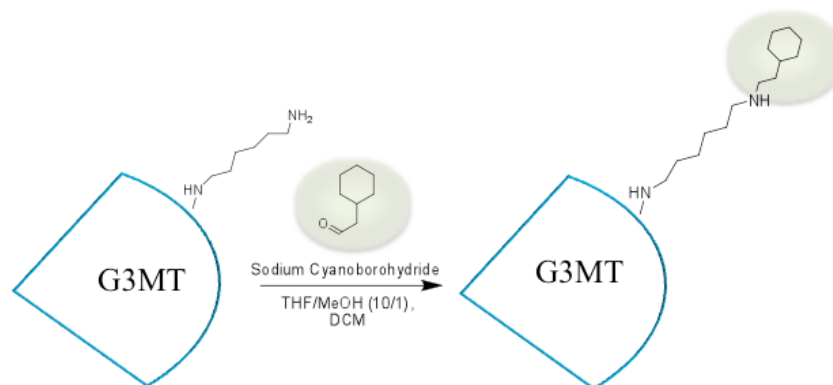


**Figure 4.2.** The amines were reacted with 2-cyclohexyl acetylaldehyde using various molar ratios.

Reductive amination was employed to couple cyclohexyl acetylaldehyde to the terminal amines using slightly modified Borch conditions for facile purification and subsequent guanidine addition.<sup>34</sup> Briefly, the transporter was modified using a slight molar excess of desired cyclohexyl groups. The reaction was conducted using a dual solvent system containing aqueous and organic layers, and following completion the aqueous layer was confirmed to possess impurities and no product. The organic layer, containing the transporter, was further purified in organic solvent using dialysis to isolate the product. This approach enhanced purification, a limitation of the second generation transporter, and provided a product that was easily characterized using <sup>1</sup>H NMR with specific emphasis on the two protons (blue; 2.75 ppm) alpha to free terminal amine and the four protons (green; 2.50 ppm) alpha to the reductively aminated amine (Figure 4.3). Once characterized, the construct would subsequently be reacted with guanidine groups.

In our initial investigation, we selected the third generation dendrimer featuring approximately equal ratios of cyclohexyl and terminal amines (Table 4.1, Trial 4). The decision to use this structure was inspired by the reports of Kelly *et al.* as they describe a

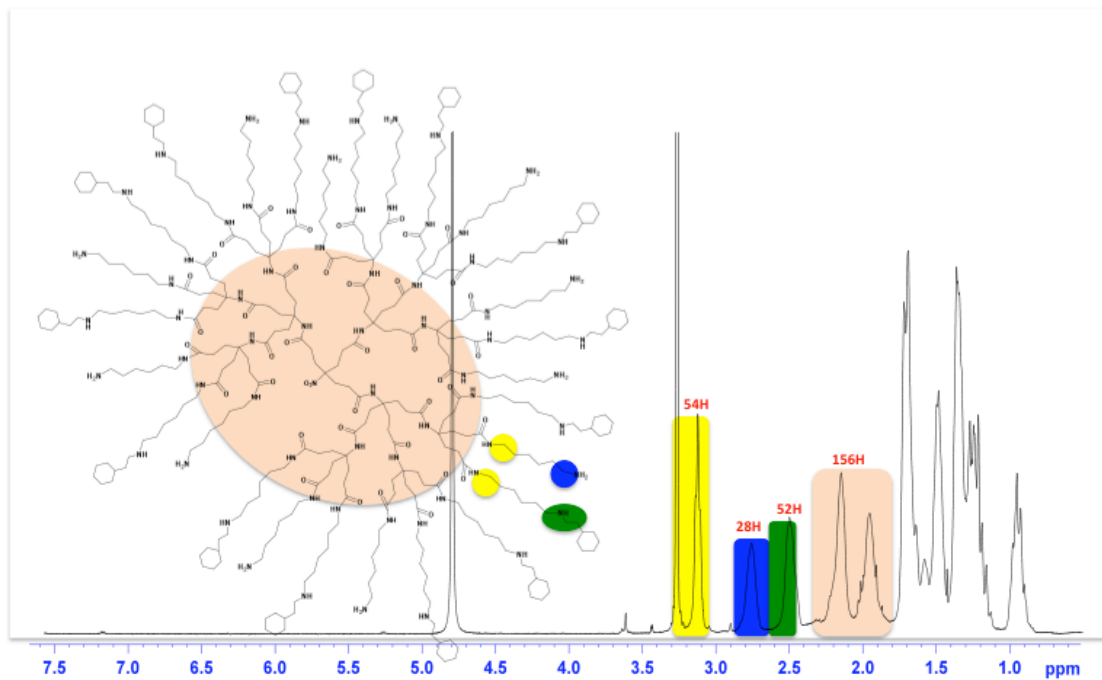


**Figure 4.3.**  $^1\text{H}$  NMR Characterization of  $\text{G3LL}(\text{NH}_2)_{14}\text{-Cyclohexyl}_{13}$ .

tat-peptide featuring equal ratios of cyclohexyl and guanidine groups proven to provide cellular uptake and mitochondria colocalization.<sup>19</sup> Based on these findings, the remaining

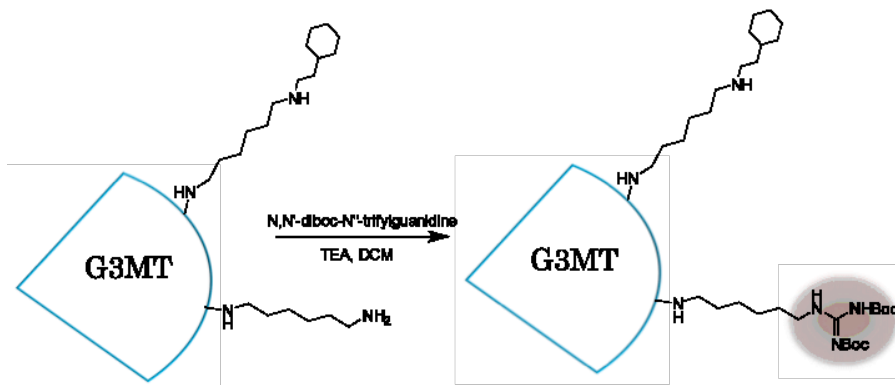


**Figure 4.4.** The remaining free amines were reacted to feature guanidine groups at the periphery.

amines were then modified with a guanidinylation reagent to add guanidine's head groups (Figure 4.4).

### Colocalization Studies

We wanted to investigate the ability of the transporter to be taken up in cells using fluorescent imaging. Therefore, the nitro group at the core focal point of the dendrimer was hydrogenated to yield an amine functionality that could be used to label one fluorophore on each dendritic macromolecule. For uptake studies, the dendrimer was attached to an Alexa Fluor 488<sup>®</sup> succinimidyl ester fluorescent probe to yield labeled transporter. Finally, the guanidine boc-protection groups were deprotected and purified, providing labeled dendrimer. The compound was found to be water soluble and was then

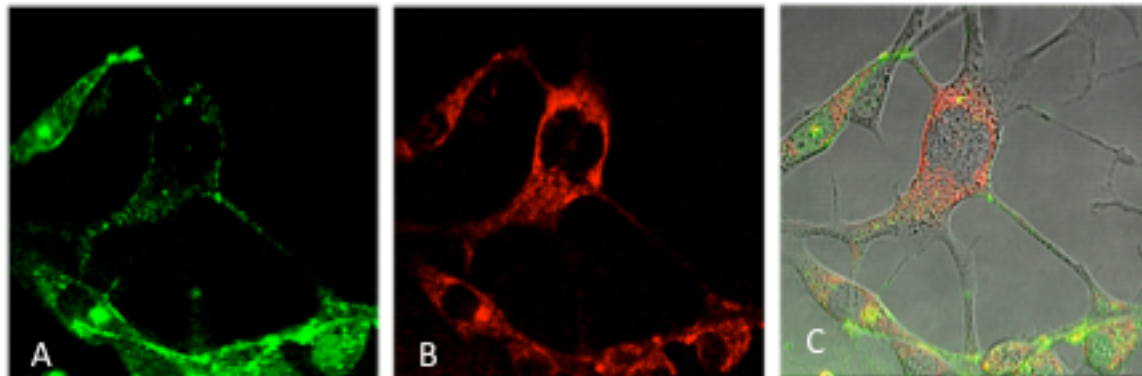


**Figure 4.5.** Confocal microscopy images of NIH-3T3 fibroblast cells. NIH-3T3 cells were grown to subconfluence and 55  $\mu\text{M}$  of the labeled transporter was applied to cells and allowed to incubate for 90 minutes. Mitotracker red (100  $\mu\text{M}$ ) was added to cells in the last 15 minutes and washed 3 times with PBS before imaging. Panel A: Green fluorescence of G3LL (Cycloheyl<sub>13</sub>) (Guanidine<sub>14</sub>) AF<sub>488</sub>. Panel B: Red fluorescence of Mitotracker CMXRos. Panel C: Merged image of green fluorescence (A), red fluorescence and DIC.

evaluated for cellular uptake and colocalization with mitochondria. Internalization was assessed using the mammalian cell line, NIH-3T3 fibroblasts. Cellular uptake and localization of the transporter was evaluated in human cells by confocal microscopy.

Several uptake experiments were performed to evaluate the transporter against mitochondria using live cell imaging. The images obtained from confocal microscopy strongly suggest that the transporter enters cells and reaches the mitochondria. As Figure 4.5 illustrates, the fluorescent signal from the transporter (green) found on panel A was observed to localize similarly to the distribution of mitochondria fluorescence (red) indicated by panel B. No entry of the labeled transporter into the nuclei was observed. A labeled third generation transporter featuring equal ratios of protected-guanidines and cyclohexyl groups was applied to cells as a control and demonstrated no cellular uptake (image not shown).

There have been limited reports of mitochondria colocalization using dendrimers, with PAMAM G4 and PAMAM G5 being the only ones to date.<sup>17, 18</sup> The approach presented here suggest several advantages over other targeted dendritic systems. The novelty in our findings suggests a more solvent-flexible approach. The transporter is able to be placed into organic solvents, which include DMF, DMSO, and dichloromethane, and also is water soluble, a characteristic potentially beneficial when used for investigations of biologically sensitive components where therapeutics would be conjugated and delivered. Our results further reconfirm the ability of guanidine groups to enable cellular uptake, as previously reported by several groups.<sup>22, 31, 32, 35</sup> Finally, it implies that an alternative to the incorporation of existing delocalizing compounds could be realized using lipophilic compounds like the cyclohexyl group, an approach that could be applied to related species.

To date, although there have been investigations of organelle colocalization using confocal imaging; few reports have taken advantage of tools capable of quantified

fluorescence. In addition to standard imaging results, calculation of Pearson's Correlation Coefficient (PCC) and expression of data using scatter plots can add additional statistical insight into colocalization exhibited by two fluorophores. The formula for calculating PCC for two channels is indicated

as follows in Figure 4.6:

$$PCC = \frac{\sum_i (R_i - \bar{R}) \times (G_i - \bar{G})}{\sqrt{\sum_i (R_i - \bar{R})^2 \times \sum_i (G_i - \bar{G})^2}}$$

**Figure 4.6.** The Pearson Correlation Coefficient (PCC) Expression.

Calculations for PCC measure the covariance between variables, and can in this case be used to elucidate the co-occurrence of two fluorophores. In this equation  $R_i$  and  $G_i$  are labeled to correspond to the intensity of the red and green channels respectively and  $\bar{R}$  and  $\bar{G}$  refer to mean intensity with the values of the correlation coefficient falling

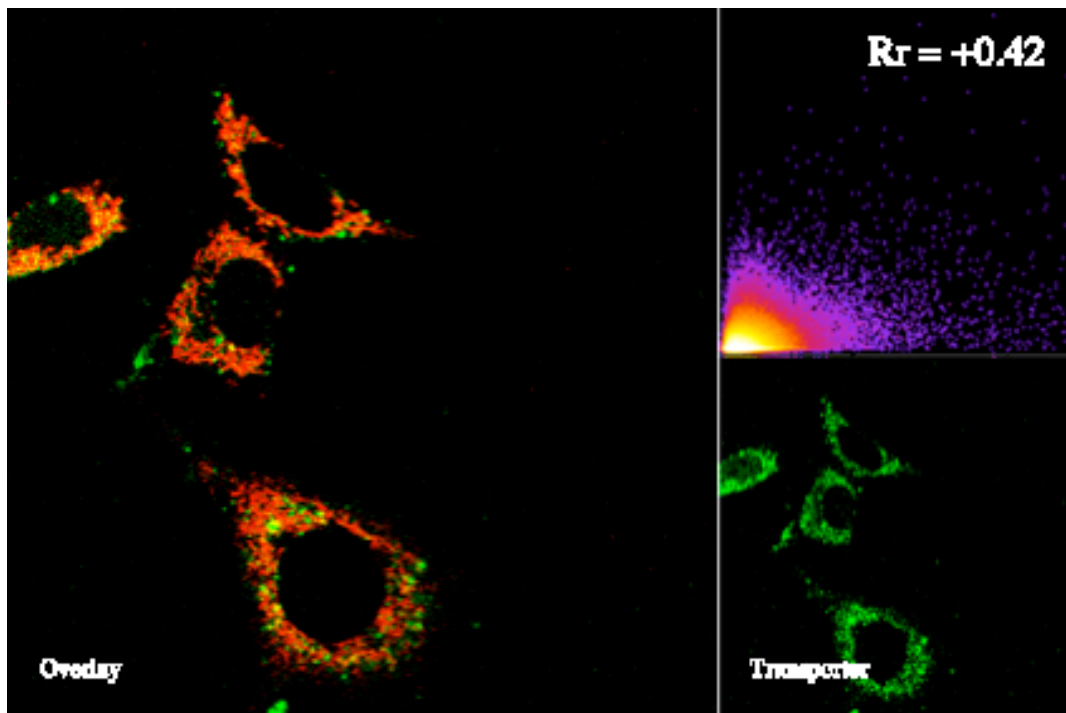


**Figure 4.7.** Left: Overlay of mitotracker (red) and transporter (green) overlay Right: Pearsons correlation value was averaged among all images to equate to + 0.42.

between -1 and 1. A value of -1 indicates incomplete correlation with a value of 1 indicating complete correlation. When applied to confocal imaging the fluorescent covariance, or more specifically colocalization, it is useful in extracting a statistical representation of how well aligned colocalization between the mitochondria probe and our transporter were. In our investigation, the correlation coefficient was calculated using Image J software and used to generate an average value. In our findings, we report a PCC value (sometimes represented by  $R_r$ ) of +0.42.

As mentioned before, a scatter plot can also provide visual insights and lead to a better understanding of the spatial co-occurrence between the fluorophore as the channels can be plotted one against the other. We show a scatter plot representative of our findings in Figure 4.7. The plot distribution suggests a positive relationship between our transporter and the mitochondria.

In understanding the plot, complete codistribution would provide a linear plot and imply a PCC value of 1. The reports of Bolte indicate that as PCC values approach 1, a stronger argument can be used to assert a correlation between two fluorophores.<sup>30</sup> While the experimentally determined PCC value does not reflect complete correlation it does suggest values comparable to other reported targeted systems.<sup>19</sup> Therefore, the values obtained do suggest our transporter can be used for mitochondria delivery. These findings are significant and add to the dendritic utility of the transporters that we have generated. As there have been limited research that report targeted delivery using macromolecular structures, with even fewer examples of colocalization corroborated with reports of PCC, our findings pave the way for future application as a targeted delivery vehicle for therapeutic treatment.



## Conclusion

The findings of this investigation support the findings reported by the Kelly group. The combination of arginine functionality cited in prior research endows the transporter with the capacity to penetrate cells.<sup>36</sup> This cationic arginine functionality has been a hallmark of many cellular delivery systems like that of tat-peptide and polyarginine, to name a few. Incorporation of the lipophilic cyclohexyl groups is key to balancing the charge distribution of our construct. Our findings align with reports suggesting that some hydrophobic character is necessary for localized delivery to the cellular mitochondria with specific focus on creating constructs featuring a 50/50 ratio of peripheral cationic charge and hydrophobic functionality.

A mitochondria-targeted third generation Newkome-type dendrimer was synthesized featuring an equal distribution of cationic guanidines and cyclohexyl groups at the periphery. The guanidine groups provided cellular uptake and the cyclohexyl groups were incorporated to provide lipophilic content. This transporter was applied to cells to investigate colocalization and demonstrate accumulation to labeled mitochondria. The recent growth in degenerative diseases linked to mitochondria disorder make the organelle a viable target for developing therapeutic treatments. In cases where selectivity is not achievable, the transporter presents a formidable option for mitochondria targeting. This construct provides potential for both current and novel drug delivery and adds to the versatility of our Newkome-type dendrimers.

## EXPERIMENTAL

**Materials.** All reagents were purchased either from Alfa Aesar, Chem-Impex Int. (Wood Dale, IL), EMD Millipore, Fisher Scientific, Life Technologies (Eugene, OR), or Sigma-Aldrich (St. Louis, MO), and used without further purification unless noted. Analytical TLC was performed on commercial Merck plates coated with silica gel 60 F<sub>254</sub>. Spectra/Por® Biotech Regenerated Cellulose Dialysis Membranes (1000 MWCO) obtained from Spectrum Laboratories, Inc. (Rancho Dominguez, CA). NIH-3T3 cells (American Type Culture Collection ATCC, Manassas, VA) were grown as subconfluent monolayers in 75 cm<sup>2</sup> cell culture plates with vent caps (Fisher Scientific) in DMEM supplemented with 10% fetal bovine serum (FBS; in a humidified incubator (70%–95%) at 37°C with 5% CO<sub>2</sub>). Cells grown to subconfluence were enzymatically dissociated from the surface with a solution of 0.25% trypsin-ethylene diamine tetra-acetic acid (Trypsin-EDTA) and plated in a glass bottom Petri dish with a 14 mm microwell (Mattek, Ashland, MA) 1–2 days prior to the experiment. These conditions produced a monolayer of cells at subconfluence.

Nuclear magnetic resonance (NMR) spectra were collected on a Bruker DPX-300 and a Bruker AV-400 Spectrometer. Chemical shifts were reported in parts per million and referenced to the corresponding residual nuclei in deuterated solvents. Hydrogenation was conducted using a Parr 3911 Hydrogenation Apparatus. Column chromatography was conducted using an Isolera Biotage, and confocal fluorescence microscopy experiments were performed using an LSM 510 laser scanning Confocal microscope (Carl Zeiss, Thornwood, NY).

### Synthesis of G3LL(Cyclohexyl<sub>13</sub>)(Guanidine<sub>14</sub>) AF<sub>488</sub>

**Synthesis of 4-(2-carboxyethyl)-4-nitroheptanedioic acid 1.** To a 250 mL round bottom flask, a solution of nitrotriester (3.00 g, 6.73 mmol) in formic acid (20 mL) was stirred at room temperature for 12 h. After the solvent was removed under reduced pressure, toluene was added and concentrated *in vacuo* to remove residual formic acid, yielding a white solid (1.87, 100%). <sup>1</sup>H NMR (400 MHz, MeOD):  $\delta$  = 2.29 (s, CH<sub>2</sub>, 12H). <sup>13</sup>C NMR (400 MHz, MeOD):  $\delta$  = 29.39, 31.40, 93.85, 175.65.

**Synthesis of di-tert-butyl 4-amino-4-(3-tert-butoxy-3-oxopropyl)heptanedioate, “Behera’s Amine” 2.** A solution of nitrotriester (10.00 g, 22.4 mmol) in ethanol/dichloromethane (10:1, 150 mL) was prepared and added to a Parr hydrogenation bottle. Raney nickel (4.5 g, 76.67 mmol) was added to the vessel and was shaken at 65 psi for 48 h at room temperature. The suspension was allowed to settle and solvent was decanted, followed by subsequent addition of dichloromethane and collection by decanting the solvent. The collected solutions were combined and concentrated under reduced pressure to yield the white aminotriester **2**. (9.05 g, 97%) <sup>1</sup>H NMR (400 MHz, MeOD):  $\delta$  = 1.445 (s, CH<sub>3</sub>, 27H), 1.62 (t, CH<sub>2</sub>, 6H), 2.26 (t, CH<sub>2</sub>, 6H). <sup>13</sup>C NMR (400 MHz, MeOD):  $\delta$  = 26.68, 26.88, 29.39, 33.61, 51.97, 80.07, 173.37.

**Synthesis of 9 Cascade: nitromethane [3]: (2-aza-3-oxopenylydyne): propionioate (Dendron: G2) 3.** To a sealed three-neck 250 mL round bottom flask, a solution of nitrotriacid, **1**, (1.11 g, 4.01 mmol) in dried THF (50 mL), 1-hydroxybenzotriazole (HOBt) (1.95 g, 14.43 mmol), and DCC (2.97 g, 14.43 mmol), were added sequentially

and stirred under argon. After 2.5 h, Behera's amine, **2**, (6.00 g, 14.43 mmol) was added to the solution and the reaction proceeded at room temperature for 40 h. The reaction mixture was filtered, and the filtrate was concentrated under reduced pressure. The crude product was purified using column chromatography, eluting with hexane/ethyl acetate (3:2) to afford the desired dendron, G1, **3**, (5.65 g, 96%). <sup>1</sup>H NMR (400 MHz, MeOD):  $\delta$  = 1.44 (m, CH<sub>3</sub>, 81H), 1.95 (m, CH<sub>2</sub>, 18H), 2.21 (m, CH<sub>2</sub>, 30H), 6.92 (s, NH, 3H). <sup>13</sup>C NMR (400 MHz, MeOD):  $\delta$  = 28.04, 29.74, 29.85, 31.28, 57.56, 80.69, 92.47, 170.46, 172.76.

**Deprotection of Dendron (G2).** To a 250 mL round bottom flask, a solution of dendron (G2) and formic acid (35 mL) was stirred at room temperature for 12 h. After the solvent was removed under reduced pressure, toluene was added and concentrated *in vacuo* to remove residual formic acid to yield nona-acid (5.58 g, 100%). <sup>1</sup>H NMR (400 MHz, MeOD):  $\delta$  = 1.95 (m, CH<sub>2</sub>, 18H), 2.21 (m, CH<sub>2</sub>, 30H), 6.92 (s, NH, 3H). <sup>13</sup>C NMR (400 MHz, MeOD):  $\delta$  = 29.74, 29.85, 31.28, 57.56, 92.47, 170.46, 172.76.

**Synthesis of (Dendron:G3) 12.** To a sealed 250 mL three neck round bottom flask, a solution of nona-acid (1.93 g, 2.01 mmol) in dried DMF (50 mL), 1-hydroxybenzotriazole (HOBt) (2.92 g, 21.65 mmol), and DCC (4.47 g, 21.65 mmol), were added sequentially and stirred under argon at 4 °C. After 2.5 h, Behera's amine, **2**, (9.00 g, 21.65 mmol) was added to the reaction mixture and the reaction was run at room temperature for 40 h. The reaction mixture was filtered and dialyzed (MWCO:1000) in methanol and then dichloromethane. After dialysis, the product was collected and concentrated *in vacuo* to yield a white solid (6.21 g, 77%). <sup>1</sup>H NMR (300 MHz, MeOD):  $\delta$  = 1.44 (s, CH<sub>3</sub>, 243H) 2.17 (t, CH<sub>2</sub>, 84H), 1.98 (t, CH<sub>2</sub>, 72H). <sup>13</sup>C NMR (400 MHz,

MeOD):  $\delta$  = 26.13, 26.99, 27.73, 28.29, 28.98, 29.20, 30.30, 30.95, 32.54, 32.70, 33.68, 33.87, 50.84, 50.92, 57.29, 67.78, 80.18, 92.59, 172.91, 177.26.

**Deprotection of Dendron G3.** To a 250 mL round bottom flask, dendron (G3), **12**, was dissolved in formic acid (40 mL) and stirred for 12 h at room temperature. The solvent was removed under reduced pressure, and the crude product was dialyzed in methanol and dichloromethane (MWCO: 1000). After dialysis, the product was collected and concentrated *in vacuo* to yield a white solid (3.52 g, 85%).  $^1\text{H}$  NMR (300 MHz, MeOD):  $\delta$  = 2.17 (t, CH<sub>2</sub>, 84H), 1.98 (t, CH<sub>2</sub>, 72H).  $^{13}\text{C}$  NMR (400 MHz, MeOD): 26.13, 27.73, 28.29, 28.98, 29.20, 30.30, 30.95, 32.54, 32.70, 33.68, 33.87, 50.84, 50.92, 57.29, 67.78, 92.59, 172.91, 177.26.

**G3(LLBoc<sub>27</sub>), (*N*-Boc-1,6-diaminohexane attachment to G3 dendron acid G3OH)**  
**14.** G3OH (1.04 g, 0.34 mmol) was dissolved in dry DMF (150 mL) and was stirred in a sealed 250 mL round bottom flask under argon at 4 °C with HOBt (3.75 g, 27.78 mmol) and DCC (5.73 g, 27.78 mmol). After 2.5 h *N*-Boc-1,6-diaminohexane (6.00 g, 27.78 mmol) was dissolved in DMF and added, and the reaction was allowed to proceed for 48 h. Upon completion, the material was filtered, concentrated, and dialyzed (MWCO: 1000) in methanol and dichloromethane and concentrated *in vacuo* to yield a brown solid (2.50 g, 87%).  $^1\text{H}$  NMR (300 MHz, MeOD):  $\delta$  = 1.44-1.35 (s, CH<sub>3</sub>, CH<sub>2</sub>, 459H) 2.17 (t, CH<sub>2</sub>, 84H), 1.98 (t, CH<sub>2</sub>, 72H), 3.03 (t, CH<sub>2</sub>, 54H), 3.16 (t, CH<sub>2</sub>, 54H).  $^{13}\text{C}$  NMR (400 MHz, MeOD): 24.62, 25.66, 26.03, 27.02, 28.73, 29.88, 30.26, 30.58, 38.92, 39.19, 57.52, 78.33, 112.41, 115.32, 118.24, 160.98, 161.32, 161.67, 174.05.

**Deprotection of G3(LLBoc<sub>27</sub>).** G3(LLBoc<sub>27</sub>) was dissolved in (50/50) dichloromethane/TFA (30 mL) solution and allowed to stir at room temperature for 12 h in a 250 mL round bottom flask. The crude product was concentrated and dialyzed (MWCO: 1000) in methanol for 2 days. After dialysis, the material was concentrated *in vacuo* to yield a white solid G3(LLNH<sub>2</sub>)<sub>27</sub>, (1.08 g, 64%). <sup>1</sup>H NMR (300 MHz, MeOD):  $\delta$  =1.10-1.60 (s, CH<sub>3</sub>, CH<sub>2</sub>, 216H) 1.7-2.2 (t, CH<sub>2</sub>, 156H), 3.03 (t, CH<sub>2</sub>, 54H), 3.16 (t, CH<sub>2</sub>, 54H). <sup>13</sup>C NMR (400 MHz, MeOD): 25.66, 26.03, 27.02, 28.73, 29.88, 30.26, 30.58, 38.92, 39.19, 57.52, 112.41, 115.32, 118.24, 160.98, 161.32, 161.67, 174.05.

**G3LL(NH<sub>2</sub>)<sub>14</sub>-Cyclohexyl<sub>13</sub>, (2-cyclohexyl acetyl aldehyde attachment) 17.** G3(LLNH<sub>2</sub>)<sub>27</sub>, (0.412 g, 72.52  $\mu$ mole) was dissolved in dry 1:1 THF/DCM (10 mL) together with dry methanol (1 mL) in a 6 dram vial. 2-cyclohexylacetyl aldehyde (0.169 g, 1.34 mmol) was added and allowed to react for 30 min at room temperature. Sodium cyanoborohydride (0.123 g, 1.96 mmol) and saturated sodium bicarbonate were then sequentially added and allowed to stir for 1 h. The crude materials were filtered and dialyzed (MWCO: 1000) in methanol. The dialyzed material was then concentrated to afford a white solid (102.1 mg, 20%). <sup>1</sup>H NMR (300 MHz, MeOD):  $\delta$  =1.20-1.85 (s, CH<sub>3</sub>, CH<sub>2</sub>, 385H) 1.98 (broad s, CH<sub>2</sub>, 72H), 2.17 (broad s, CH<sub>2</sub>, 84H), 2.59 (broad s, CHNHCH<sub>2</sub>, 52H), 2.87 (broad s, NH<sub>2</sub>CH<sub>2</sub>, 28 H), 3.16 (broad s, CONHCH<sub>2</sub>, 54 H). <sup>13</sup>C NMR (400 MHz, MeOD): 24.65, 24.69, 24.74, 25.74, 25.87, 25.93, 26.01, 26.11, 26.36, 26.48, 29.02, 29.02, 32.42, 32.68, 32.77, 32.92, 33.02, 35.90, 41.24, 44.81, 51.17, 68.23, 160.98, 161.32, 161.67, 174.14.

**G3LL(Cyclohexyl<sub>13</sub>)(Guanidine<sub>14</sub>) 18.** A solution of G3LL(NH<sub>2</sub>)<sub>14</sub>-Cyclohexyl<sub>13</sub> dendrimer (102.1 mg, 14.36  $\mu$ mmol), was dissolved in cooled dichloromethane (12 mL)

in a 100 mL round bottom flask. Triethylamine (TEA) (0.315 mL) was added, followed by addition of *N,N'*-diboc-*N''*-triflylguanidine (101.1 mg, 0.258 mmol) and the reaction was stirred for 48 h at room temperature. The crude material was dialyzed (MWCO: 1000) in methanol and after dialysis concentrated to yield a white solid (75.1, 31%). <sup>1</sup>H NMR (400 MHz, MeOD): δ = 1.20-1.85 (s, CH<sub>3</sub>, CH<sub>2</sub>, 459H) 1.98 (broad s, CH<sub>2</sub>, 72H), 2.17 (broad s, CH<sub>2</sub>, 84H), 2.59 (broad s, CHNHCH<sub>2</sub>, 52H), 2.87 (broad s, NH<sub>2</sub>CH<sub>2</sub>), 3.16 (broad s, CONHCH<sub>2</sub>, 54). <sup>13</sup>C NMR (400 MHz), MeOD): δ = 25.68, 25.75, 25.84, 25.91, 25.99, 26.71, 26.80, 26.87, 27.22, 27.24, 29.70, 30.44, 32.39, 32.59, 32.64, 35.38, 50.86, 50.97, 80.66, 82.48, 82.57, 83.88, 115.01, 115.11, 115.21, 118.20, 118.28, 118.40, 121.39, 121.45, 121.59, 124.57, 124.63, 124.78, 149.97, 151.72, 151.75, 153.00, 157.19, 173.91.

**Hydrogenation of G3LL(Cyclohexyl<sub>13</sub>)(Guanidine<sub>14</sub>) dendrimer 19.** To a Parr hydrogenation bottle G3LL(Cyclohexyl<sub>13</sub>)(Guanidine<sub>14</sub>) dendrimer (47.1 mg, 22.4 μmole) was added and dissolved in dichloromethane (5 mL). Raney nickel (200 mg) and ethanol (100 mL) were added to the Parr vessel and the reaction mixture was hydrogenated at 65 psi for 5 days. Product development was confirmed using thin layer chromatography, and the material was filtered through filter paper and concentrated to afford a brown solid (32.3 mg, 68%). <sup>1</sup>H NMR (400 MHz, MeOD): δ = 1.20-1.85 (s, CH<sub>3</sub>, CH<sub>2</sub>, 459H) 1.98 (broad s, CH<sub>2</sub>, 72H), 2.17 (broad s, CH<sub>2</sub>, 84H), 2.59 (broad s, CHNHCH<sub>2</sub>, 52H), 2.87 (broad s, NH<sub>2</sub>CH<sub>2</sub>), 3.16 (broad s, CONHCH<sub>2</sub>, 54). <sup>13</sup>C NMR (400 MHz), MeOD): δ = 25.68, 25.75, 25.84, 25.91, 25.99, 26.71, 26.80, 26.87, 27.22, 27.24, 29.70, 30.44, 32.39, 32.59, 32.64, 35.38, 50.86, 50.97, 80.66, 82.48, 82.57, 83.88,

115.01, 115.11, 115.21, 118.20, 118.28, 118.40, 121.39, 121.45, 121.59, 124.57, 124.63, 124.78, 149.97, 151.72, 151.75, 153.00, 157.19, 173.91.

## **Labeling**

Amine G3LL(Cyclohexyl<sub>13</sub>)(Guanidine<sub>14</sub>) dendrimer (8.33 mg, 0.793  $\mu$ mole) was dissolved in DMSO (20  $\mu$ L). Alexa Fluor  $\text{\textcircled{R}}$  488 succinimidyl ester (2.00 mg, 3.11  $\mu$ mole) dissolved in DMSO was added to the solution in a 1 dram vial and allowed to stir for 2 h at room temperature. The crude material was dialyzed (MWCO: 1000) in methanol and dichloromethane. Then the dialyzed material was concentrated to afford the labeled product (7.12 mg, 71%). The labeled Cyclohexyl<sub>13</sub> Guanidine<sub>14</sub> G3 dendrimer was dissolved in (50/50) dichloromethane/TFA (30 mL) solution and allowed to stir at room temperature for 3 h in a 1 dram vial. The crude product was concentrated, and then dialyzed (MWCO: 1000) in methanol and dichloromethane. The dialyzed material was then concentrated to yield product (4.31 mg, 89%).

## **Confocal Microscopic Analysis**

For colocalization studies, the culture medium was removed, and the cells were washed in phosphate-buffered saline (PBS), pH 7.4. The cells were incubated with  $\sim$ 5  $\mu$ M Cyclohexyl<sub>13</sub> Guanidine<sub>14</sub> G3 dendrimer in serum-free MEM ( $\alpha$ -MEM [no phenol red]; Invitrogen) for 45 min. Mitotracker CMXRos was added to achieve a final concentration of 100 nM for the last 15 min of the incubation. Cells were washed three times with serum-free MEM. After washing, serum-free MEM was added and live cell imaging was performed using an inverted Zeiss LSM 510 confocal microscope (40 $\times$ ).



The excitation wavelength for imaging of the labeled dendrimer was 488 nm, and emission was collected from 505 to 530 nm. The excitation wavelength for visualization of Mitotracker CMXRos was 543 nm, and emission was collected with a long-pass 560 nm filter. Differential interference contrast (DIC) images were taken along with both fluorescence channels, and no bleed-through was observed during colocalization studies using these parameters. The fluorescence images were processed using Image J software program to determine Pearson's Correlation Coefficient (Rr), and values reported reflect an average of values obtained from cells (~30 cells) over multiple experiments ( $\geq 3$  days). The background was subtracted from the images with a manually selected region of interest. Mitotic and unhealthy cells, as assessed by DIC, were excluded from analysis. To avoid large differences in signal intensity between fluorescence channels that can introduce artifacts, cells with comparable signals from both channels were used for calculations.

## References

1. Lemasters, J. J.; Holmuhamedov, E., Voltage-dependent anion channel (VDAC) as mitochondrial governor - Thinking outside the box. *Biochimica Et Biophysica Acta-Molecular Basis of Disease* **2006**, *1762* (2), 181-190.
2. Shaw, J. M.; Winge, D. R., Shaping the mitochondrion: mitochondrial biogenesis, dynamics and dysfunction Conference on Mitochondrial Assembly and Dynamics in Health and Disease. *Embo Reports* **2009**, *10* (12), 1301-1305.
3. Andreyev, A. I.; Kushnareva, Y. E.; Starkov, A. A., Mitochondrial metabolism of reactive oxygen species. *Biochemistry-Moscow* **2005**, *70* (2), 200-214.
4. Wallace, D. C., Mitochondrial diseases in man and mouse. *Science* **1999**, *283* (5407), 1482-1488.
5. Horton, K. L.; Pereira, M. P.; Stewart, K. M.; Fonseca, S. B.; Kelley, S. O., Tuning the Activity of Mitochondria-Penetrating Peptides for Delivery or Disruption. *Chembiochem* **2012**, *13* (3), 476-485.
6. Xu, Y.; Chen, X. M.; Kelley, M. R., Targeting human O6-methylguanine DNA methyltransferase (MGMT/AGT) to the mitochondria affords protection against BCNU, temozolomide and MMS. *Cancer Gene Therapy* **2003**, *10*, S28-S28.
7. Murphy, M. P., Slip and Leak in Mitochondrial Oxidative-Phosphorylation. *Biochimica Et Biophysica Acta* **1989**, *977* (2), 123-141.
8. Murphy, M. P.; Smith, R. A. J., Drug delivery to mitochondria: the key to mitochondrial medicine. *Advanced Drug Delivery Reviews* **2000**, *41* (2), 235-250.
9. Weissig, V.; Torchilin, V. P., Cationic bolosomes with delocalized charge centers as mitochondria-specific DNA delivery systems. *Advanced Drug Delivery Reviews* **2001**, *49* (1-2), 127-149.
10. Johnson, L. V.; Walsh, M. L.; Chen, L. B., Localization of Mitochondria in Living Cells with Rhodamine-123. *Proceedings of the National Academy of Sciences of the United States of America-Biological Sciences* **1980**, *77* (2), 990-994.
11. Rideout, D.; Bustamante, A.; Patel, J., Mechanism of Inhibition of Fadu Hypopharyngeal Carcinoma Cell-Growth by Tetraphenylphosphonium Chloride. *International Journal of Cancer* **1994**, *57* (2), 247-253.
12. Biswas, S.; Dodwadkar, N. S.; Sawant, R. R.; Koshkaryev, A.; Torchilin, V. P., Surface modification of liposomes with rhodamine-123-conjugated polymer results in enhanced mitochondrial targeting. *Journal of Drug Targeting* **2011**, *19* (7), 552-561.

13. Weissig, V.; Boddapati, S. V.; Cheng, S. M.; D'Souza, G. G. M., Liposomes and liposome-like vesicles for drug and DNA delivery to mitochondria. *Journal of Liposome Research* **2006**, *16* (3), 249-264.
14. Torchilin, V. P., Recent approaches to intracellular delivery of drugs and DNA and organelle targeting. *Annual Review of Biomedical Engineering* **2006**, *8*, 343-375.
15. Yamada, Y.; Shinohara, Y.; Kakudo, T.; Chaki, S.; Futaki, S.; Kamiya, H.; Harashima, H., Mitochondrial delivery of mastoparan with transferrin liposomes equipped with a pH-sensitive fusogenic peptide for selective cancer therapy. *International Journal of Pharmaceutics* **2005**, *303* (1-2), 1-7.
16. Yamada, Y.; Akita, H.; Kamiya, H.; Kogure, K.; Yamamoto, T.; Shinohara, Y.; Yamashita, K.; Kobayashi, H.; Kikuchi, H.; Harashima, H., MITO-Porter: A liposome-based carrier system for delivery of macromolecules into mitochondria via membrane fusion. *Biochimica Et Biophysica Acta-Biomembranes* **2008**, *1778* (2), 423-432.
17. Samuelson, L. E.; Dukes, M. J.; Hunt, C. R.; Casey, J. D.; Bornhop, D. J., TSPO Targeted Dendrimer Imaging Agent: Synthesis, Characterization, and Cellular Internalization. *Bioconjugate Chemistry* **2009**, *20* (11), 2082-2089.
18. Biswas, S.; Dodwadkar, N. S.; Piroyan, A.; Torchilin, V. P., Surface conjugation of triphenylphosphonium to target poly(amidoamine) dendrimers to mitochondria. *Biomaterials* **2012**, *33* (18), 4773-4782.
19. Yousif, L. F.; Stewart, K. M.; Kelley, S. O., Targeting Mitochondria with Organelle-Specific Compounds: Strategies and Applications. *ChemBiochem* **2009**, *10* (12), 1939-1950.
20. Horton, K. L.; Stewart, K. M.; Fonseca, S. B.; Guo, Q.; Kelley, S. O., Mitochondria-penetrating peptides. *Chemistry & Biology* **2008**, *15* (4), 375-382.
21. Chung, H. H.; Harms, G.; Seong, C. M.; Choi, B. H.; Min, C. H.; Taulane, J. P.; Goodman, M., Dendritic oligoguanidines as intracellular translocators. *Biopolymers* **2004**, *76* (1), 83-96.
22. Huang, K.; Voss, B.; Kumar, D.; Hamm, H. E.; Harth, E., Dendritic molecular transporters provide control of delivery to intracellular compartments. *Bioconjugate Chemistry* **2007**, *18* (2), 403-409.
23. Svenson, S.; Chauhan, A. S., Dendrimers for enhanced drug solubilization. *Nanomedicine* **2008**, *3* (5), 679-702.
24. Nanjwade, B. K.; Bechra, H. M.; Derkar, G. K.; Manvi, F. V.; Nanjwade, V. K., Dendrimers: Emerging polymers for drug-delivery systems. *European Journal of Pharmaceutical Sciences* **2009**, *38* (3), 185-196.

25. Chauhan, A. S.; Sridevi, S.; Chalasani, K. B.; Jain, A. K.; Jain, S. K.; Jain, N. K.; Diwan, P. V., Dendrimer-mediated transdermal delivery: enhanced bioavailability of indomethacin. *Journal of Controlled Release* **2003**, *90* (3), 335-343.
26. Neerman, M. F.; Chen, H. T.; Parrish, A. R.; Simanek, E. E., Reduction of drug toxicity using dendrimers based on melamine. *Molecular Pharmaceutics* **2004**, *1* (5), 390-393.
27. Patri, A. K.; Kukowska-Latallo, J. F.; Baker, J. R., Targeted drug delivery with dendrimers: Comparison of the release kinetics of covalently conjugated drug and non-covalent drug inclusion complex. *Advanced Drug Delivery Reviews* **2005**, *57* (15), 2203-2214.
28. Gewirtz, P., "On 'I Know It When I See It'. *Yale Law Journal* **1996**, *105*, 1023-1047.
29. Dunn, K. W.; Kamocka, M. M.; McDonald, J. H., A practical guide to evaluating colocalization in biological microscopy. *American Journal of Physiology-Cell Physiology* **2011**, *300* (4), C723-C742.
30. Bolte, S.; Cordelieres, F. P., A guided tour into subcellular colocalization analysis in light microscopy. *Journal of Microscopy-Oxford* **2006**, *224*, 213-232.
31. Rothbard, J. B.; Kreider, E.; Vandeuken, C. L.; Wright, L.; Wylie, B. L.; Wender, P. A., Arginine-rich molecular transporters for drug delivery: Role of backbone spacing in cellular uptake. *Journal of Medicinal Chemistry* **2002**, *45* (17), 3612-3618.
32. Fonseca, S. B.; Pereira, M. P.; Kelley, S. O., Recent advances in the use of cell-penetrating peptides for medical and biological applications. *Advanced Drug Delivery Reviews* **2009**, *61* (11), 953-964.
33. Hamilton, S. K.; Ikizler, M. R.; Wallen, C.; Wright, P. F.; Harth, E., Effective delivery of IgG-antibodies into infected cells via dendritic molecular transporter conjugate IgGMT. *Molecular Biosystems* **2008**, *4* (12), 1209-1211.
34. Borch, R. F.; Bernstein, M.; Durst, H. D., Cyanohydridoborate Anion as a Selective Reducing Agent. *Journal of the American Chemical Society* **1971**, *93* (12), 2897-&.
35. Wender, P. A.; Galliher, W. C.; Goun, E. A.; Jones, L. R.; Pillow, T. H., The design of guanidinium-rich transporters and their internalization mechanisms. *Advanced Drug Delivery Reviews* **2008**, *60* (4-5), 452-472.
36. Fittipaldi, A.; Giacca, M., Transcellular protein transduction using the Tat protein of HIV-1. *Advanced Drug Delivery Reviews* **2005**, *57* (4), 597-608.

## CHAPTER V

### CONCLUSION AND FUTURE OUTLOOK

The work presented demonstrates the development of dendrimer systems as delivery platforms. The systems were created using two structural approaches, which include second generation and third generation molecular transporters. In one approach, the second generation transporter was attached to a recombinant antibody to form a bioconjugate. To construct the conjugate, several investigations were conducted to determine the optimized attachment conditions. The bioconjugate was then used to provide delivery of the antibody to the cytosol for neutralization against rotavirus *in vitro*. The neutralization of rotavirus by the bioconjugate indicates promise as an effective design for viral treatment and suggest potential to be used for other applications. Furthermore, as cellular entry is a critical component in many forms of therapeutics and other compounds alike, providing transport of compounds for biological application, cellular labeling, or even diagnostic approaches are viable directions for using the second generation dendrimer.

In another investigation, third generation dendrimers were developed with the desire to investigate new libraries of dendritic structures. The macromolecules were synthesized to feature ethyl and alkyl dendritic peripheral arms. In addition, structures were synthesized that could be well characterized. Future investigations to evaluate cellular distribution of dendrimers *in vitro* are of interest. Furthermore, because the higher order generation structures feature regions of void space, these regions can be

investigated for compound retention as an additional approach for delivery of therapeutics.

Due to the ability to synthesize facile structures using third generation platforms, several compounds were synthesized to feature multi-valent peripheries. The investigation of the constructs was found to provide targeting to cellular mitochondria. This was achieved using a variation in termini head groups to feature a 50/50 ratio of lipophilic and cationic functionality. The results from these findings highlight the ability of to develop structures for organelle targeting to mitochondria. Using this strategy, additional structures featuring different end group functionalities may prompt further advancement as an approach for delivery systems. The use of structures featuring large generations of structures enables the most facile approach for creating such architectures and may be expanded to incorporate other functional groups. Furthermore, there are other intracellular compartments that would benefit from targeted systems and the manipulation of these termini groups suggest potential for creating additional targeted structures specific to those organelles. The development and application of targeted structures provide a means of intracellular identification and vehicle of delivery for therapeutic treatment and could be used to probe further understanding of other deleterious conditions linked to organelle dysfunctions.

The macromolecules reported provide a useful platform for the use of dendrimers as compounds for potential vehicles for selective delivery. They also suggest potential as effective building blocks that could enhance the delivery of current and novel therapeutic formulations. While guanidine functionalized dendrimers suggest the greatest

potential *in vitro* system combinatorial approaches using hybrid systems featuring dendrimers may pave the way for further uses of dendrimers *in vivo*.